FUNDAMENTAL CHARACTERIZATION OF ALTERNATE FUEL EFFECTS IN CONTINUOUS COMBUSTION SYSTEMS

EXXON RESEARCH AND ENGINEERING CO.,
LINDEN, NJ. GOVERNMENT RESEARCH LAB

11 SEP 1978

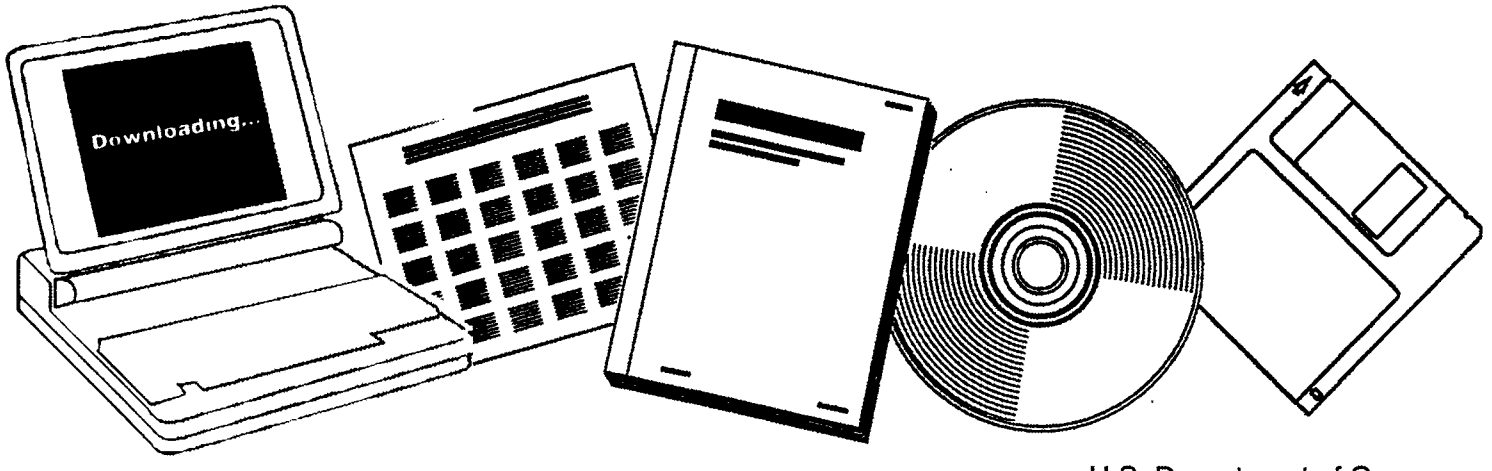

One Source. One Search. One Solution.

NTIS

Providing Permanent, Easy Access to U.S. Government Information

National Technical Information Service is the nation's largest repository and disseminator of government-initiated scientific, technical, engineering, and related business information. The NTIS collection includes almost 3,000,000 information products in a variety of formats: electronic download, online access, CD-ROM, magnetic tape, diskette, multimedia, microfiche and paper.

Search the NTIS Database from 1990 forward

NTIS has upgraded its bibliographic database system and has made all entries since 1990 searchable on **www.ntis.gov.** You now have access to information on more than 600,000 government research information products from this web site.

Link to Full Text Documents at Government Web Sites

Because many Government agencies have their most recent reports available on their own web site, we have added links directly to these reports. When available, you will see a link on the right side of the bibliographic screen.

Download Publications (1997 - Present)

NTIS can now provides the full text of reports as downloadable PDF files. This means that when an agency stops maintaining a report on the web, NTIS will offer a downloadable version. There is a nominal fee for each download for most publications.

For more information visit our website:

www.ntis.gov

U.S. DEPARTMENT OF COMMERCE
Technology Administration
National Technical Information Service
Springfield, VA 22161

SAN-1543-12
Distribution Category UC-96

EXXON RESEARCH AND ENGINEERING COMPANY

FUNDAMENTAL CHARACTERIZATION OF ALTERNATE FUEL EFFECTS IN CONTINUOUS COMBUSTION SYSTEMS

SUMMARY TECHNICAL PROGRESS REPORT

FOR PERIOD AUGUST 15, 1977 - AUGUST 14, 1978

by

W. S. Blazowski
Exxon Research and Engineering Company
Government Research Laboratories
Linden, New Jersey 07036

and

R. B. Edelman
P. T. Harsha
Science Applications, Inc.
Woodland Hills, California

September 11, 1978

Prepared for

the Department of Energy

Under Contract EC-77-C-03-1543

P. O. BOX 8 ■ LINDEN, NEW JERSEY 07036

TABLE OF CONTENTS

FOREWORD

This is the first annual Summary Technical Progress Report for DOE Contract EC-77-C-03-1543, "Fundamental Characterization of Alternate Fuel Effects in Continuous Combustion Systems". It includes descriptions of experimental and analytical information generated during the first year of the subject program, August 15, 1977-August 14, 1978. Effort during the first three months of the program was directed towards evaluation of experimental and analytical needs. This work resulted in a quarterly Technical Progress Report thoroughly describing our assessment of the problem. Since the previous report is available through the same sources of technical information, this information has not been reported here.

Experimental information was generated by Exxon Research and Engineering Company (ER&E) and analytical work was performed by Science Applications, Inc. (SAI). Dr. Raymond B. Edelman is responsible for activities at SAI. ER&E is the prime contractor for this program and is responsible for overall program direction and performance.

The Principal Investigator wishes to acknowledge the efforts of Mr. Robert W. Schroeder who conducted the experimental efforts described herein with expert skills and diligence. Further, the development of a data reduction procedure for the Jet Stirred Combustor was performed by Mr. Dominic C. Rigano to whom I am also grateful.

W. S. BLAZOWSKI
Principal Investigator

ABSTRACT

The overall objective of this contract is to assist in the development of fuel-flexible combustion systems for gas turbines as well as Rankine and Stirling cycle engines. The primary emphasis of the program is on liquid hydrocarbons produced from non-petroleum resources. Fuel-flexible combustion systems will provide for more rapid transition of these alternate fuels into important future energy utilization centers (especially utility power generation with the combined cycle gas turbine). The specific technical objectives of the program are: a) develop an improved understanding of relationships between alternate fuel properties and continuous combustion system effects, and b) provide analytical modeling/correlation capabilities to be used as design aids for development of fuel-tolerant combustion systems. Efforts this past year have been to evaluate experimental procedures for studying alternate fuel combustion effects and to determine current analytical capabilities for prediction of these effects. Jet Stirred Combustor studies during this period have produced new insights into soot formation in strongly backmixed systems and have provided much information for comparison with analytical predictions. The analytical effort included new applications of quasi-global modeling techniques as well as comparison of predictions with the experimental results generated.

I. INTRODUCTION

With increased emphasis on the utilization of U.S. energy resources for national self-reliance, coal and alternate (synthetic) fuels are expected to play an important role in future energy developments. In many stationary applications, where significant non-petroleum energy is already utilized, widespread conversion to the usage of coal from oil is anticipated. While new exhaust emissions control technologies must be developed to accomplish this task in an environmentally acceptable manner, the engineering know-how to utilize coal and experience previously developed can be expected to facilitate conversion.

Other applications for which direct coal utilization may not be technically or economically viable, however, must rely on liquid hydrocarbons or gases produced from non-petroleum sources. The major North American resources from which future synthetic fuels (synfuels) will be derived are coal, shale, and tar sands deposits. Fuels derived from these resources will include coal liquids, methanol, and low, intermediate, and high BTU coal gas products as well as hydrocarbon liquids derived from oil shale and tar sands.*

Characteristics of the basic feedstocks from which the future liquid fuels will be made are significantly different from typical petroleum properties. Liquid synfuels, especially those derived from coal, are likely to be more aromatic and have significantly decreased hydrogen content. These characteristics can be expected to result in increased soot formation, increased flame radiation (which can affect the integrity of combustor hardware), and increased deposit forming tendency, possibly resulting in plugging and fouling of equipment. Another significant difference between conventional petroleum and synthetic crudes is nitrogen content. Depending on the extent of refining performed, increased NO_x emission from fuel bound nitrogen may also be a problem. Finally, as a result of the generally lower volatility of synthetic crudes, synfuels might be expected to be less volatile than petroleum-derived fuels thereby causing problems associated with fuel droplet burning.

Optional approaches for the future utilization of synfuels consist of energy-intensive refining steps to match conventional fuel specifications or devising ways of altering combustion systems to allow combustion of fuels not meeting current specifications. In his plenary session paper "Synthetic Fuels and Combustion" at the 16th International Combustion Symposium, J. P. Longwell discussed the rationale for the utilization of synthetic liquid fuels without extensive refining (Reference 1). The incentives for following this route were shown to be very significant from the standpoints of energy conservation and cost.

For the combustion system designer, the task at hand is one of evaluating the impact of changes in fuel character and defining the range of fuel characteristics within which the system can operate. The U.S. Air Force has initiated one such program for defining future military aircraft fuels. The combustion effects of future fuels are to be characterized along with

*Limited synfuel production from tar sands is already a reality, but this resource is small compared to the potential of coal or oil shale reserves.

other system factors (e.g., fuel tank design, pumps, handling requirements, etc.) and fuel processing information is to be acquired. A trade-off analysis will then determine the characteristics (a future fuel specification) which will result in minimum total operating cost and adequate availability without significant sacrifice in safety, performance, or environmental impact. With respect to availability, geographic variability in the staple resource and in refining capability will cause combustion system flexibility to be an important asset. Future development of "fuel flexible engines" may receive high priority.

Indeed, each application to utilize future synfuels or expanded-specification petroleum fuels must develop such a program. It is anticipated that the outcome of such studies will be the realization that future fuels should be significantly different than those now in use. Naturally, these findings should strongly influence future synfuel process design.

Regardless of the application, the impact of the fuel on the combustion system would be expected to play the major role. Unfortunately, the investigation of fuel impact on combustion systems is almost entirely empirical and expensive, large-scale testing is necessary. Our current understanding of the fundamental combustion phenomena which influence a fuel's practical combustion characteristics is extremely limited. The extensive efforts to develop combustor models during the past decade have avoided the complexity of input details which would define fuel characteristics and the existing ability to predict, or even extrapolate, fuel effects is nearly non-existent.

The current situation, although understandable in light of the previous assumed availability of low-cost fuel of consistent high quality, must now be corrected. Fundamental understanding of the combustion phenomena influencing a fuel's performance (gas phase fuel pyrolysis kinetics, soot formation and oxidation, droplet evaporation and combustion, and aerodynamic/chemical interactions) must be developed. Further, models to be used by the combustion system designer for prediction of fuel effects in real systems (i.e., means to utilize the details discussed above) are required.

This program addresses the serious weakness in our ability to relate fuel characteristics to combustion effects. A multi-year effort is being conducted to satisfy two primary objectives: a) to provide an improved understanding of the relationships between fuel properties and combustion characteristics and b) to develop analytical modeling/correlation capabilities for the prediction of fuel effects. The work is limited to investigation of alternate liquid fuels used in continuous combustion systems, with gas turbine systems receiving special attention. Future electric power generation with combined cycle gas turbines makes it imperative that technology be developed to allow operation on liquid synfuels with minimum refining (2). Development of such fuel-flexible gas turbine will encourage the utilization of synthetic fuels as they enter the marketplace, have major impact on future conservation of petroleum supplies, and reduce the cost of power production. The results of this program will also benefit the second important gas turbine application, aircraft propulsion. In this case, the future use of lower hydrogen content fuels can improve availability (a vital consideration for military applications) and reduce cost.

The program philosophy is to relate fundamental combustion phenomena to fuel characteristics using analytical models developed with and eventually verified by data obtained in carefully designed experiments. Figure 1 describes this approach schematically. The model can be envisioned as a combination of chemical and fuel related elements, thermodynamic and

FIGURE 1

Schematic Representation of a Combustor Model

CHEMICAL AND FUEL RELATED ELEMENTS

* Fuel Vaporization and Spray Dynamics
* Fuel Pyrolysis
* Soot Formation
* Bound N → NO_x Conversion
* H_2 and CO Oxidation
* Soot Oxidation
* Aerodynamic/Chemical Interactions

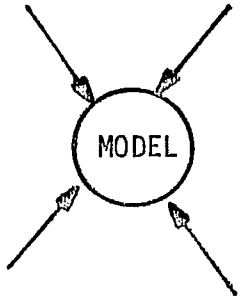

THERMODYNAMIC AND HEAT TRANSFER ELEMENTS

- Conduction
- Convection
* Radiation
- Turbulence Effects
- Energy Balance and Temperature Determination

GAS PHASE ELEMENTS

- Mass and Species Conservation
- Momentum Conservation
- Energy Conservation
- Species Diffusion
- Turbulence Model

SOLUTION SCHEME

- Simplification of Equations
- Solution Procedure
- Criteria for Solution Acceptance

heat transfer elements, and gas phase elements. A solution scheme provides the mathematical procedures for solving the many complex mathematical relationships. The subject program focuses on the fuel related elements appearing in the upper left portion of the schematic but includes devoting sufficient attention to other elements to result in the development of a successful model. The program proceeds along two parallel, strongly-interactive paths involving both modeling and experimental tasks. ER&E is responsible for overall program direction and experimentation, while Science Applications, Inc. (SAI) is responsible for analytical modeling undering subcontract to ER&E.

These results will allow engine designers to better understand fuel effects in existing systems and will provide a vital tool necessary for the future development of fuel flexible systems. Four key goals of the DOE Principal Alternate Fuels Planning Network will be pursued in this program:

- quantify engineering chemical kinetics of alternate fuels
- develop combustion models for alternate fuels
- characterize and quantify emissions from alternate fuels
- evaluate combustion performance of alternate fuels

While the primary thrust in this program is towards the gas turbine application, many direct contributions will be made to alternate fuel usage in other applications such as spark ignition and diesel engines. Specific contributions will include improved understanding of soot formation/oxidation chemistry and information regarding fuel nitrogen-to-NO_x conversion.

Effort during the first phase of this program (August 15, 1977-September 30, 1978) provided a well-developed plan for subsequent years of the program. Key combustion properties and ranges of fuel variation of interest to our subsequent efforts were surveyed. The first quarterly report of this program (3) provides a thorough accounting of this evaluation. Experimental and analytical needs were identified and prioritized. Experimental work included utilization of the Jet Stirred Combustor for evaluation of fuel combustion characteristics. The analytical modeling effort included new applications of quasi-global modeling techniques as well as predictions of and comparisons with the experimental results generated.

This report provides an extensive description of program efforts from January 1978 to August 1978. Presentation is organized into three main sections. Section II describes the status of the experimental effort, Section III describes the progress in analytical modeling, and Section IV gives an overview of the future program.

II. EXPERIMENTAL EFFORT

This section describes the status of the experimental portion of the subject program. Major subsections which follow describe the Jet Stirred Combustor apparatus being used, present the results, discuss and interpret the results, and provide summary conclusions of the experimental effort to date.

A. Apparatus

The first-year experimental program focused on study on the soot formation process using the Jet-Stirred Combustor (JSC). This device is a modification of the Longwell-Weiss reactor (4) with hemispherical geometry. The JSC has been used extensively in fluid mechanic and combustion modeling because combustion rates are limited by chemical kinetics as opposed to transport effects. A key advantage of the JSC for the present program is that the strongly backmixed nature of this combustion process provides a simulation of the recirculating characteristics of the gas turbine primary zone. It is in this zone where mixture conditions are sufficiently rich to produce soot. Consequently, the JSC allows study of soot formation in an aerodynamic situation relevant to gas turbine systems. Another advantage of the stirred combustor is that the reactor is homogeneous in species concentration as well as temperature; each operating condition is characterized by a single set of temperature and concentration data rather than profiles of these parameters. This simplifies the tasks of obtaining and interpretating the data.

The reactor (Figure 2) consists of an outer shell of castable refractory shaped as two halves of a sphere, 15.2 cm in diameter. Materials used in fabricating these reactors are Super Castable 3200, Fractocrete 3400, and Castable 141A, all products of Combustion Engineering Refractories. The upper hemisphere is solid with the exception of the hole through which the reactants are brought to the injector. The lower portion is hollowed out to a hemispherical reaction zone of 2.54, 3.81, or 5.08 cm diameter and has twenty-five holes of 3.2 mm diameter through which the burned mixture exhausts. Combustion experiments are conducted at atmospheric pressure with a range of residence times from 0.6 to 4 ms. Thermocouples are utilized to determine the temperature within the reactor as well as temperature gradients within the refractory (for calculation of heat loss).

Fuel and air are metered separately through calibrated rotameters, preheated to the desired inlet temperature and then mixed before entering the combustor. Air and fuel heating to temperatures of 350°C (and fuel prevaporization in the case of liquids) is accomplished in an aluminum block heater. Separate coils for fuel and air are embedded in the solid aluminum block which is wrapped with electrical resistance heaters. In the case of liquid fuels, a small flow of N_2 is maintained through the fuel coil to atomize the fuel and provide for smooth vaporization. Atomization was achieved at the entrance to the heater with a Spraying Systems Company 1/4 JSS air atomizing nozzle. In this configuration, a central jet (0.2 mm diameter) of fuel is atomized by the strong shearing forces caused by a co-axial jet (between diameters of 1.2 and 1.6 mm) of N_2.

The temperature of the fuel/air stream is determined immediately before injection. This measurement is input to a digital controller which provides power to the block heater to maintain injector inlet temperature within ± 10°C of the set point. The fuel-air mixture enters the reaction zone through an Inconel injector which is a hemisphere of 1.27 cm diameter into which are drilled forty radial holes of 0.5 mm diameter. Reactants

FIGURE 2

The Jet Stirred Combustor

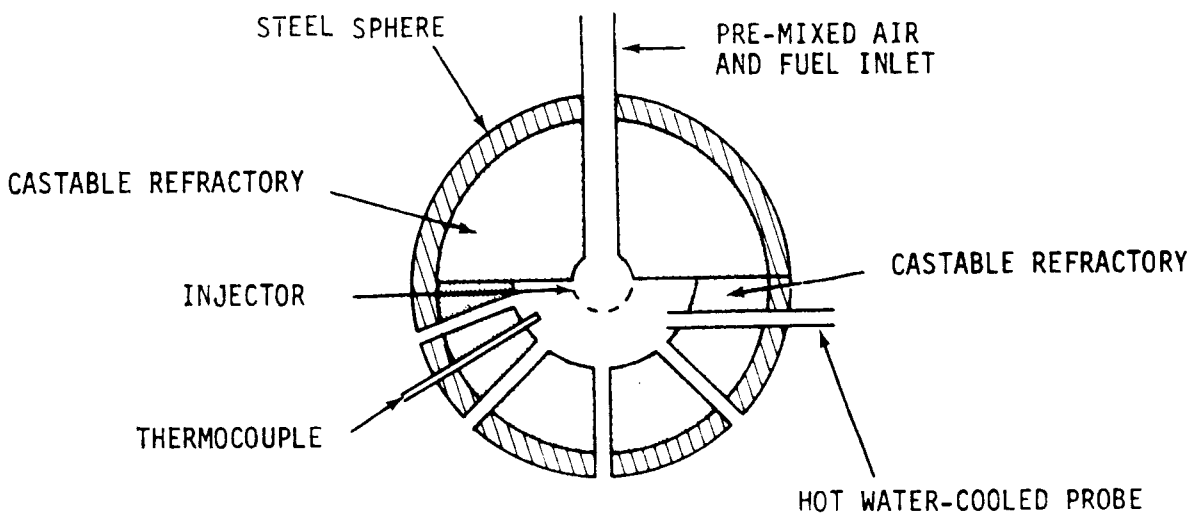

enter the reaction zone as small sonic jets which stir the reactor contents and produce a mixture of essentially uniform temperature and composition in a characteristic time which is very short compared with the average residence time. An overall view of the fuel and air system as well as the JSC is shown in Figure 3.

A probe is inserted through one of the twenty-five exhaust ports to extract a sample. Special care has been taken to prevent condensation of water or unburned hydrocarbons within the probe and sample lines, as high concentrations of these constituents are expected at mixture ratios of interest in this study. The sampling probe (Figure 4) is hot-water cooled and sample transfer is accomplished using electrically heated sample lines. All sample conditioning (pumping, filtering, and valving) is accomplished within a Blue-M Model OV-18A oven maintained at 150°C. Valves have been selected which are rated for operation at temperatures up to at least 175°C and design characteristics are such that lubricated valve components are sealed from the gas path. The pump selected is a high temperature metal bellows type (Model MD-158 HT) driven by a 1/4 horsepower motor external to the oven. The sample conditioning system is shown in Figure 5.

Gas sampling is accomplished with conventional process instrumentation. A filter within the oven removes particulates from gases passing to instrumentation. A first gas stream leaving the oven is transferred through hot (~150°C), electrically-heated lines to a Beckman Model 402 analyzer for total hydrocarbon (THC) measurement. This instrument has a vast dynamic range allowing determination of hydrocarbon concentrations ranging from the parts-per-million level through tens of mole percent. The hydrocarbon instrument was calibrated with a mixture containing CH_4 and all reported THC results are "as methane". A second sample gas stream leaving the oven is chilled to eliminate condensable water (to a dew point of about 10°C) and hydrocarbons prior to introduction into NDIR analyzers for CO and CO_2 measurements. These were both Beckman Model 864 instruments with the maximum CO range being 10 mole percent and the maximum CO_2 range being 20 mole percent. An overall view of the gas analysis system is shown in Figure 6.

The particulate sampling system uses different filters located within the sample-conditioning oven. Two 47 mm filters sealed in a stainless steel holder were used in "series". The first was a Millipore Mitex (Teflon) filter with a 5 μm pore size; the second was a Gellman Type AE with a 0.3 μm pore size. The Teflon filter was found to be necessary to prevent the glass fiber material from sticking to the Viton O-Ring sealing the filter holder. Nearly all the soot collected was found on the first (Teflon) filter.

The incipient soot formation equivalence ratio was the simplest determination of sooting characteristics pursued during this program. For this information, data is taken at increasing equivalence ratio* increments of 0.1 until a filter deposit is observed. Results presented will, therefore, represent an equivalence ratio value midway between test points at which soot was observed.

---

*Equivalence ratio, ϕ, is the actual fuel-air ratio divided by the stoichiometrically correct fuel-air ratio. Values less than one correspond to lean operation while values greater than one indicate fuel rich operation.

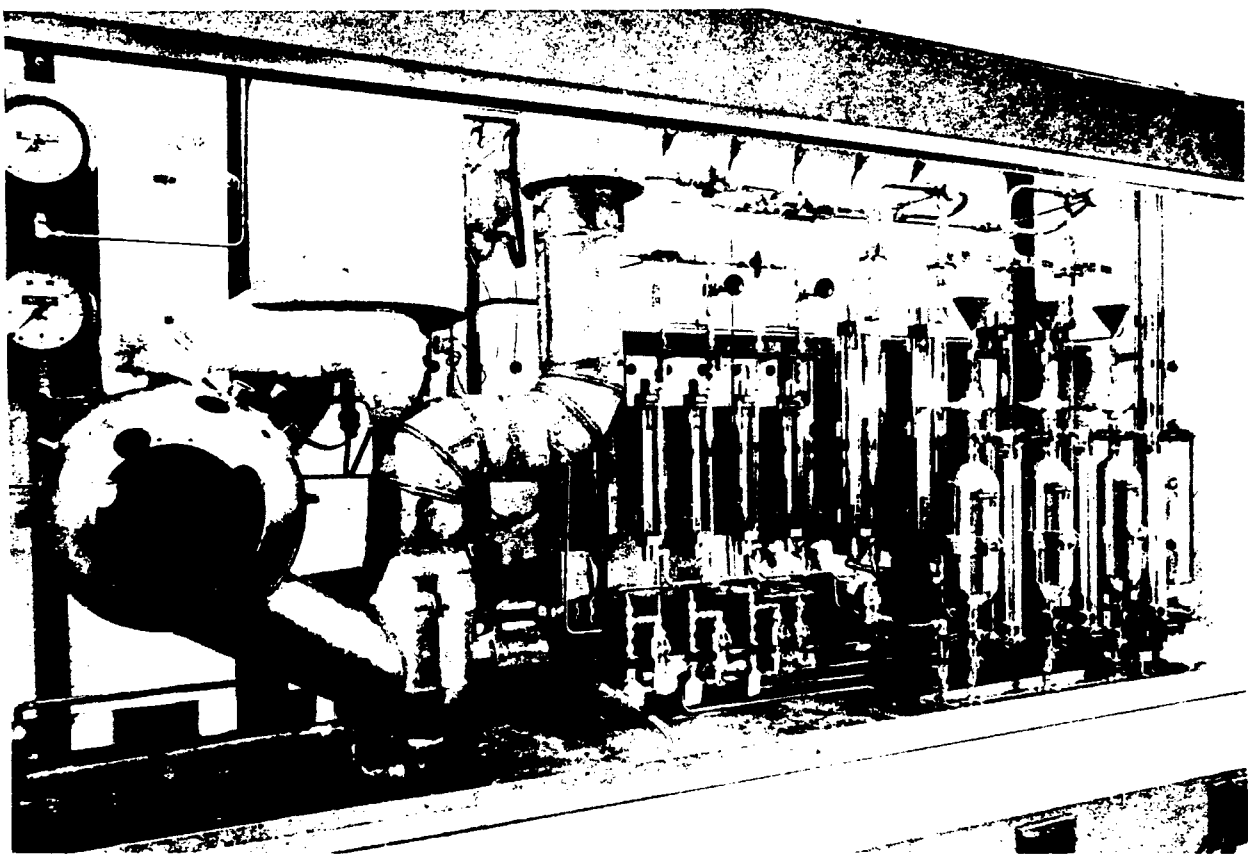

FIGURE 3: Overall View of Experimental System

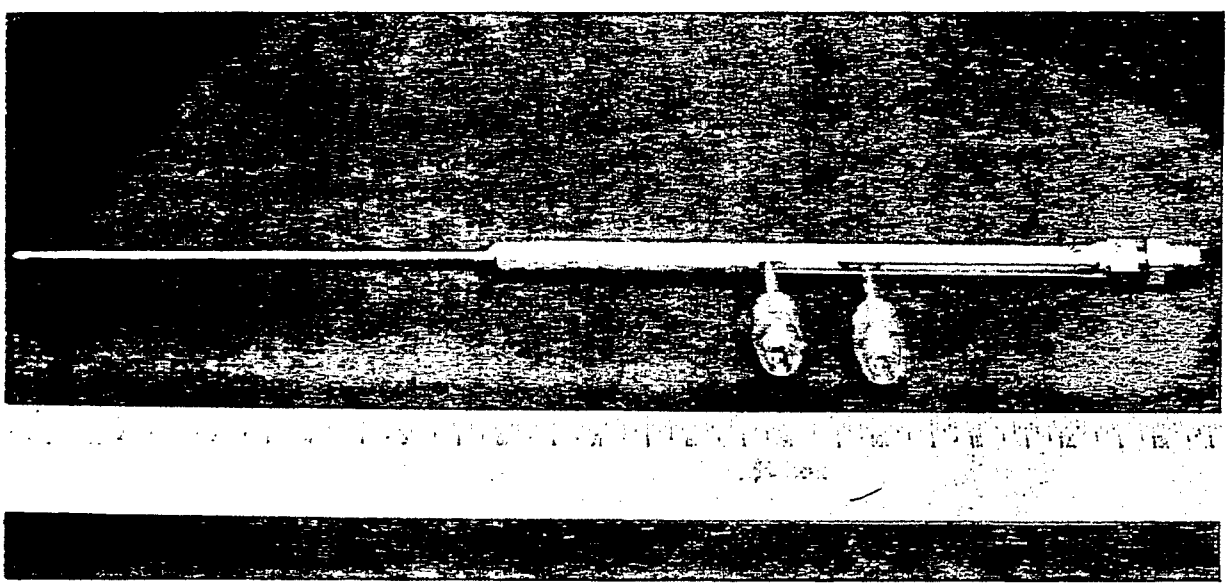

FIGURE 4: Sample Probe

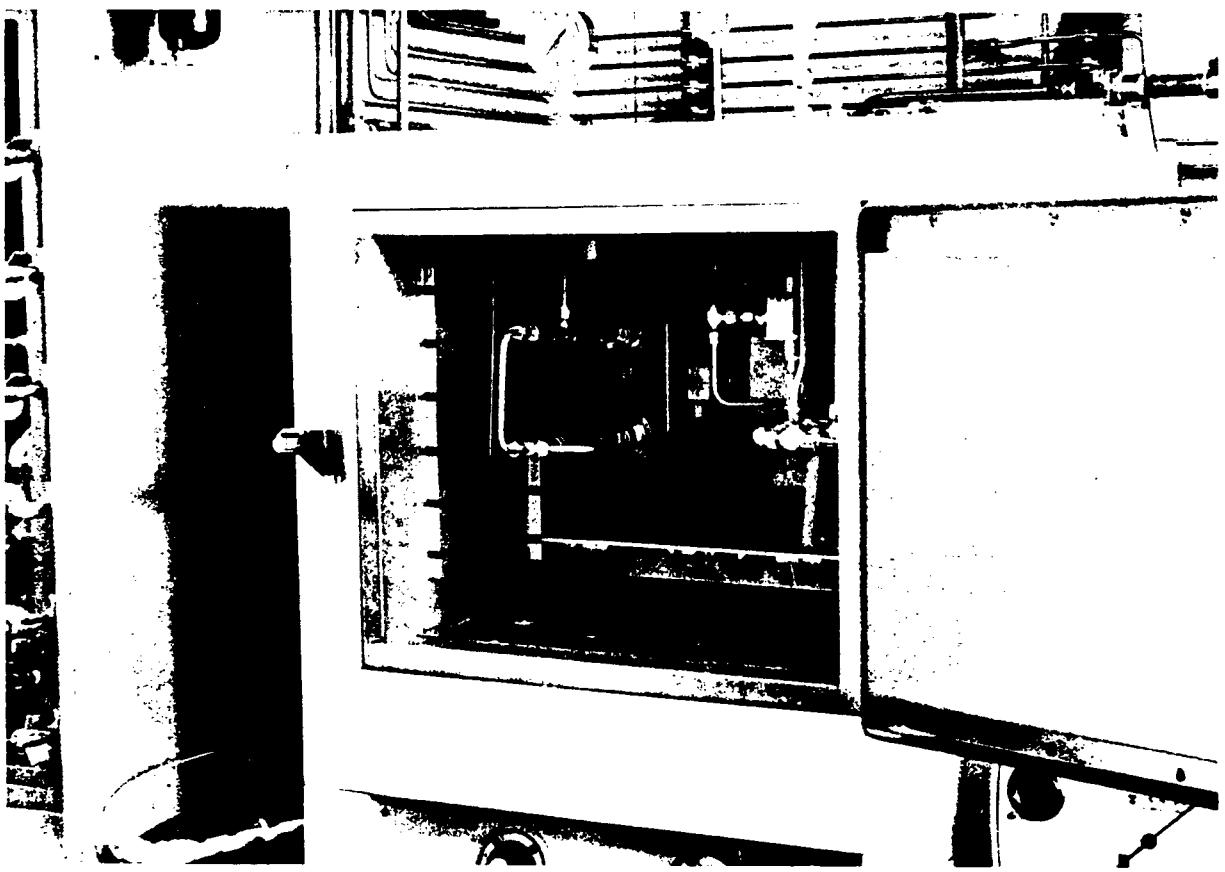

FIGURE 5: Sample Conditioning System

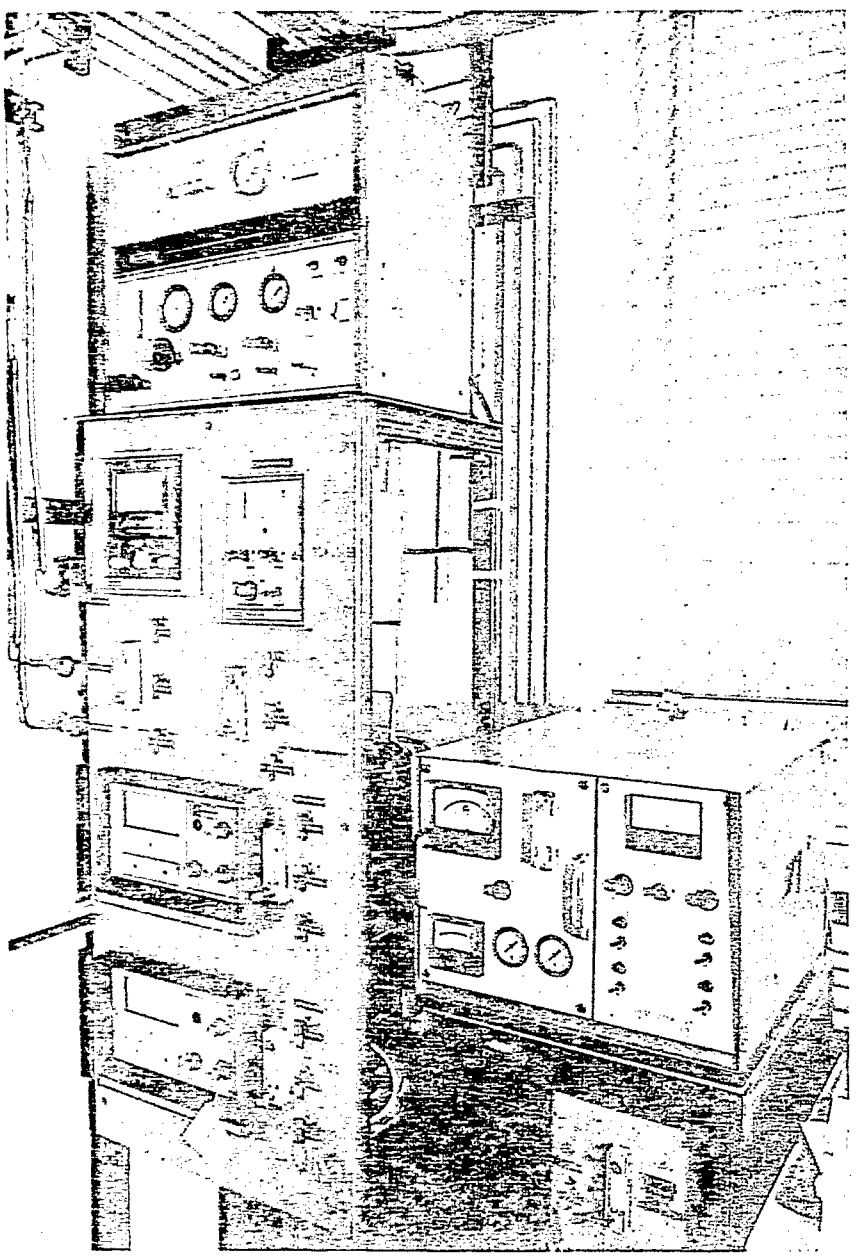

FIGURE 6: Gas Analysis System

The Teflon filters were not preconditioned to drive off moisture--it was experimentally found that this is not necessary. The glass-fiber filters were conditioned by overnight drying in an oven at 150°C followed by at least four hours in a desicator. The Teflon and dried glass-fiber filters were then pre-weighed and stored in the desicator until actual use. After soot collection the samples were kept in a desicator overnight to drive-off moisture remaining from the combustion gases which had passed through. Final weighing was then performed on a Metler H20 balance. In general, 10 standard liters of gas passed through each filter produced a collection of soot sufficient for weighing. A wet test meter was used to determine this total volume throughput which usually required less than ten minutes to accomplish.

Under many conditions it was evident that significant soot had deposited at the tip of the probe during sampling. In these cases the deposited soot was limited to a few mm of the probe tip and was removed with a fine wire to be included with the filters in the differential weighing procedure. Under lightly-sooting conditions the fraction of the total soot determination attributed to the deposit was a small fraction of that on the filters. However, at highly-sooting conditions, the deposit weight could be equivalent to the filter contribution.

The temperature within the reactor was determined with a platinum/platinum-13% rhodium thermocouple positioned such that the thermocouple bead was continuously exposed to the highly turbulent flow characteristic of the JSC at the entrance to one of the exhaust ports. This temperature has been tabulated in an uncorrected form in our data reduction procedure to be described below. Six other thermocouple measurements were made. One was to determine temperature deep within the refractory of the bottom reactor hemisphere with a platinum/platinum-13% rhodium thermocouple. Two chromel/alumel thermocouples determined the temperature of the outside steel shell of the bottom hemisphere. These three temperatures were then used to calculate heat loss through the lower-half of the JSR. A similar procedure was used for top-half heat loss; in this case, a chromel/alumel thermocouple embedded in the refractory and two chromel/alumel thermocouples to determine outside shell temperature were utilized.

A data reduction procedure was developed to accomplish calculation of gas phase species concentration, inside reactor temperature (from millivolt readings), reactor heat loss by conduction and radiation, and inside reactor temperature from gas analysis. Figure 7 presents a sample output of the data reduction program.

Calibration curves for each gas analysis instrument were incorporated into the program so that input would involve specification of instrument range and scale reading. Measurements were corrected to a "wet" basis with the knowledge that all species but hydrocarbons were made after water removal to a 10°C dew point. Since all carbon-containing exhaust products were determined, a carbon balance was performed to check the consistency between fuel-air ratios measured from air and fuel feed rates and that determined from exhaust concentrations of CO, CO_2, and hydrocarbons.

JET STIRRED REACTOR DATA OUTPUT

RUN NUMBER STPOSR138

No Soot

FUEL

TYPE	FEED RATE (GRAMS/MIN) MEASURED	FROM FLUE GAS ANALYSIS	PERCENT DIFFERENCE	HEATING VALUE (CAL/GRAMS)	TEMPERATURE (K)
TOLUENE	10.80	NOT APPLICABLE		9769.7	574.1

AIR

FLOW RATE (GRAMS/MIN) MEASURED	FROM FLUE GAS ANALYSIS	PERCENT DIFFERENCE	TEMPERATURE (K)
112.50	NOT APPLICABLE		574.1

FUEL AIR MIXTURE CONDITIONS

STIOCHIOMETRIC FUEL TO AIR RATIO	BASED ON MASS FEEDRATES FUEL TO AIR RATIO	EQUIVALENCE RATIO	BASED ON FLUE GAS ANALYSIS FUEL TO AIR RATIO	EQUIVALENCE RATIO
0.07	0.10	1.29	NOT APPLICABLE	

WET FLUE GAS ANALYSIS (MOLE PERCENT)

TOTAL GRAM MOLES/MIN	CO	CO2	O2	N2	NO	NOX	HC	H2	H2O
4.63	10.44	7.27	1.12	71.02	0.0	0.0	0.0300	2.33	7.78

HEAT BALANCE

ENERGY INPUT (CAL/HR) FUEL	AIR	NITROGEN	TOTAL	SENSIBLE HEAT RISE (CAL/HR)
6421130.0	485395.1	25499.0	6932024.0	4103178.0

HEAT LOSSES (CAL/HR)

CONDUCTIVE TOP HALF OF REACTOR	BOTTOM HALF OF REACTOR	RADIATIVE	TOTAL	PERCENT
93292.7	248098.4	147226.9	488618.0	7.0

TEMPERATURES (K)

T1	T2	T3	T4	T5	T6	T7
575.6	678.5	495.9	446.6	733.1	1669.5	1964.9

CALCULATED REACTOR TEMPERATURE	MEASURED REACTOR TEMPERATURE	PERCENT DIFFERENCE
2039.8	1964.9	3.8

NOTE A TEMPERATURE OF 0.0 INDICATES A VALUE WAS NOT RECORDED

In some cases of fuel rich operation the combustion product CO concentration exceeded the maximum range of the instrument, 10%. The data reduction program then performed a carbon balance to compute the CO concentration. In this situation it is not possible to compare feed-rate and exhaust-product-implied fuel-air ratios as described above.

Heat losses were then calculated. The temperatures determined from the six thermocouples within the reactor were utilized to determine conduction heat losses. Radiative losses through the twenty-five exhaust ports were determined in an iterative calculation involving the reactor temperature calculated via the thermochemical procedure described below and knowledge of the appropriate radiation view factor for the known exhaust port geometry.

Inside reactor temperature was calculated by an enthalpy balance between incoming total enthalpy, outgoing total enthalpy, conduction heat loss, and radiative heat loss. Note that since the radiative heat loss is a sensitive function of reactor temperature, the iterative calculation between this enthalpy balance and radiative heat loss was necessary. The enthalpy balance required knowledge of H_2 and H_2O concentrations. Since these concentrations were not measured, they could be determined only with the assumption that the combustion products are in partial equilibrium where the water-gas equilibrium relationship is obeyed. H_2 and H_2O concentration values on the output shown in Figure 7 embody this assumption. The calculated temperature produced in this manner was then compared with the directly measured value.

B. Results

During this first program year the JSC was used primarily to obtain data which could give an improved understanding of soot formation with alternate fuels. Hydrocarbons investigated during Phase I included normal, branch and cyclic paraffins, olefins, single and double ring aromatics, 2-component blends, and commercial Jet A. The key combustion parameters investigated were blowout and species concentration variation at lean operating conditions, incipient soot mixture conditions, gaseous species variation at rich operating conditions, and soot production at rich operating conditions. A particularly important consideration in developing our plan was the intent to use the information to evaluate whether existing quasi-global models predict the important effects observed. The following presentation of program status reflects this orientation--experimental results and interpretations will be discussed immediately below, followed by Section III which describes the analytical treatment of this information.

1. Combustion at Lean Operating Conditions

Initial experimentation was conducted using ethylene as the fuel. Lean blowout limits as a function of total mass flow and inlet temperature were acquired. The trends observed are in agreement with expectations that lean blowout equivalence ratio should increase as reactor

mass flow is increased. Figure 8 illustrates data obtained with a 3.81 cm diameter JSC where an ethylene-air mixture at an inlet temperature of 240°C was investigated. Our experience in obtaining lean blowout data has been that the actual blowout point is difficult to determine--the thermal inertia of the reactor can allow combustion to occur sporatically below the minimum equivalence ratio value at which steady-state combustion can be maintained. Because of this, data taking is tedious and the results indicate much scatter.

More valuable information for lean operating conditions involves the gas-phase species behavior as fuel-air ratio is varied. It has been found that hydrocarbons are only present near the lean blowout limit. This implies that hydrocarbon pyrolysis and partial oxidation (to CO and H_2) is the dominant process influencing extinction and that blowout data can be valuable in evaluation of quasi-global kinetic characterizations of these processes. Carbon monoxide increases as the fuel-air ratio is lowered to approach the lean blowout point and also increases at the highest fuel-air ratios. Consequently, a minimum value is observed (see Figure 9). Similar results were obtained for iso-octane and toluene. As will be discussed in Section III, these results are of value in developing quasi-global models of combustion chemistry. In particular, global chemical kinetic rates for CO oxidation can be determined using these data.

The results presented in Figure 9 also imply that surface effects are not important to the overall global kinetics of heat releasing reactions in the JSR. This inference is reached by considering the data for two different diameter reactors. In the absence of surface effects and in the case where heat loss is similar, two reactors should behave identically when reactor volumetric loading is constant. That is:

$$\text{Constant} = \frac{\dot{m}}{V} = \frac{3\ \dot{m}}{\pi\ d^3}$$

where $\dot{m}$ is total reactor mass flow, V is reactor volume, and d is reactor diameter. The differences in heat loss between the two reactors are thought to be insignificant (<5% of total heat release) for these data. Note that a 5% difference in temperature would correspond to a very small horizontal shifting (fuel air ratio compensation) in Figure 9.

Using the above relationship the 5.08 cm reactor with an air flow of 112.5 gm air/min should behave as a 3.81 cm reactor with an air flow of $112.5\ (3.81/5.08)^3 = 47.5$ gm/min. As indicated in Figure 8 the results are in reasonable agreement with this behavior; the data for the 5.08 cm reactor falls slightly below that for 67 gm air/min in the smaller reactor. Naturally, it would have been better to conduct the tests at exactly analgous flow rates, but even in this case the complicating factor of heat loss might cause some small disagreement in results. Indeed, the best check on the consistency between reactor sizes would be testing at the correct flow rates and determining reactor temperature so that CO mole percent may be plotted against reactor temperature. Coincidence of the data on this basis would provide conclusive evidence of the absence of surface effects.

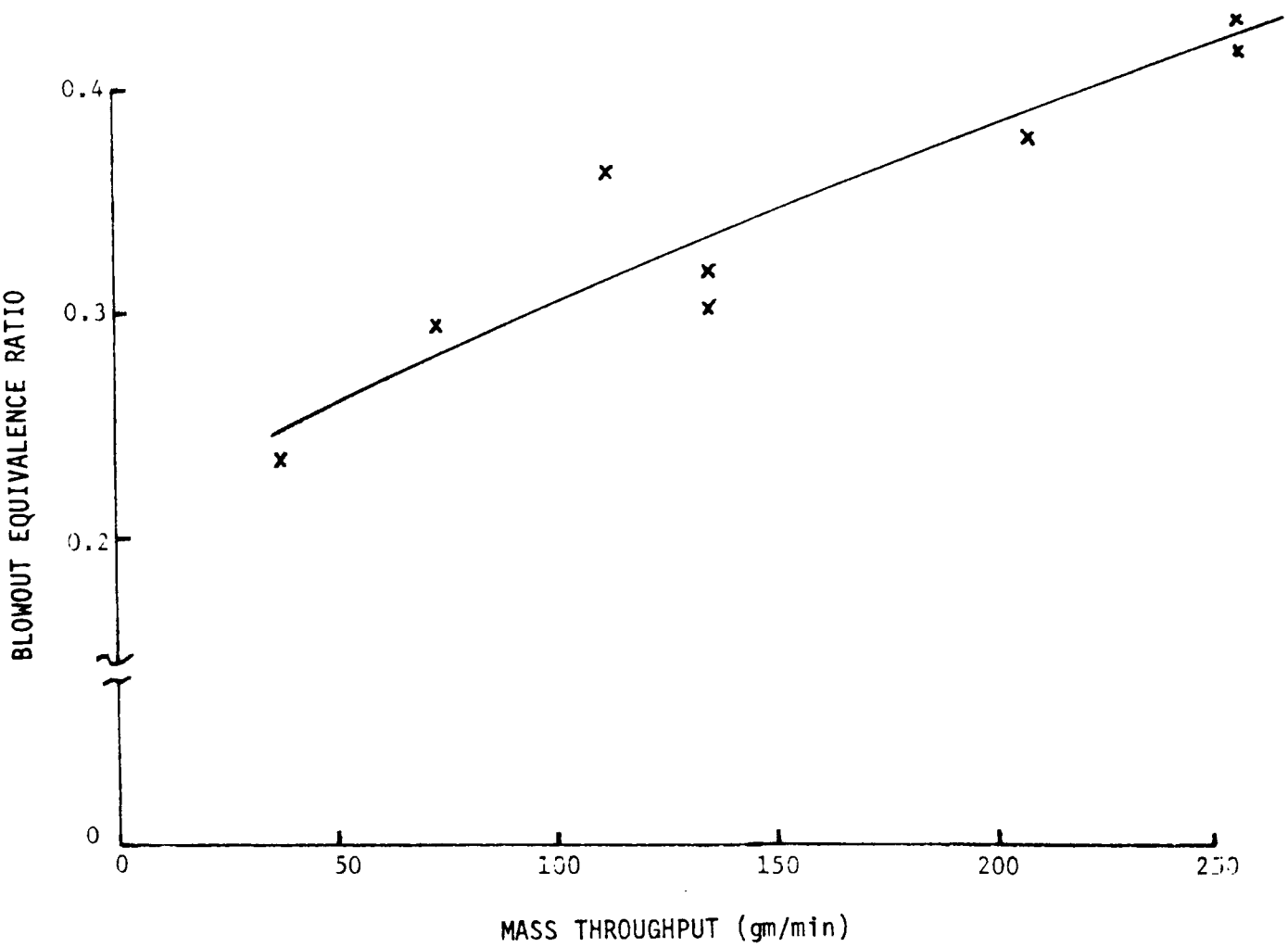

FIGURE 8: Dependence of Lean Blowout Equivalence Ratio on Mass Throughput for Ethylene-Air Combustion with an Initial Temperature of 240°C

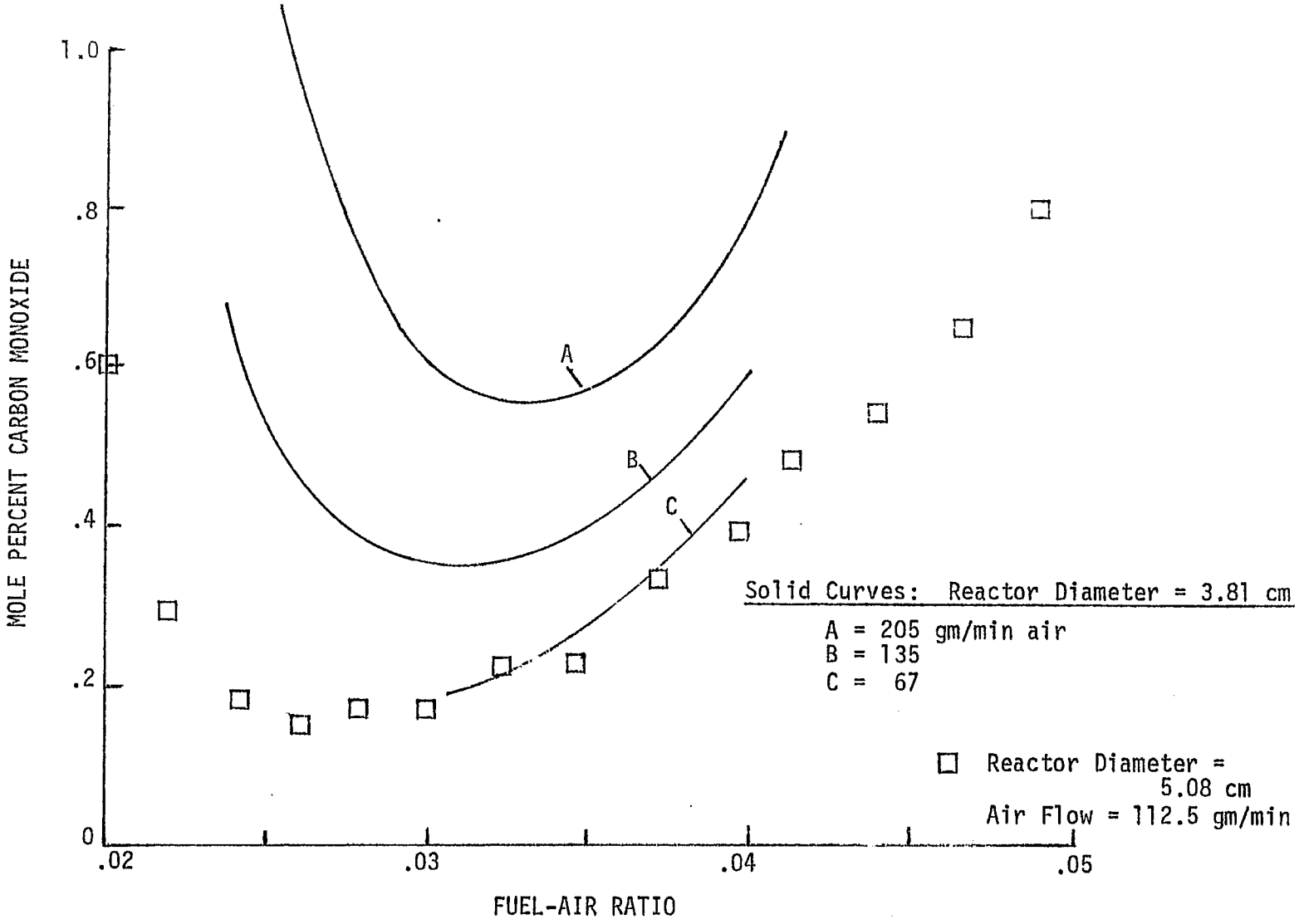

FIGURE 9: Carbon Monoxide in Exhaust Products for Lean Ethylene-Air Combustion at an Inlet Temperature of 300°C

2. Fuel Rich Operation with Ethylene

Ethylene was the first fuel studied under fuel-rich conditions at which soot may form. However, the amount of soot produced with ethylene is very small and no measurements of soot production were made. Experimental observations are limited to the incipient soot mixture ratio and the gas species concentrations in the neighborhood of the incipient soot limit.

The dependence of the incipient soot formation limit on reactor inlet mixture flow rate and inlet temperature was determined. Figure 10 illustrates the dependence of the incipient soot formation limit on inlet mass flow rate for ethylene-air combustion at an inlet temperature of 25°C. The flow rate effect appears to be significant with soot limit equivalence ratio increasing from 1.85 to 2.25 over the flow range tested (70-160 gm air/min). This is an interesting observation in that at the lower flow rate conditions the equivalence ratio for incipient soot approaches the accepted premixed laminar flame value of 1.8. It can be postulated that residence time effects--the effect of reduced burnedness as JSR loading is increased--are important to ethylene's soot formation process in the well mixed situation.

Data presented in Table 1 indicate that the temperature effect on the incipient soot limit is not measurable over the range of ethylene air combustion conditions investigated (25-300°C). Wright (5,6) reported a continuous increase in incipient soot equivalence ratio with increasing temperature in a JSC experiment but considered a broader range of temperatures and identified the critical O/C by observing flame color. It has been our observation that ethylene is a difficult fuel to study in soot formation investigations. Compared with toluene, for example, very small amounts of soot are formed.

A notable temperature effect observed during this testing was that the darkness of the filter observed at the lowest sooting equivalence ratio increased with mixture inlet temperature. At 25°C the darkness of the soot deposit was very slight with increasing darkness as temperature was elevated. Another observation was that beyond the soot limit equivalence ratio the soot deposit on the filter became darker and then lighter as the blowout mixture ratio was approached.

Gas species at the incipient limit were determined for ethylene-air mixtures at 25°C and a number of air mass flows. Figure 11 illustrates typical results for the incipient soot limit behavior of ethylene air mixtures at an air flow rate of 160 gm/min at 25°C. CO was the major carbon-containing species and remained at a concentration of about twelve mole percent for all equivalence ratios tested. Total hydrocarbons increased significantly with equivalence ratio but CO_2 decreased. Oxygen concentration was very low at an equivalence ratio of 1.77 but steadily increased at higher equivalence ratios--an indication of poor reactedness as the mixture was further enriched.

As mentioned in Section IIA, the concentrations of H_2 and H_2O as well as the reactor temperature were calculated from these data. These results are shown in Figure 12. Temperature varies from about 1900 to

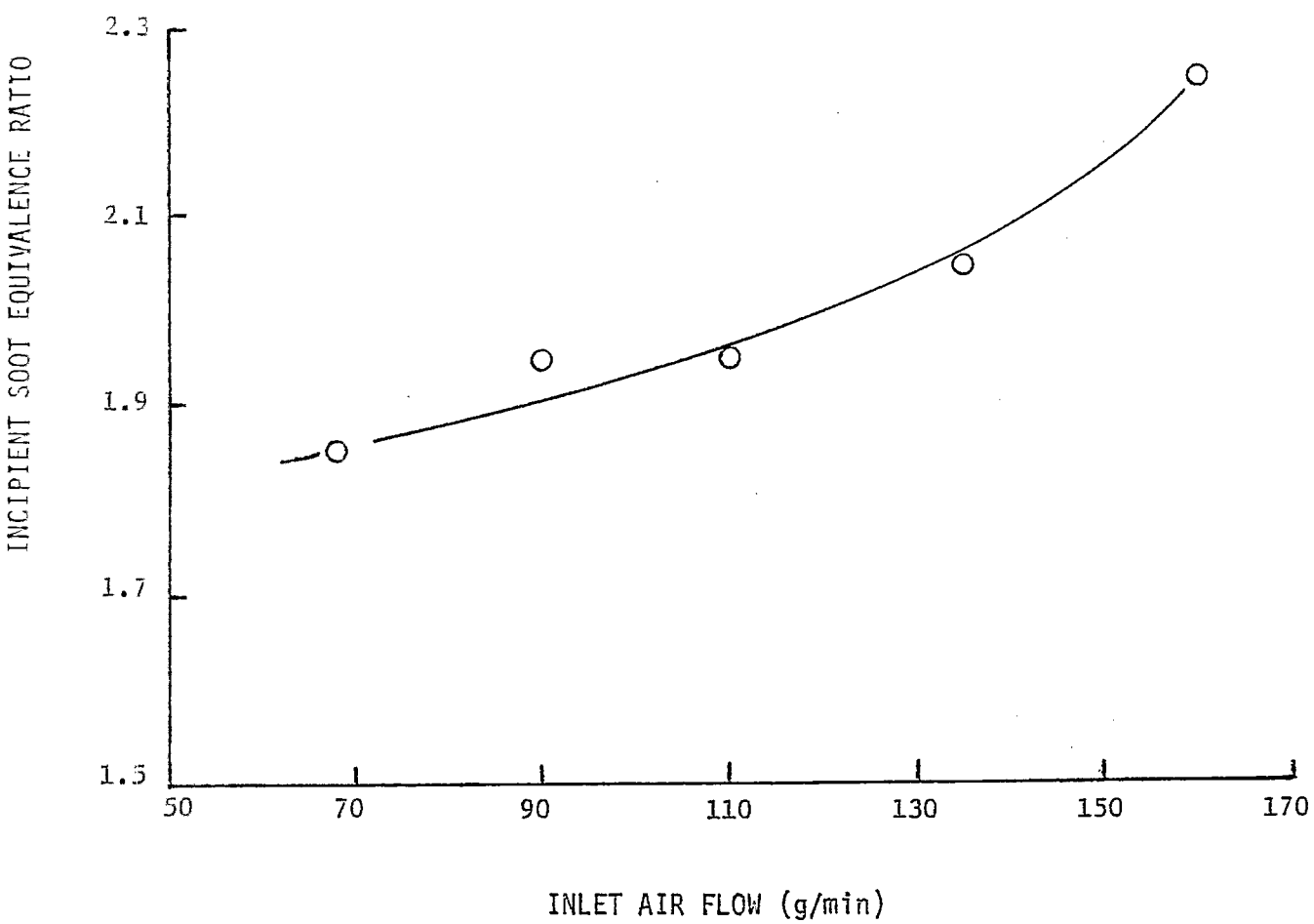

FIGURE 10: Incipient Soot Limit Equivalence Ratio Dependence on Mass Flow for Ethylene-Air Combustion (Inlet Temperature = 25°C)

TABLE 1

Incipient Soot Limit Dependence on Inlet Temperature for Ethylene-Air Combustion

($\dot{m}_{air}$ = 110 g/min)

Temp.	ϕ	% HC
25°C	1.95	5.0
100°C	1.85	3.2
200°C	1.95	4.3
300°C	1.95	3.4

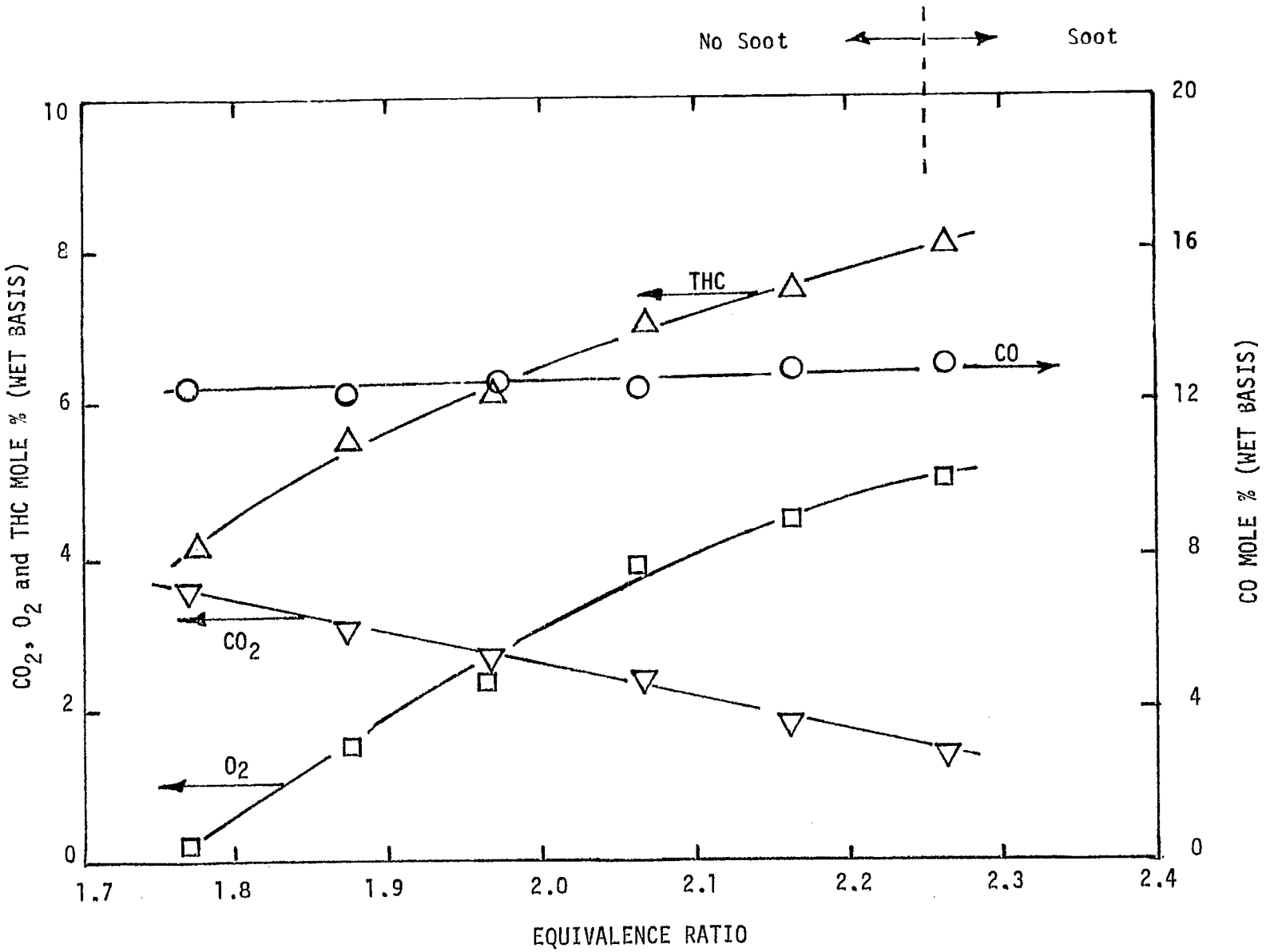

FIGURE 11: Measured Combustion Product Concentrations for Rich Ethylene-Air Combustion (Air Flow = 160 gm/min, Inlet Temperature = 25°C)

EQUIVALENCE RATIO

FIGURE 12: Calculated H_2 and H_2O Concentrations and Reactor Temperature for Rich Ethylene Air Combustion (Air Flow = 160 gm/min, Inlet Temperature = 25°C).

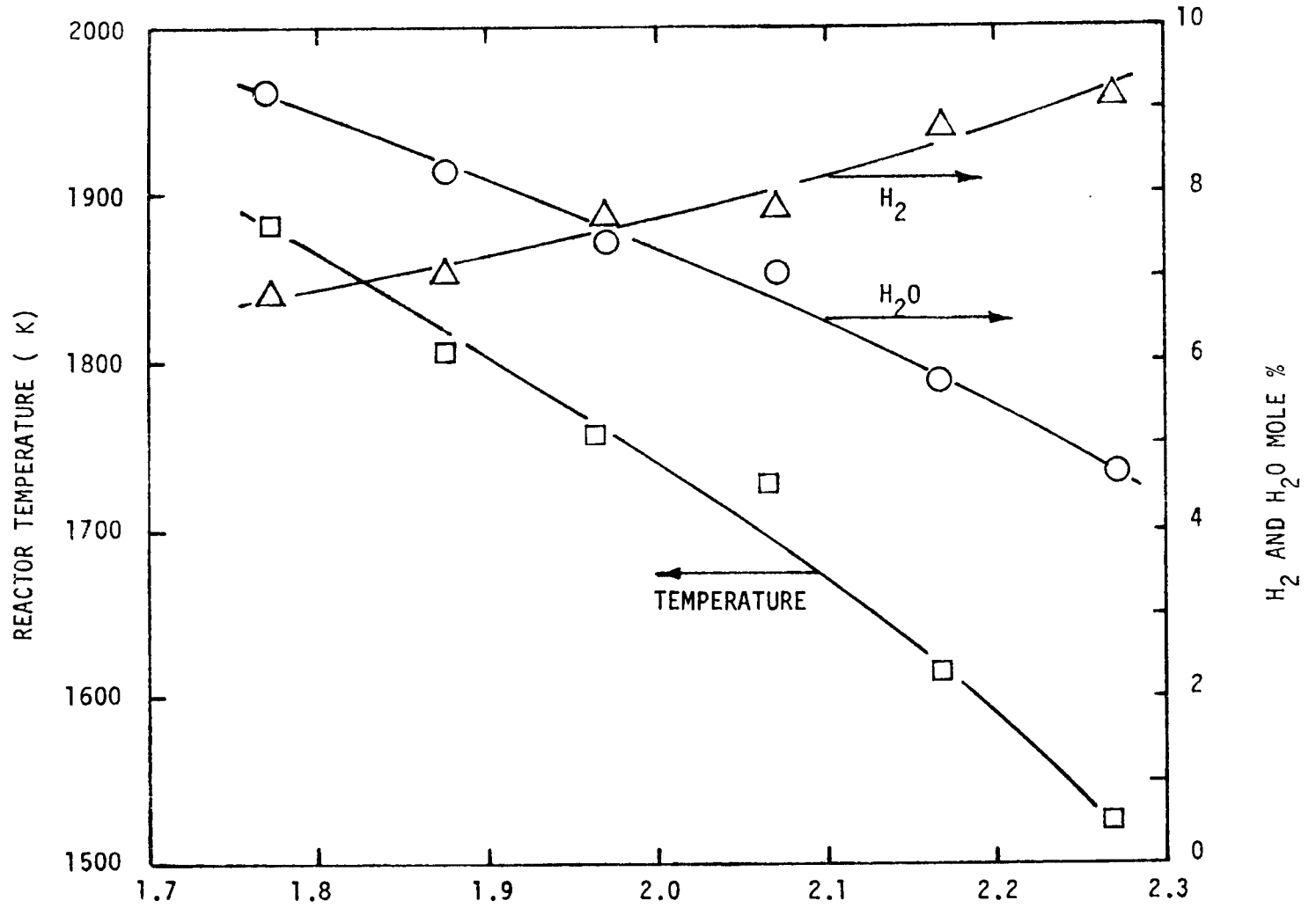

1520 K over the 1.77 to 2.27 range of equivalence ratio studied. Unfortunately, temperature was not measured directly during these experiments and a calculated/experimental comparison cannot be made. Parallel data is available for fuels other than ethylene and these will be discussed later. Calculated hydrogen concentration increases with equivalence ratio to about 9.6 mole percent at $\phi = 2.27$. H_2O decreases from about 9.2 at $\phi = 1.77$ to 4.7 mole percent.

Finally, it is of interest to examine the fraction of fuel carbon which is converted to each carbon-containing exhaust product, CO, CO_2 or THC. Figure 13 illustrates the portions of fuel carbon converted to CO, CO_2, and total hydrocarbons for these same conditions of ethylene air combustion. As indicated, CO is by far the predominant species. It is important to note that THC concentrations are very significant at and even below the incipient soot formation limit in the case of C_2H_4 combustion--a sharp contrast to this behavior will be described below for toluene-air combustion.

3. Toluene Sooting Characteristics

The incipient soot limit behavior of toluene was determined as a function of inlet mass flow and inlet mixture temperature (at 200, 250, and 300°C). No distinct relationship between the incipient soot limit and these parameters was uncovered. Using the same technique used in evaluating C_2H_4--leanest operation at which a soiled filter was observed--the limit was consistently found to be 1.35.

Gas phase species concentrations at and beyond the incipient soot limit were obtained and are presented in Figure 14. These data were obtained at an inlet temperature of 300°C with an inlet air flow rate of 112.5 gm/min. The plot illustrates typical gas phase behavior by displaying the portions of fuel carbon converted to CO, CO_2, and total hydrocarbons. These data have a lower bound on equivalence ratio of 1.29 because at ϕ below this value, reactor temperature exceeds refractory material limitations (about 2033°K). As with ethylene, CO is the predominant specie. However, a substantial difference between these data and C_2H_4 results was observed. Whereas with toluene incipient soot occurs as hydrocarbons begin to "break thru" under rich operating conditions, ethylene's soot limit occurs at conditions where hydrocarbon concentration is high (a factor of 36 times that for toluene).

Typical results for toluene soot production are shown in Figure 15. These data correspond to operation at air mass flows of 50, 80, and 112.5 gm/min and at an inlet mixture temperature of 300°C. Note that while the incipient soot limit was not significantly affected by mass flow, soot production was substantially less at the lower air mass flow condition. The results of Figure 15 also indicate that soot production increases very significantly as the mixture equivalence ratio increases. However, translation of the data to fraction of fuel carbon or soot indicates that, even at the worst condition, less than 1% of the fuel carbon is converted to soot.

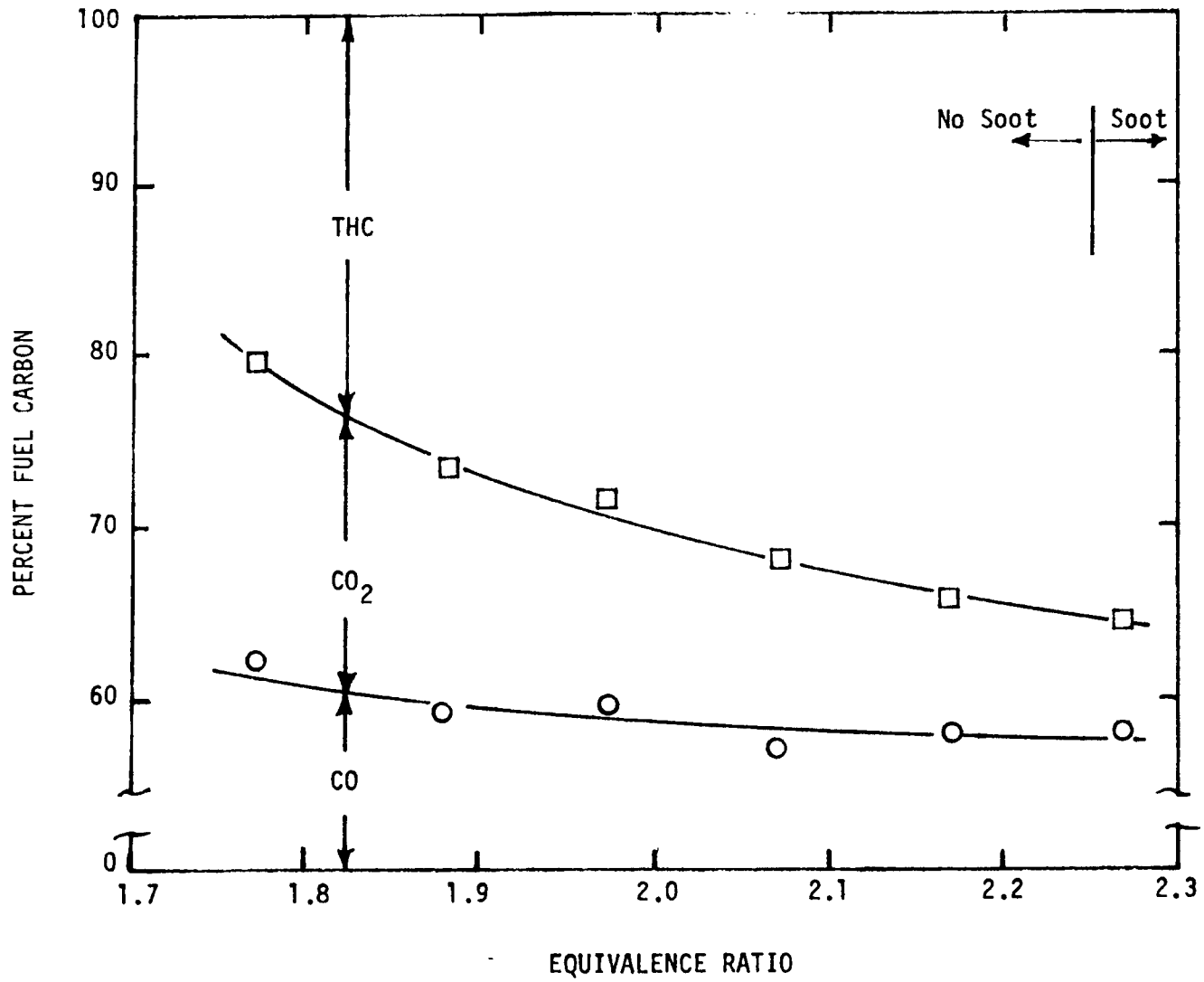

FIGURE 13: Fraction of Fuel Carbon Converted to Each Exhaust Product For Ethylene-Air Combustion (Data from Figure 11).

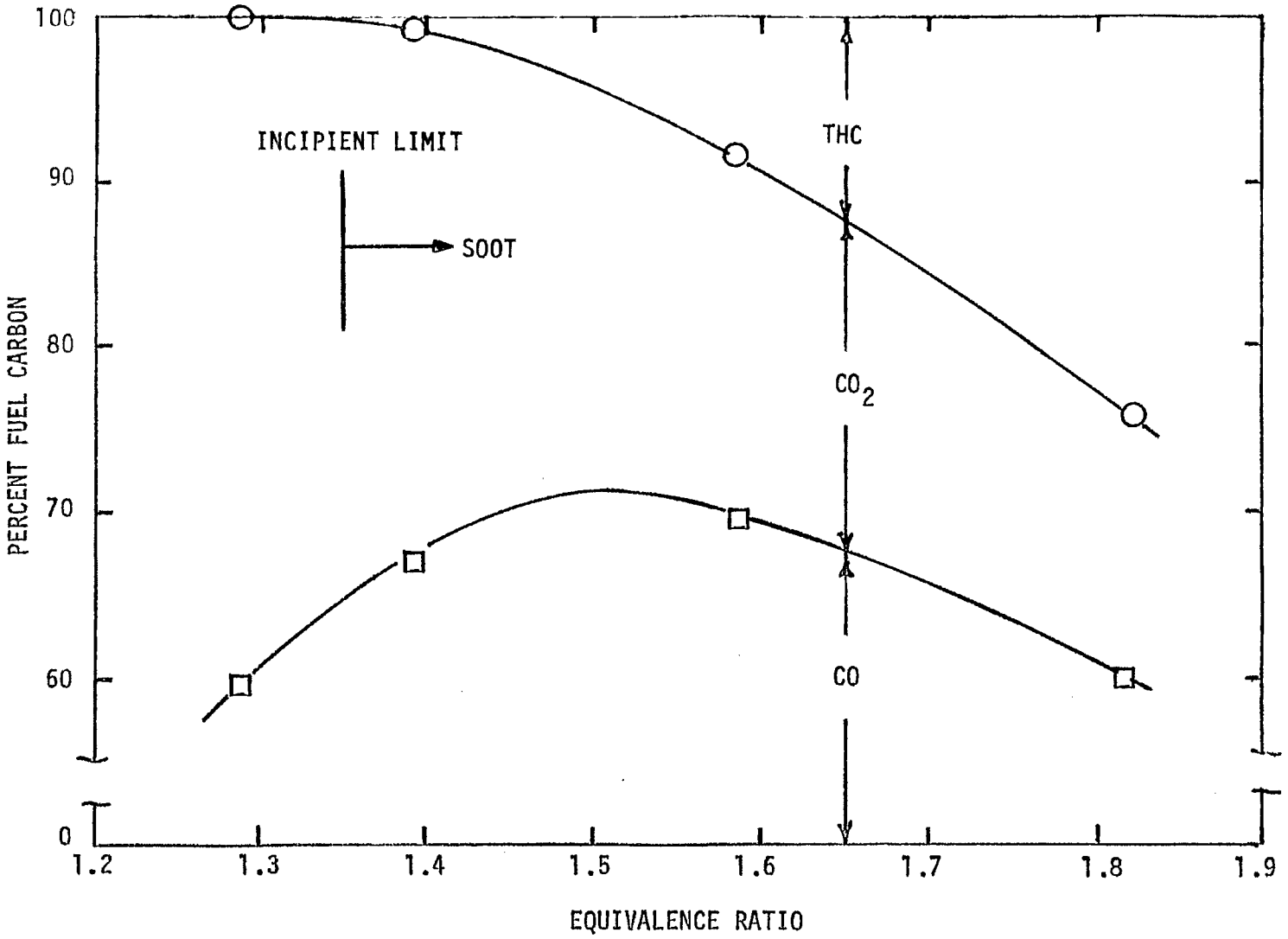

FIGURE 14: Fraction of Fuel Carbon Converted to Each Exhaust Product for Toluene-Air Combustion (Air Mass Flow = 112.5 gm/min, Inlet Temperature = 300°C).

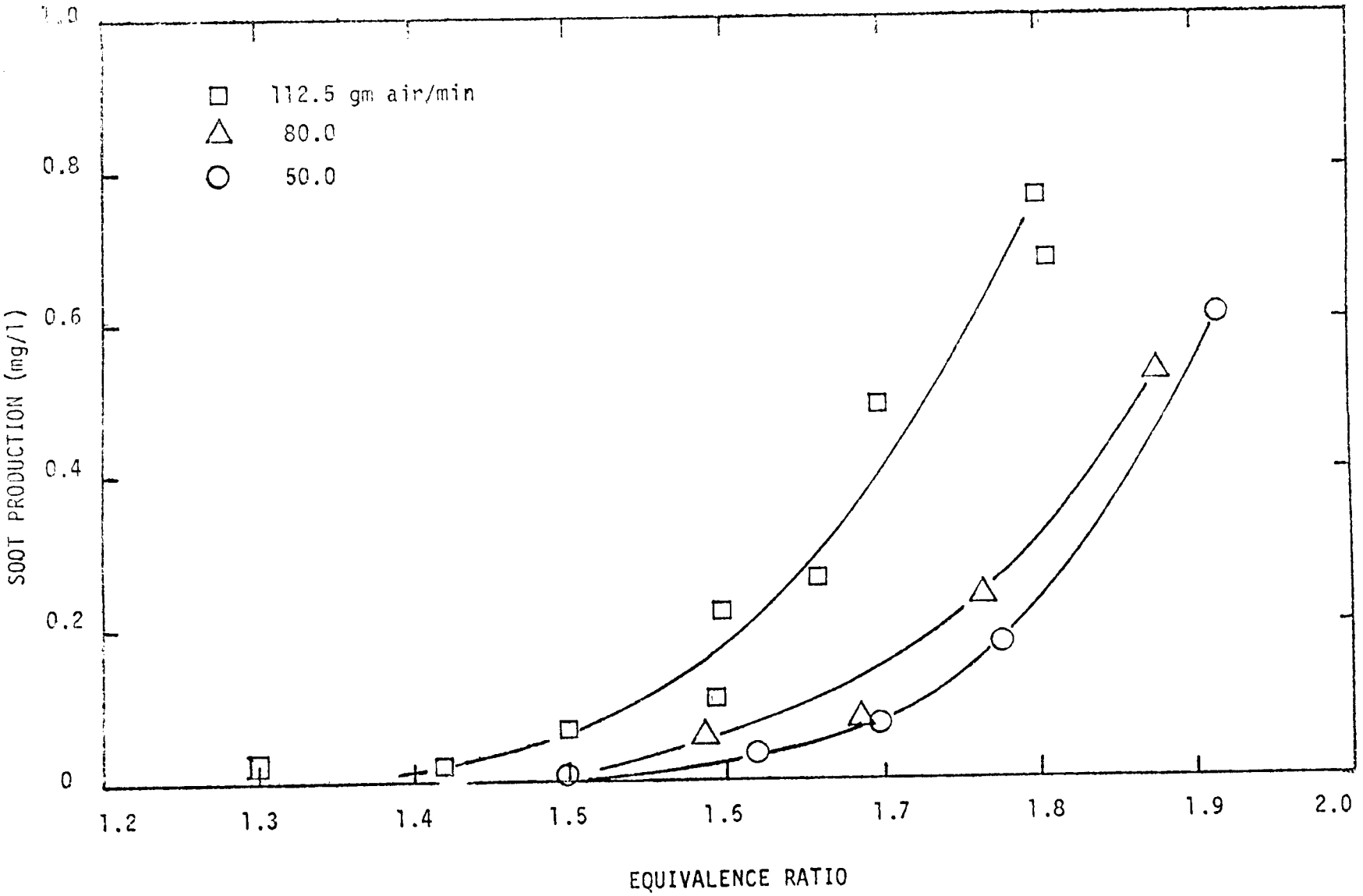

FIGURE 15: Dependence of Toluene Soot Production on Mass Loading (Inlet Temperature = 300°C)

Figure 16 illustrates the dependence of soot production on mixture inlet temperature for toluene-air mixtures. As has been noted previously, the incipient soot limit was not substantially influenced by inlet temperature. However, these data illustrate that mixture inlet temperature (and flame temperature) increases result in greater soot production at the higher equivalence ratios.

These results for toluene indicate a number of potentially important differences between the soot formation processes of ethylene and toluene:

a) Toluene soots at a much lower equivalence ratio (1.35) than ethylene (1.95) and the amount of soot formed with ϕ beyond the incipient limit is much larger.

b) The incipient soot limit for ethylene was found to vary with mass flow, but this was not the case for toluene.

c) In the case of C_2H_4 combustion, significant amounts of hydrocarbons ($\sim$3-8% as CH_4) were present at equivalence ratios leaner than the soot limit but with toluene the incipient soot limit corresponded approximately to the equivalence ratio for the initial presence of hydrocarbons in the combustion products.

4. Sooting Characteristics of Other Hydrocarbon Types

The observations described above indicate a fundamental difference in the soot formation mechanisms for C_2H_4 and $C_6H_5CH_3$ under the strongly backmixed conditions of the Jet Stirred Combustor. The promise of our originally-proposed approach--quasi-global characterization of soot formation characteristics based on hydrocarbon type--is supported by these findings. In order to further develop this concept it was necessary to screen a large number of other fuel types to determine whether they behave like C_2H_4, $C_6H_5CH_3$ or have soot formation characteristics distinctly different than C_2H_4 or $C_6H_5CH_3$.

Results are summarized in Table 2. Air flow was set at 112.5 gm/min and the fuel-air mixture entered the reactor at 300°C for these tests. The first column lists the fuels tested. They are grouped into alkanes and alkenes, single-ring aromatics, and double-ring compounds. Incipient soot formation limit values of equivalence ratio, hydrocarbon concentration, and measured reaction temperature have been listed in the second column. In cases where rich blowout was achieved without observation of sooting, the values for the richest condition prior to blowout are recorded. One fuel, n-octane, could not be tested under fuel-rich conditions as the reactor temperatures achievable prior to blowout exceeded the reactor material limitations.

Table 2 illustrates that the alkanes and alkenes tested behave like ethylene--significant concentrations of hydrocarbons (>1%) are present at fuel rich conditions without soot formation. All of the single ring

FIGURE 16: Effect of Inlet Temperature on Soot Production of Toluene

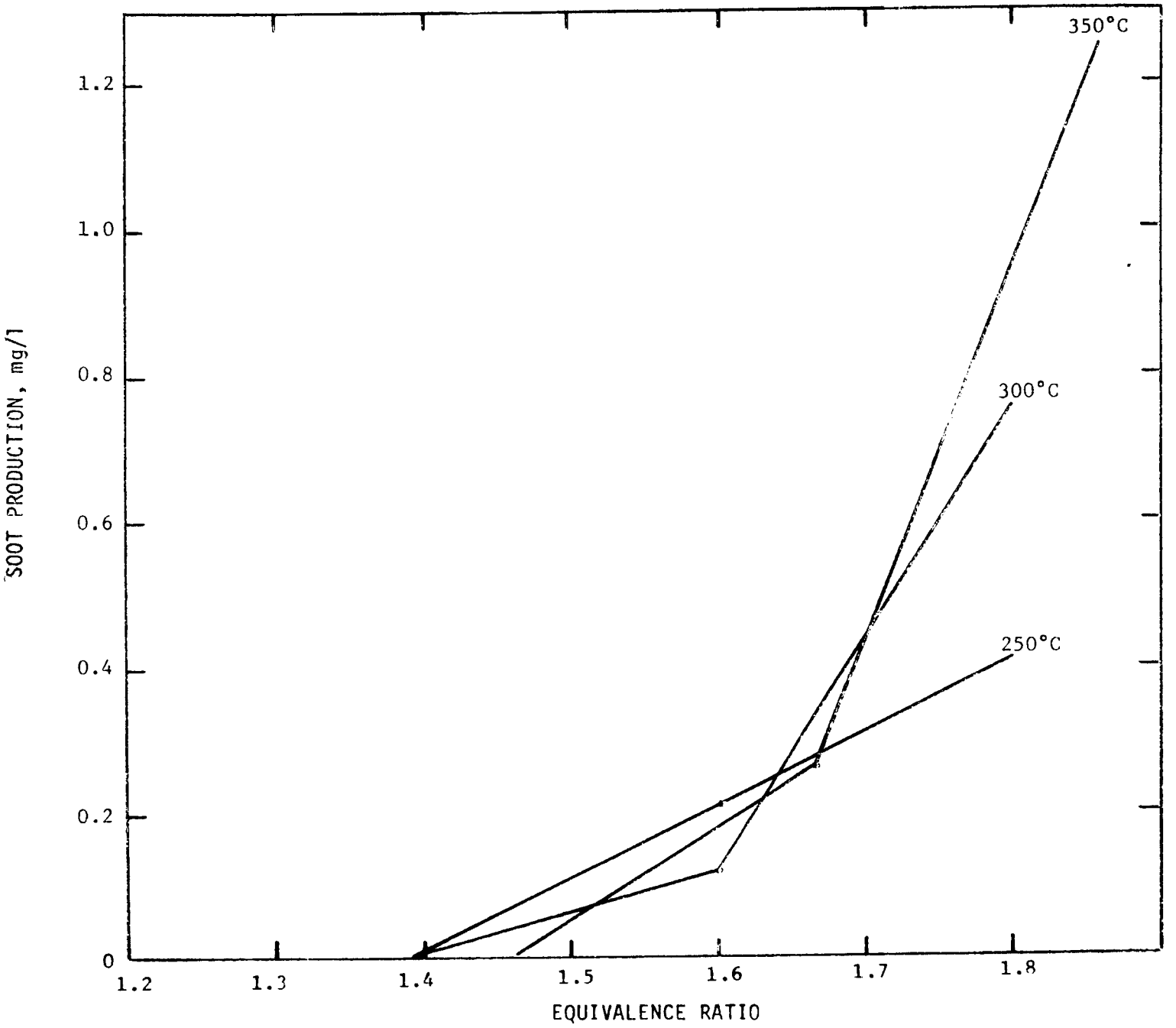

TABLE 2

Pure Fuels Screening Results

Fuel	Incipient Soot Limit (1)			S_T (2) @ ISL + 0.2φ		S_T @ ISL + 0.4φ	
	φ	% HC	Measured Temperature (K)	mg/l	% HC	mg/l	% HC
Ethylene	2.0	3.4	1550	(5)			
Hexane	1.61(3)	9.25	1478				
Cyclo-hexane	1.70(3)	8.88	1426				
N-octane	(4)	(4)	-				
Iso-octane	1.70(3)	7.5	1546				
1-Octene	1.89(3)	8.5	1530				
Cyclo-octene	1.70(3)	7.8	1615				
Toluence	1.39	0.20	1951	0.118	1.72	0.765	5.88
O-xylene	1.31	0.37	1889	0.152	5.88	(5)	
M-xylene	1.30	0.52	1846	0.189	3.88	(5)	9.0
P-xylene	1.30	0.62	1858	0.166	4.62	(5)	
Cumene	1.40	0.65	1855	0.178	3.62	0.455	7.38
Decalin	1.61(3)	7.25	1510				
Tetralin	1.31	0.62	1836	0.356	4.75	(5)	(5)
1-Methylnaphthalene	1.21	0.39	1905	0.926	2.5	(6)	(6)
Dicyclopentadiene	1.39	0.78	1890	0.255	3.62	1.485	7.62

(1) For screening purposes. Incipient soot limit (ISL) is condition at which soot was first noticed on a clean filter.
(2) S_T = Total soot combination of soot on filter and in probe.
(3) Does not soot--highest equivalence ratio value obtained prior to blowout.
(4) Too hot to burn.
(5) Rich blowout occured before condition could be reached.
(6) Soot concentration very high; probe plugged before data could be taken.

aromatics tested were found to produce soot with incipient soot limit equivalence ratios ranging from 1.3 to 1.4 Reactor temperature at the soot limit ranged from 1800-1950 K. As with toluene, the soot limit occurs at an equivalence ratio when small amounts of hydrocarbons begin to appear in the exhaust. Not all of the double-ring compounds produced soot. Decalin, a completely saturated double-ring compound, did not soot and behaved like the alkanes/alkenes in terms of exhaust hydrocarbon concentration. Tetralin, 1-methyl-napthalene, and dicyclopentadiene did produce soot at equivalence ratios ranging from 1.21 to 1.39.

The final two columns in Table 2 illustrate soot production at equivalence ratios above the incipient limit. These same results have been illustrated in Figure 17. One striking feature of these results is the similarity in the initial slope of the plots for all of the unsaturated ring compounds. When the equivalence ratio is increased further, however, the soot production of these hydrocarbons varies substantially.

As will be discussed in Section IIC, it is believed that the data at higher equivalence ratios for each hydrocarbon are unreliable as the Jet Stirred Combustor is operating very near rich blowout with some hydrocarbon passing through entirely unignited at times (sporatic operation is observed at the richest operating conditions). Consequently, the reactor may be behaving partially as a high temperature pyrolysis device or coker during operation at the very highest equivalence ratios. Very high THC concentrations at these equivalence ratios lends support to this explanation.

The behavior of 1-methyl-napthalene cannot be rationalized in this manner. It produces large amounts of soot at relatively low equivalence ratios and the reactor temperature is much higher than encountered at rich blowout of the other hydrocarbons in Figure 17. Further, THC at these high sooting conditions was lower than that of the others implying that 1-methyl-napthalene is an especially strong soot producing hydrocarbon.

In summary, it was found that all hydrocarbons tested might be grouped into three categories as follows:

Like C_2H_4	Like $C_6H_5CH_3$	Unlike C_2H_4 or $C_6H_5CH_3$
Hexane	O-xylene	1-methyl-napthalene
Cyclo-hexane	M-xylene	
N-octane	P-xylene	
Iso-octane	Cumene	
1-octene	Tetralin	
Cyclo-octane	Dicyclopentadiene	
Decalin		

The first group produced large amounts of exhaust hydrocarbons without sooting as did ethylene and in no case was significant soot observed. The second group produced soot at the mixture ratio which corresponded to hydrocarbon breakthrough. In all cases the measured hydrocarbon composition was less than one percent at the incipient limit. Another commonality in the second group is that the amount of soot produced as equivalence ratio was increased beyond the incipient limit was similar (within a factor of two) for all the hydrocarbons. 1-methyl napthalene was significantly different in this respect producing much higher soot quantities than those in the second category.

FIGURE 17: Soot Production for Various Pure Hydrocarbons at 300 C Inlet Temperature and 112.5 gms/min Air Flow

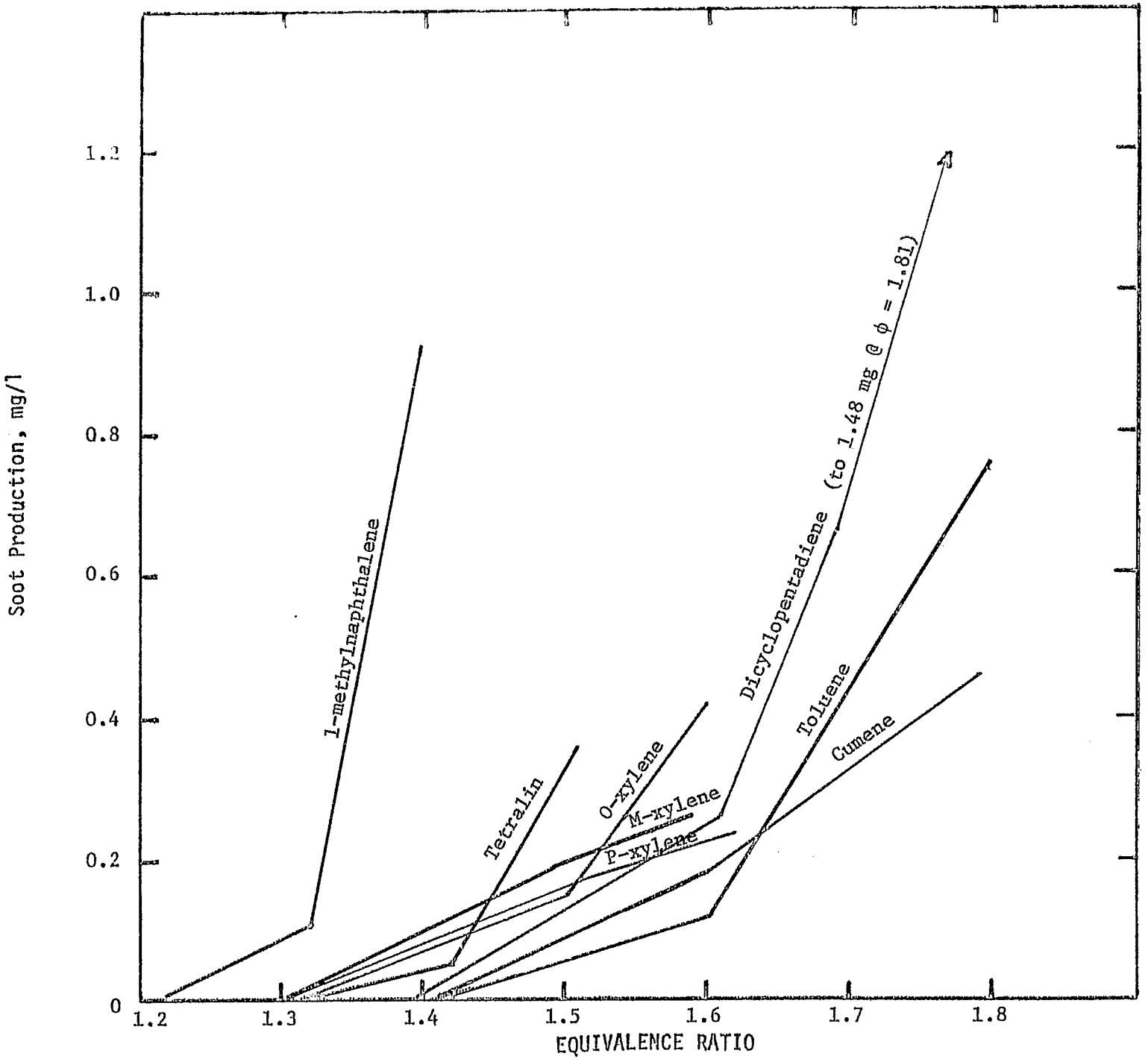

5. Sooting Characteristics of Fuel Blends

Blends of toluene and iso-octane were tested to determine the behavior of a two-component mixture with like-C_2H_4 and like-$C_6H_5CH_3$ hydrocarbons. These results are shown in Figure 18 and Table 3. Mixtures with 50 or more percent toluene produced soot while a 25% toluene blend did not. Clearly, for the mixtures which did soot, increases in the volume percent toluene result in increased soot production at all equivalence ratios. It was also determined that with less toluene in the blend, the concentration of hydrocarbons at the incipient limit tended to increase. For example, with 50% toluene, the hydrocarbon concentration was 2.4%, while with 100% toluene this value was 0.20%. These results imply that a combination of the analytical descriptions for toluene and iso-octane might be a reasonable approach for prediction of the sooting characteristics of fuel blends.

A commercial aviation turbine fuel, Jet A, was also tested. This fuel produced soot, but in amounts less than the 50% toluene/50% iso-octane blend discussed above. Further, the incipient soot limit equivalence ratio was found to be greater than that of the 50% blend (ϕ = 1.7 vs. 1.5). These results are consistent with the previous observations in that the Jet A has a hydrogen content of about 13.9%, midway between the 50% toluene blend (11.9%) and the 25% toluene blend (14.6%) which did not soot.

Attempts to test two coal liquids were made. These were both COED samples supplied by FMC of Princeton, New Jersey. The first was produced from Utah coal while the second utilized a Western Kentucky coal. Both tests failed as these fuels were found to plug the atomizing nozzle utilized in the fuel prevaporizer. The 0.008 inch diameter fuel orifice became plugged with a gum-like substance which prevented fuel flow.

C. Discussion

The effort conducted in the first year of this program was intended to examine experimental procedures for studying alternate fuel combustion characteristics. It has been a very productive year in which new insights into soot formation have been developed with application of the Jet Stirred Combustor. Nevertheless, there are limitations to the current information which require that much additional work be performed.

A significant drawback to the current results is that the flame ionization detector measures only total hydrocarbons. Understanding of the soot formation mechanism and construction of quasi-global models would require more detailed information where the types of hydrocarbons present are identified. A second experimental difficulty deals with the accuracy of the soot production results. Repeat tests which were performed allowed repeatability to be assessed--up to the moderately sooting conditions (about 0.4 mg/ℓ) data were repeatable to better than 20% but at heavier sooting conditions repeatability was not this good. As will be discussed below, it is believed that many of the heavily sooting conditions were actually beyond the rich blowout condition where sporatic operation resulted in rather undefined reactor conditions.

TABLE 3

Fuel Blend Screening Results

Fuel	Incipient Soot Limit (1)		S_T (2) @ ISL + 0.2ϕ		S_T @ ISL + 0.4ϕ	
	ϕ	% HC	mg/l	% HC	mg/l	% HC
100% Toluene	1.39	0.20	0.118	1.72	0.765	5.88
87.5% Toluene/12.5% Iso-octane	1.41	0.15	.160	2.2	0.63	5.25
75% Toluene/25% Iso-octane	1.40	1.21	.122	4.88	(4)	
62.5% Toluene/37.5% Iso-octane	1.49	0.82	.165	3.85	(4)	
50% Toluene/50% Iso-octane	1.50	2.4	.060	6.75	(4)	
25% Toluene/75% Iso-octane	1.61(3)	7.12				
10% Toluene/90% Iso-octane	1.51(3)	6.25				

(1) For screening purposes. Incipient soot limit (ISL) is condition at which soot was first noticed on a clean filter.
(2) S_T = Total soot combination of soot on filter and in probe.
(3) Does not soot--highest equivalence ratio value obtained prior to blowout.
(4) Rich blowout occured before condition could be reached.

FIGURE 18: Soot Production vs. Equivalence Ratio for Toluene and Toluene/Iso-Octane Blends at 300°C Inlet Temperature & 112.5 gms/min Air Flow

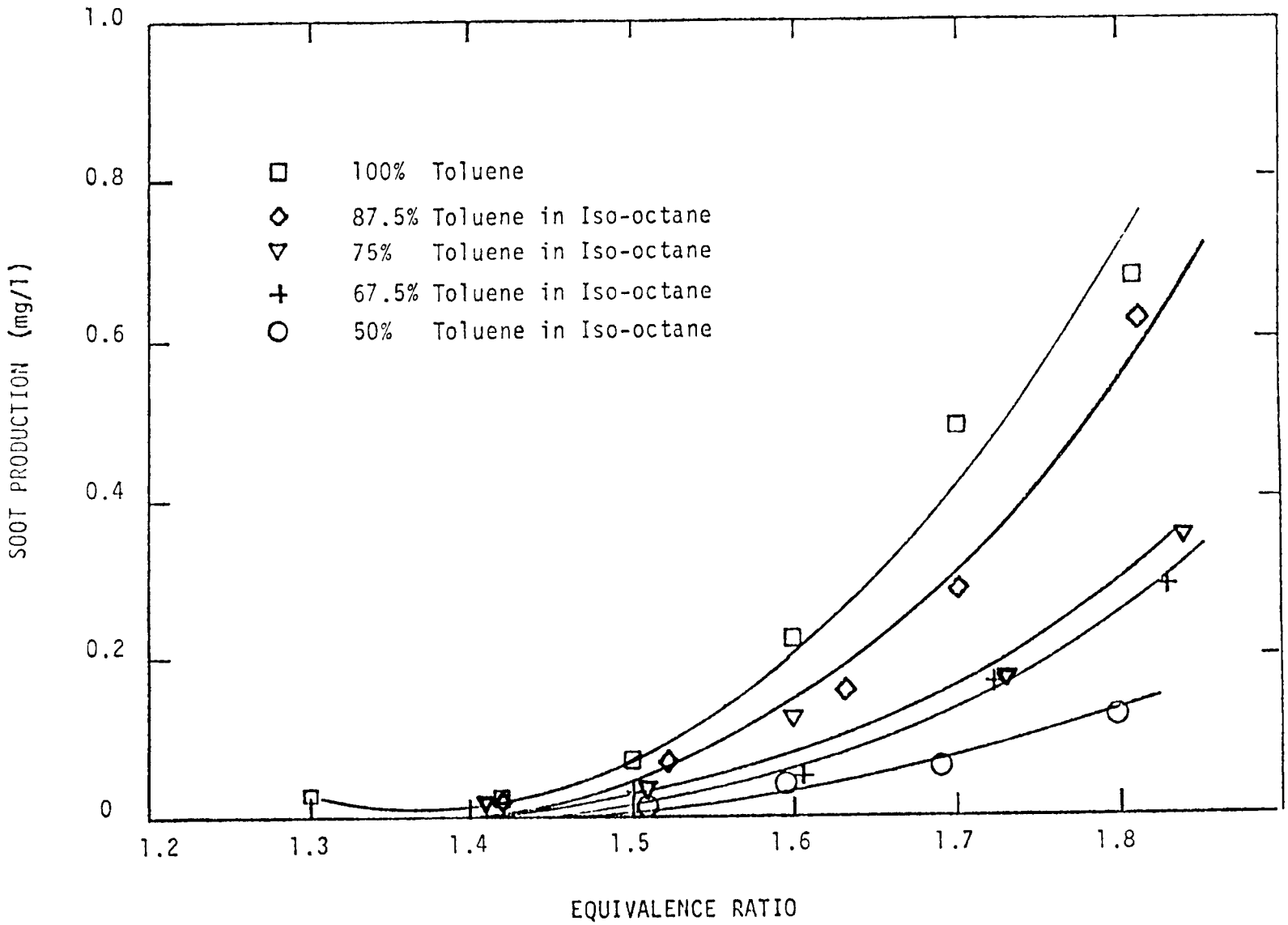

A final problem with the current results is that results were obtained at reactor temperatures which correspond to input values of equivalence ratio and inlet temperature; no attempt was made to study soot formation at constant ϕ variable T or constant T variable ϕ. This type of information will be necessary for the construction of quasi-global models of soot formation. Such experiments involve reactor temperature control with mixtures of N_2 and O_2 rather than air. This testing is significantly more complex and time consuming and was considered to be inappropriate for our first year assessment study.

Other limitations to the current information are that results are limited to one atmosphere operation and premixed fuel and air entering the JSC. Pressure is known to be an important parameter in soot formation studies and must be included as an important variable in our quasi-global models of soot formation. Obtaining such data is an important objective of our future program. Our use of a premixed fuel and air entering the JSC was intended to simplify the nature of the process under study. While this approach is an essential first step to our basic understanding of the process, practical devices usually involve independent introduction of fuel and air into the combustion zone with the fuel being liquid droplets at the injection point. Capability to predict soot formation in practical devices will require analytical methods of compensating for this inhomogeneity and our future program has been designed to generate experimental information which will lead to development of these modeling techniques.

While the above limitations are worthy of attention in planning for our future program, it is evident that the first year program has produced a substantial new body of information regarding soot formation. The discussion below provides further interpretation of these results. Key items to be addressed are:

- Correlation of fuel blend soot production results with blend overall hydrogen content
- Assessment of soot production trends with exhaust product THC
- Comparison of current results with soot formation theories

1. Hydrogen Content Correlation

The toluene iso-octane soot production data illustrated in Figure 18 may also be examined to evaluate the effect of fuel hydrogen content, a parameter often reported as useful in correlating sooting characteristics. At constant equivalence ratios of 1.6 and 1.8, an excellent correlation implying a linear relationship is evident (see Figure 19). Actual gas turbine combustor testing has also found an approximately linear relationship between fuel hydrogen content and soot production and the results discussed here indicate an important similarity between sooting in the well-characterized JSC and that in an actual combustor.

Another interesting implication of the Figure 19 correlation is that the JSC might be a tool useful in better relating fundamental fuel characteristics to combustion behavior. In this context, it will be useful to examine the Figure 19 correlation for other two component blends and for three and four component blends. In this manner the means of using

FIGURE 19: Dependence of Soot Production in Hydrogen Content of Toluene/Iso-Octane Blends

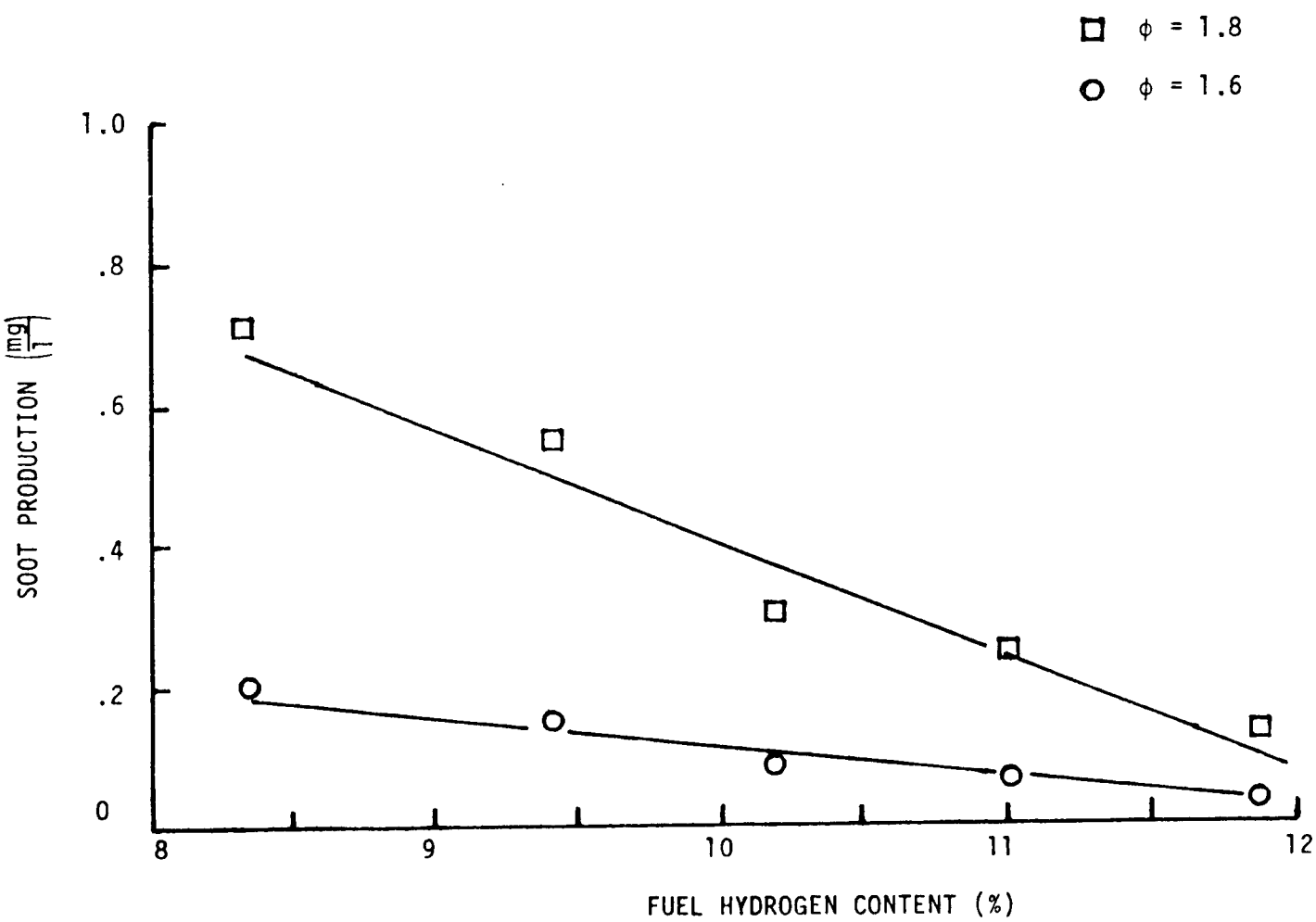

quasi-global models for various hydrocarbon types can be developed. For example, it is likely that an iso-octane/1-methyl-napthalene blend will produce a steeper soot production/hydrocarbon content trend than is evident for the toluene/iso-octane blend. Carrying this train of thought a bit further, it is reasonable to expect that such testing might result in a new method of ranking soot production potential based on JSC results.

2. Trends with THC

Throughout this report the concept that total hydrocarbon content is a key parameter in soot formation has been offered. In analyzing the data obtained it has been found that two useful correlations can be developed. Before presentation of this information, however, it is necessary to more closely examine the data which has been produced very near the rich blowout point. It will be concluded below that some of the data presented previously corresponded to operation beyond the blowout point. In these cases, the reactor operated sporatically with fuel passing through uncombusted at times and the system behaving as a pyrolysis or coker system.

Points at which this situation existed have been identified by close examination of the temperature information obtained. Figure 20 compares the calculated and measured values of reactor temperature. All data for each pure fuel which has been tested under rich conditions are included. Boundaries have been drawn to indicate equivalence to within $\pm$10%. It is evident that the majority of results involve calculated and measured temperatures which agree to well within 10%. However, there is significant disagreement below about 1600 K--equivalence ratios generally in excess of 1.7. Close examination of these data points indicate that in many cases the measured and/or calculated reactor temperature is less than that of the thermocouple embedded furthest within the castable refractory. That is, the reactor is hotter than the combustion products and consequently is supplying heat to the reactants. Naturally, this is an unstable process which leads to the sporatic combustion which was observed. These points have been indicated by shading in Figure 20. Such information must be considered as not directly relevant to the current study and have been discriminated against in the correlations which are to be discussed below.

The first correlation involving THC as the key parameter involves the previously-reported results for toluene soot production variation with JSC mass loading. It was determined that the data for 50, 80, and 112.5 gm air/min (Figure 15) could be correlated with combustion product total hydrocarbon concentration. These results are illustrated in Figure 21. The shaded data points in this graph correspond to operating conditions believed to be beyond the rich blowout point and are not considered in developing the correlation. The implication of the trend pictured in Figure 21 is that regardless of residence time the factor most important to soot production is the reactor hydrocarbon composition. Consequently, reduced reactor mass loading (longer residence time) increases reactedness (or combustion efficiency) and the decrease in hydrocarbon soot precursors results in less soot production. This information has the practical implication that soot production (and flame luminosity) in gas turbines can be minimized by reducing primary zone mass loading.

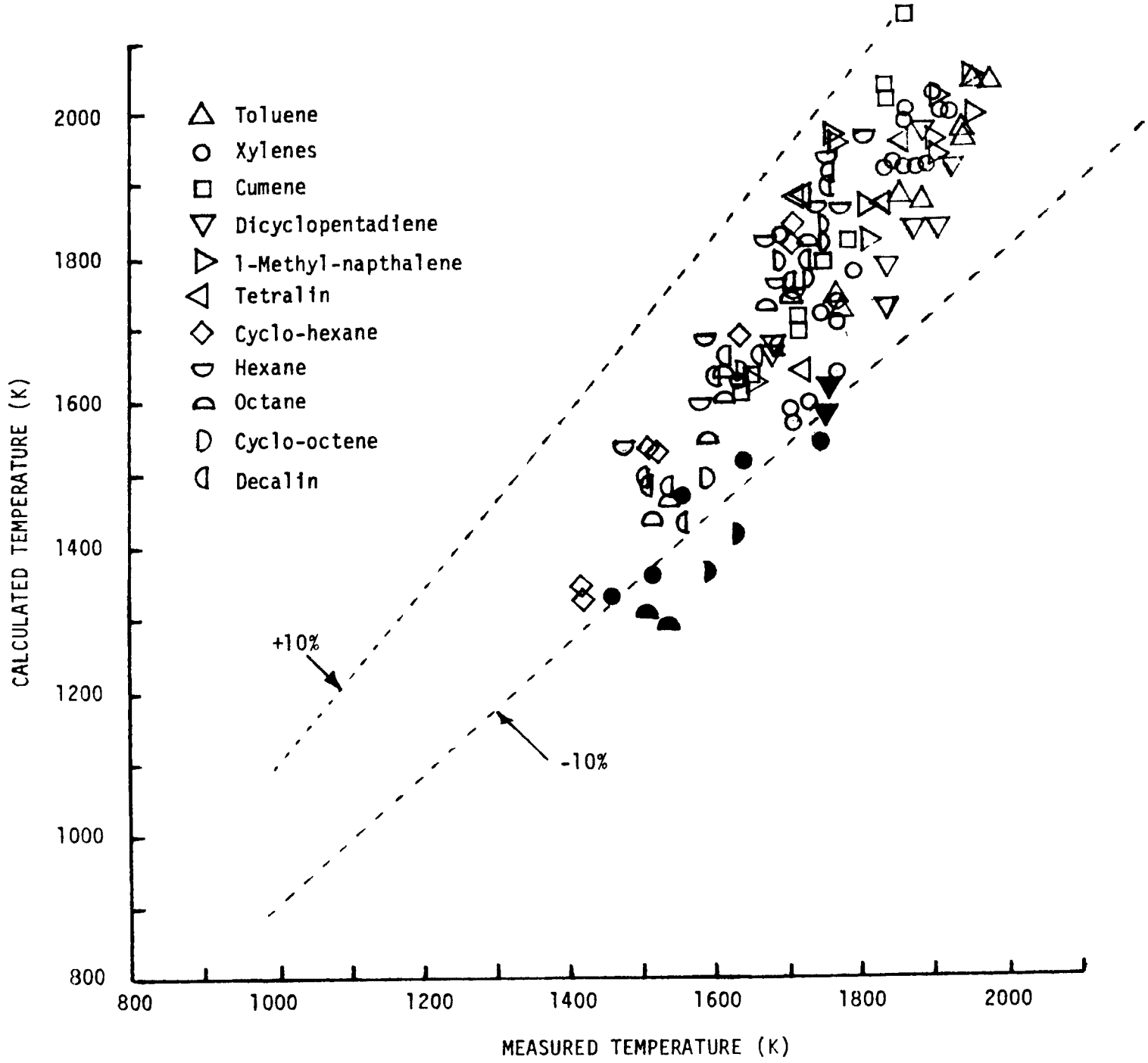

FIGURE 20: Comparison of Measured and Calculated Reactor Temperature

FIGURE 21: Correlation of Figure 15 Soot Production Data with Hydrocarbon Concentration
(Shaded data points indicate operation beyond rich blowout.)

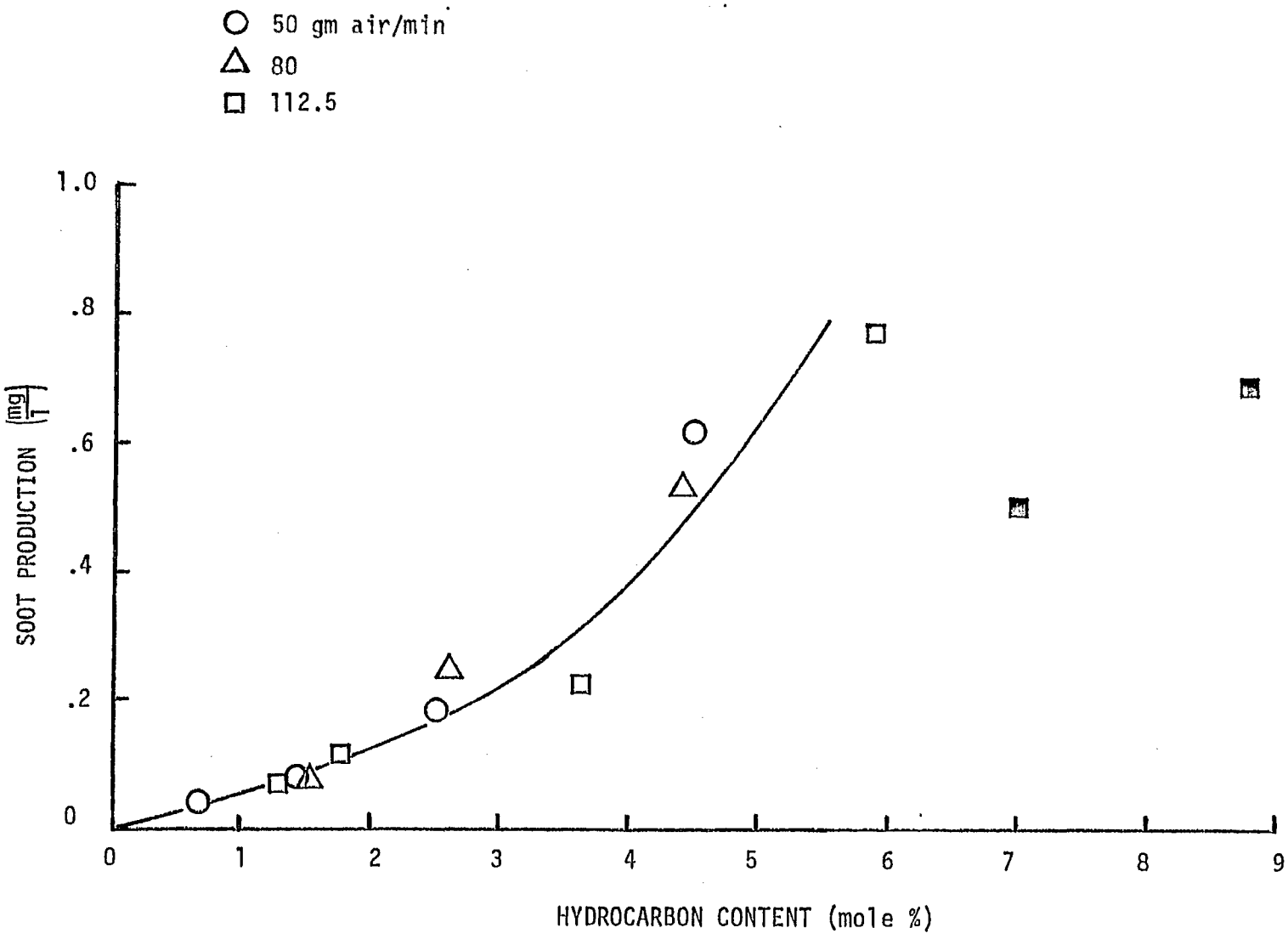

The correlation of soot production with hydrogen content was extended to all soot-producing fuels studied and results are presented in Figure 22. The current data below a THC of 5% (those not beyond the blowout point) provide for two important inferences. First, a correlation band can be drawn about data for the xylenes, cumene, dicyclopentadiene, and tetralin. While the band is fairly wide, it does represent a trend worthy of further exploration vis-a-vis the implementation of quasi-global models for soot production based on broad classifications of molecular structure. Secondly, the data indicate 1-methyl-napthalene is certainly not a member of this family. The soot production dependence on hydrocarbon concentration is much steeper for 1-methyl-napthalene and will likely require a different quasi-global characterization of soot-production chemistry.

3. Comparison with Theory

Many mechanistic models for soot formation have been proposed (8-26). Generally, it is recognized that condensed ring aromatic hydrocarbons can produce soot via a different mechanism than do aliphatic hydrocarbons. A simplified mechanism following Graham, et al (14,15) is as follows:

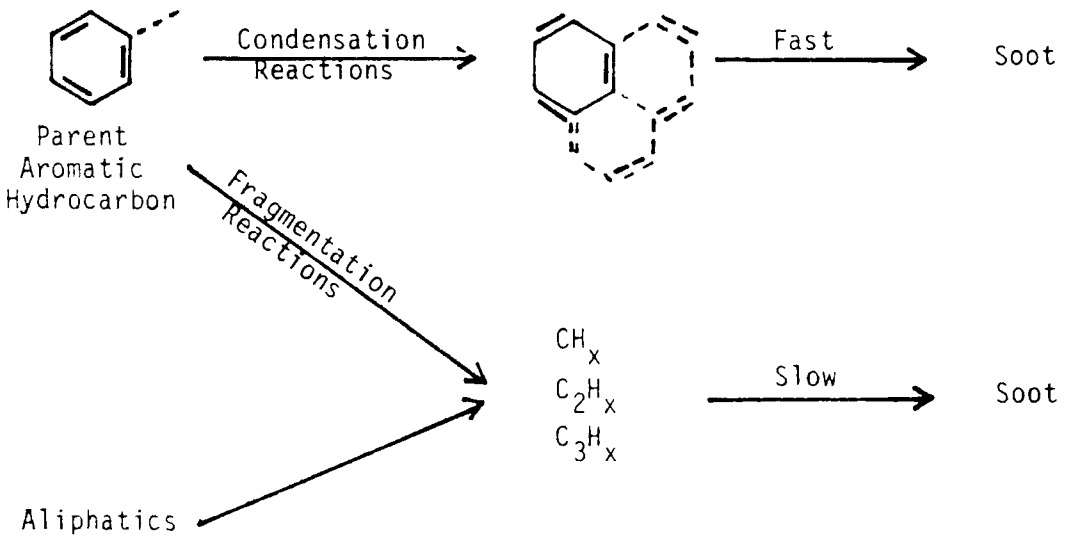

Aromatic hydrocarbons can produce soot via two mechanisms: a) condensation of the aromatic rings into a graphite-like structure, or b) breakup to small hydrocarbon fragments which then polymerize to form larger, hydrogen deficient molecules which eventually produce soot nucleation sites. Based on his shock tube studies of soot formation, Graham concludes that the condensation route is much faster than the fragmentation/polymerization route. Further, he has found that the mechanism by which an aromatic forms soot changes with temperature; below 1800 K the condensation path is favored while above this temperature the fragmentation/polymerization route is followed. Consequently, increases in temperature beyond 1800 K may result in a reduction in soot production.

FIGURE 22: Soot Production/Hydrocarbon Correlation for All Sooting Pure Fuels Tested

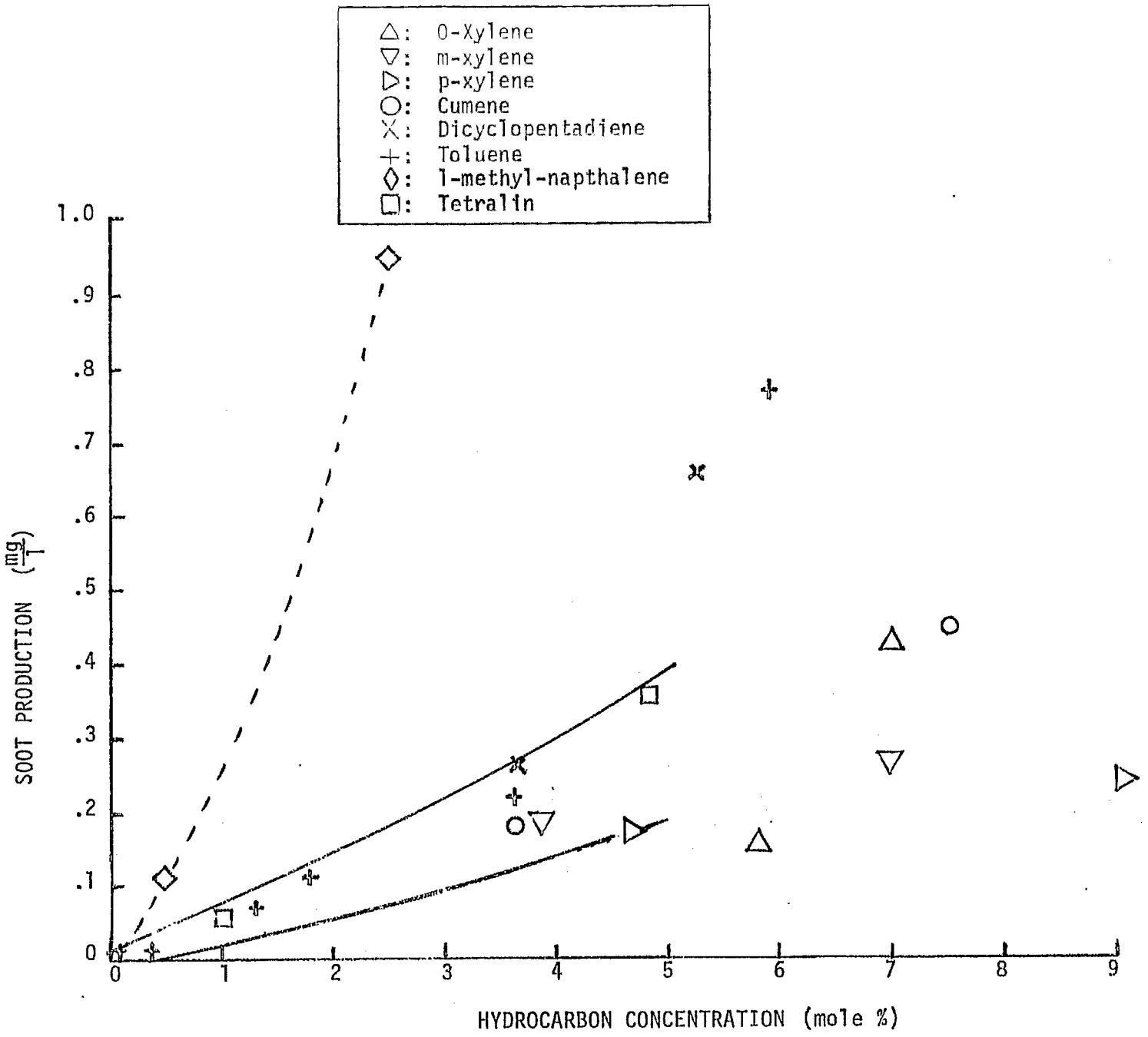

According to this simple model, aliphatics produce soot via the fragmentation/polymerization mechanism only. As a result, these hydrocarbons do not form the quantities of soot produced by the aromatics. Indeed, during the fuel rich combustion of a fuel blend composed of aromatics and aliphatics at a temperature less than 1800 K, the aromatic hydrocarbons would produce the major quantity of soot. The aliphatic combustion process would influence temperature and hydrocarbon fragment concentration but soot formation via fragmentation/polymerization would be minimal. Above 1800 K, however, the both aliphatic and aromatic hydrocarbons would produce soot via the fragmentation/polymerization route resulting in a net reduction in soot production.

The experimental results are consistent with this model. It has been observed that for condensed-ring aromatic materials soot formation commences with the initial presence of hydrocarbons in the exhaust. If we assume that these breakthrough hydrocarbons maintain their aromatic character, this observation reflects the fast kinetics of the ring-building or condensation reactions. Further, the results for 1-methyl-napthalene indicate that a double-ring aromatic provides the most rapid soot formation of the hydrocarbons studied. The observation is consistent with the ring building view.

On the other hand, the aliphatic hydrocarbons investigated allowed substantial concentrations of hydrocarbons to participate in the combustion process without soot formation. This observation reflects the slow kinetics of the process involving polymerization of small hydrocarbon fragments.

Fuel blends tested in the JSC also agree with the simple chemical mechanism. As the amount of toluene in the toluene/iso-octane blend increased, more soot was formed and the incipient limit equivalence ratio increased with decreasing percent toluene. Further, the quantity of hydrocarbons present at the soot limit increased so the amount of iso-octane in the blend increased.

It was found that soot production was more pronounced as equivalence ratio increased. This increase coincides with temperature decreases from an incipient soot value of 1850-1950 K. Despite this apparent consistency, the empirical results are not sufficient to examine changes in soot formation mechanism at 1800 K. Such evaluation would require constant ϕ variable T data as discussed in Section IIC1. Further experimental work of this nature will be given high priority, as the implication that soot production can be reduced at higher temperature is potentially very important. If soot production from aromatic hydrocarbons is minimized at higher temperatures, combustion systems might be designed to accommodate optimal conditions.

These experimental/analytical comparisons are not intended to firmly establish the validity of any theory. Instead, they are presented to illustrate that the results of our first year effort do complement existing views of the soot formation process. It is true that the comparisons are limited by the scope of the existing JSC data base (one atmosphere pressure, lack of combustion product hydrocarbon breakdown, non constant T results, etc.)--our approach to developing a more thorough base is described in Section IV. Most importantly, the current results lend optimism to our originally proposed approach, that of quasi-global modeling of the soot formation process for various categories of hydrocarbons.

D. Conclusions of Experimental Work

The following conclusions have been drawn from the Phase I experimental effort.

- Ethylene and toluene have distinctly different soot formation characteristics in backmixed combustion.
- The hydrocarbon concentration at and beyond the incipient soot limit appears to be a dominant factor influencing sooting characteristics.
- Other hydrocarbons may be categorized as like-C_2H_4 or like-$C_6H_5CH_3$ with 1-methyl-napthalene being a more powerful soot-producing compound.
- Fuel blend testing indicates a combination of like-C_2H_4 and like-$C_6H_5CH_3$ behavior.
- Results are consistent with existing mechanistic understanding of the soot formation process and provide encouragement for our initially-proposed approach of generating quasi-global soot formation models for categories of hydrocarbons.

III. ANALYTICAL EFFORT

During this phase of the program an approach has been defined for the development of a model for combustor chamber analysis. The emphasis has been to delineate a model framework in which sensitivity to fuel properties is a key component.

The model structure is being formulated to accomodate the new information on fuel effects developed in this program as well as information that exists or is being developed elsewhere. Specific mechanisms included in the model development are gas phase pyrolysis and oxidation kinetics, soot formation and oxidation, fuel nitrogen combustion chemistry, droplet evaporation and combustion and aerodynamic and chemical interactions.

Another major aspect of the model development is its tailoring to meet the needs of the designer. These needs are varied but generally fall within a set of desired information including heat transfer, lean blowout, ignitability, pattern factor, combustion efficiency and gas and particulate emissions. Design guidance for control of these factors is of most direct value to the combustion system designer.

To assist in defining an approach to meet these objectives, a state-of-the-art survey was conducted and reported upon in the first quarterly program report (Reference 3). The major conclusions are that a modular approach be used for the overall combustor model framework with quasiglobal kinetics and turbulent kinetic energy and micromixing methods to characterize mixing and aerodynamic/chemical interactions. The modular model and the quasiglobal kinetics model are discussed in the following sections.

A. Modular Modeling Approach

The computation of a generalized combustor flowfield is a formidable task, involving as it must a number of complex physical and chemical processes, which include turbulent, recirculating flow, swirl, finite-rate chemical kinetics, droplet evaporation and combustion, and heat transfer. Despite the problems involved, considerable progress has been made in recent years in the development of calculation methods for these flows, in terms of both techniques for the solution of the elliptic governing equations and the development of simpler yet physically perceptive modeling techniques.

Since most practical combustion chamber flowfields involve large regions of recirculating flow, in which axial diffusion is important, direct calculation of these flows involves the numerical solution of the elliptic form of the governing equations. A considerable amount of research effort has been put into the development of numerical techniques for these problems, and successful comparison of calculation with experiment for recirculating flows with large heat release has been reported by Hutchinson et al. (27) and by Abou Ellail, et al. (28), for example. Significantly, in both cases a careful adaptation of the numerical model to the specific experimental configuration was reported to be required, and in both of these papers it was noted that the details of the computation required careful handling to obtain the accuracy demonstrated. Furthermore, Abou Ellail, et al. (28) note that it is not possible to provide sufficient resolution in a detailed combustor flowfield computation to adequately

describe processes such as fuel injection for which the mixing process initially occurs on a scale much smaller than that of the overall combustion chamber.

Thus, while the development of numerical models capable of providing direct solution of the equations governing specific combustion chamber flowfields continues, a need exists for the development of physically perceptive yet mathematically simpler models. This requirement arises from both the need to provide a model which allows reasonably rapid computation of a number of different, complex combustor geometries, and the need to develop models for those processes, such as fuel injection, which occur on scales smaller than can be adequately resolved in a detailed overall flowfield computation. The development of approximate methods - modular models - is a response to the requirements just outlined.

The basic interest in the application of approximate techniques is to avoid the complexities inherent in a direct calculation of an elliptic flowfield by making suitable assumptions that allow the flow to be computed using simpler approaches. Clearly the simplest possible procedure is to assume that the flowfield is effectively one-dimensional thus avoiding any necessity for definition or calculation of velcoity or species profile effects. A somewhat more sophisticated approach is to assume that the combustor flowfield can be broken down into separate zones, each of which can be calculated individually in some detail, and then coupled together in some fashion to obtain an overall computational analog of the combustor flow. Such approaches are termed modular models, examples of which have been reported by Roberts, et al. (29), Swithenbank, et al. (30) and Edelman and Harsha (31).

In order to describe each of these models in sufficient detail to point out the similarities and differences between them, consider the representative gas turbine combustor shown schematically in Figure 23. Conceptually, this flowfield can be broken down into three regions: the central recirculation zone, shown cross-hatched and an outer, swirling air flow surrounding this central zone (both of which occur in the combustor primary zone) and a mixing and combustion region downstream of this region in the combustor secondary zone.

The model described by Roberts, et al. (29) is a three-zone streamtube model, in which the flow in a gas-turbine combustor can is broken down into a primary zone (the central recirculation region), an outer streamtube of reacting flow surrounding the primary zone, and a single-streamtube secondary zone downstream of the primary zone, in which the products of the outer streamtube are mixed with additional air and further reaction takes place. The model includes physical descriptions for fuel droplet burning and either equilibrium or kinetic-limited hydrocarbon-air thermochemistry; the flows in each of the three zones are assumed to be one-dimensional. In all zones mixing of gaseous species is assumed instantaneous, while droplets in the streamline surrounding the recirculation zone are assumed to vaporize following a d^2 law; this vaporization rate governs the reaction rate in the outer zone. Gas phase chemistry is computed using a quasiglobal kinetics model following Edelman and Fortune (32).

In the Roberts et al. modular model a key feature is the division of the mass flow entering the combustor into the rates feeding the three zones, shown schematically in Figure 24. The size of the primary, recirculation zone

FIGURE 23: Representative Gas Turbine Combustor Can Schematic

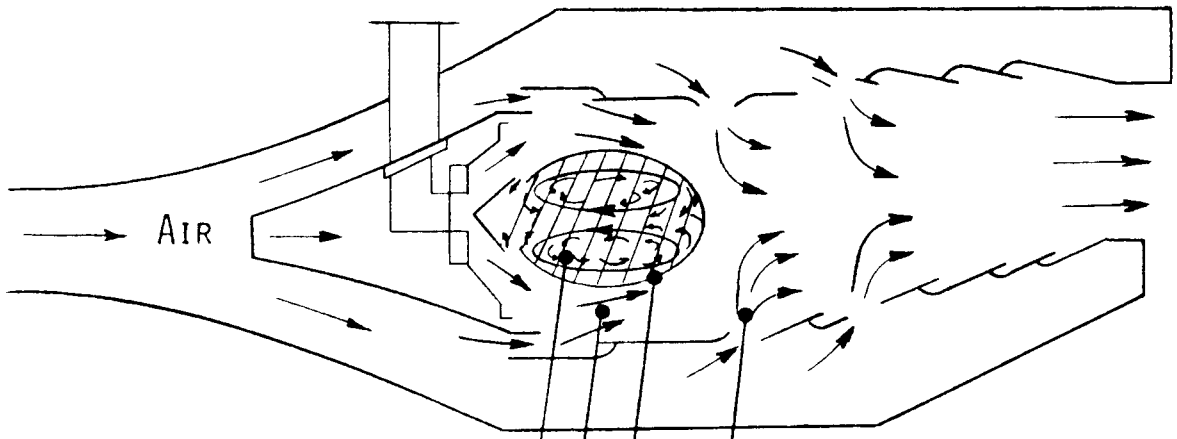

MAJOR FLOW ELEMENTS

- RECIRCULATION ZONE
- NON-RECIRCULATING, SWIRLING MIXING ZONE
- SHEAR LAYER COUPLING ZONE
- SECONDARY LATERAL INJECTION

MAJOR DESIGN PARAMETERS

- GEOMETRY
- AIR INFLOW STATE
- FUEL INJECTION STATE
- BOUNDARY CONDITIONS

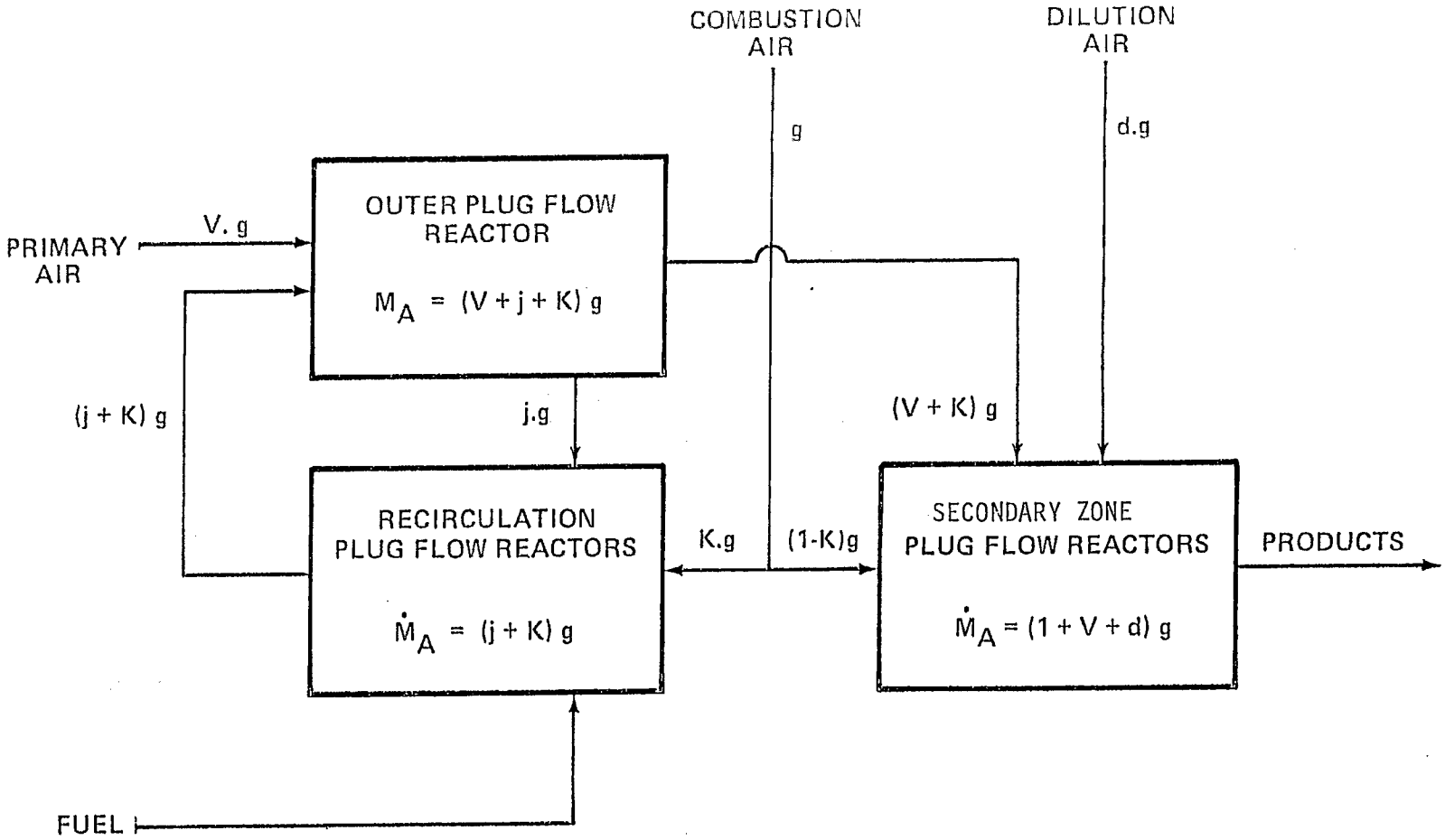

FIGURE 24: Schematic of Modular Model of Roberts, et al. (29)

is obtained using an empirical relationship for recirculation zone boundaries in gas turbine combustion chambers. It is then assumed that air enters the recirculation zone only from the combustion air feed to the combustor can, at the downstream boundary, and the fraction of the total combustion air which enters the recirculation (the remainder flows into the dilution zone) is given by an empirical correlation. This air instantly mixes with the fuel in the primary region, and an equilibrium hydrocarbon combustion model is used, with finite-rate NO_x reactions proceeding for a residence time given by the volume of the recirculation region divided by the volumetric flow rate in this region. All fuel in this recirculation region is assumed to be in vapor phase, and the fraction of the total fuel flow in this region is given by the ratio of the recirculation region gas flow to the total flow (vapor and liquid phases) in the outer streamtube. The output from the recirculation region (equal to the input mass flow) mixes instantly with the unburned vapor phase fuel in the outer streamtube, initiating finite-rate reactions in this region.

This modular approach is obviously highly simplified. No direct comparison with data is reported in Ref. 29, although it is noted that the prediction of absolute levels of NO_x at the combustor exit is good. Capability to predict fuel nitrogen-to-NO_x conversion or soot production is not included in this model.

Because the elements of the modular model of Roberts, et al. (29) are one-dimensional plug flow computations, conditions at the start of the calculation must be such that sustained combustion will be maintained. Such an initial assumption is not necessary when stirred reactor models are incorporated in the modular approach, as for example by Swithenbank et al. (30). In this approach the combustor is modeled as a set of perfectly-stirred and plug flow reactors, arranged both in series and parallel, as shown schematically in Fig 25. Here the perfectly-stirred reactors represent regions of intense recirculation. While this approach will provide predictions of blowout phenomena and allow the use of arbitrary initial conditions, like the model of Roberts, et al. (29) it rests on the ability to prescribe a priori the relative mass fluxes into each component of the model.

The modular approach used in the present work, described earlier by Edelman and Harsha (31) is, like the other models just outlined, an attempt to avoid some of the problems of elliptic flow field computation by devising an approximate treatment of a complex combustor flowfield. There are however, very significant differences in the assumptions made in the development of this modular approach compared to those involved in the models of Roberts et al. (29) and Swithenbank, et al. (30) and these differences offer the potential for the present modular approach to handle considerably more complex problems than are possible with the earlier techniques.

In the present modular approach the combustor flowfield is broken down into three major components: a non-recirculating flow, which is treated as parabolic, recirculation zones assumed to be represented by well-stirred reactor(s), and turbulent shear layers along the diving streamlines separating the directed flow and ricirculation regions. The shear layer serves as the coupling region between the other two model components; fluxes of species and energy across this shear layer form the boundary conditions on the two computational regions. Full finite-rate chemistry, based on the quasiglobal model (32), is included in both the directed flow and the well-stirred reactor,

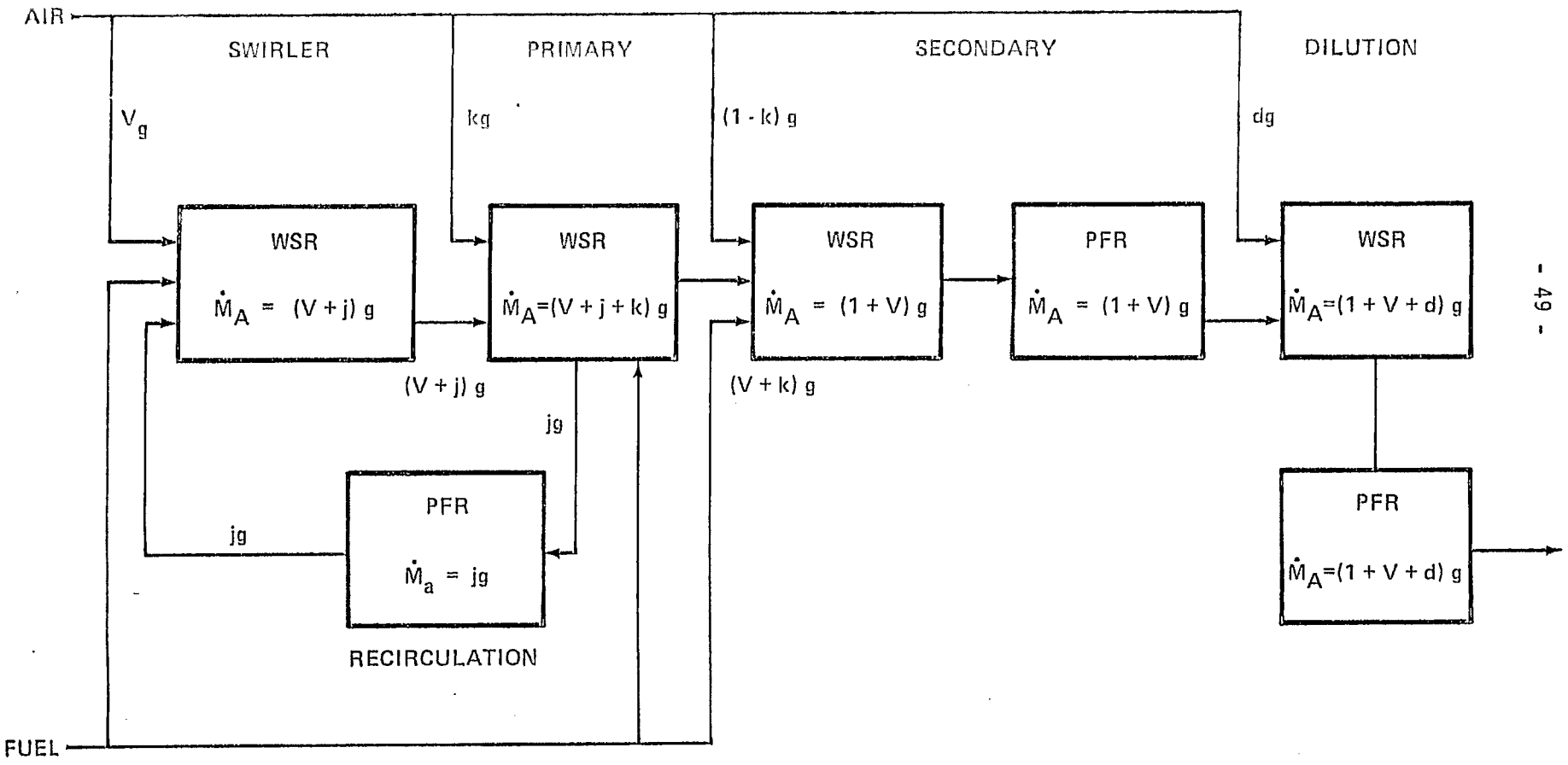

FIGURE 25: Schematic of Modular Model of Swithenbank, et al. (30)

and particle and droplet effects can also be computed. The directed flow is assumed to be fully turbulent. Although the modular formulation is not restricted to any one turbulence model, in this description a one-equation turbulent kinetic energy model (used to obtain the turbulent shear stress in the directed flow) is assumed for present purposes.

A schematic representation of the present modular model is shown in Fig. 26. The key difference between this approach and the other modular models just described is the provision for the shear layer coupling region in the current model. Through the use of this element of the model, the division of the mass flux between the directed flow and the recirculation region is computed iteratively rather than specified empirically. Furthermore, the directed flow region is computed in detail as a two-dimensional parabolic flowfield, rather than through a one-dimensional approximation, allowing the use of detailed computations of the mixing and chemical reactions in this region of the combustor.

The features of the three modular models discussed in this section are summarized in Table 4. Although the present model is computationally more complex than the models of Roberts et al. (29) and Swithenbank, et al. (30), and requires an iterative solution; the additional complexity allows the development of an overall combustor flowfield computation which can include far more detailed modeling than is possible with either of these approaches. Furthermore, each element of the present modular model--the well-stirred reactor, the non-uniform, swirling flow, and the shear layer can be systematically developed. For example, the effects of unmixedness can be introduced into both the stirred reactor module, using techniques such as the Monte Carlo simulation reported by Kattan and Adler (33), and into the parabolic flow computation, using

TABLE 4: Comparison of Modular Models

	Roberts et al. (29)	Swithenbank, et al. (30)	Present Model
Elements	Plug Flow Reactors	Plug Flow/Perfectly Stirred Reactors	Parabolic Flow/ Stirred Reactors
Coupling Conditions	Empirical Flow Division	Empirical Flow Division	Iterative Solution For Flow Division
Turbulent Flow Characterization	None	None - Enters Empirical Flow Division	Turbulent Kinetic Energy Model
Chemistry Model	Quasi-Global H/C Kinetics	Global H/C Kinetics	Quasi-Global H/C Kinetics

FIGURE 26: Schematic of Present Modular Model

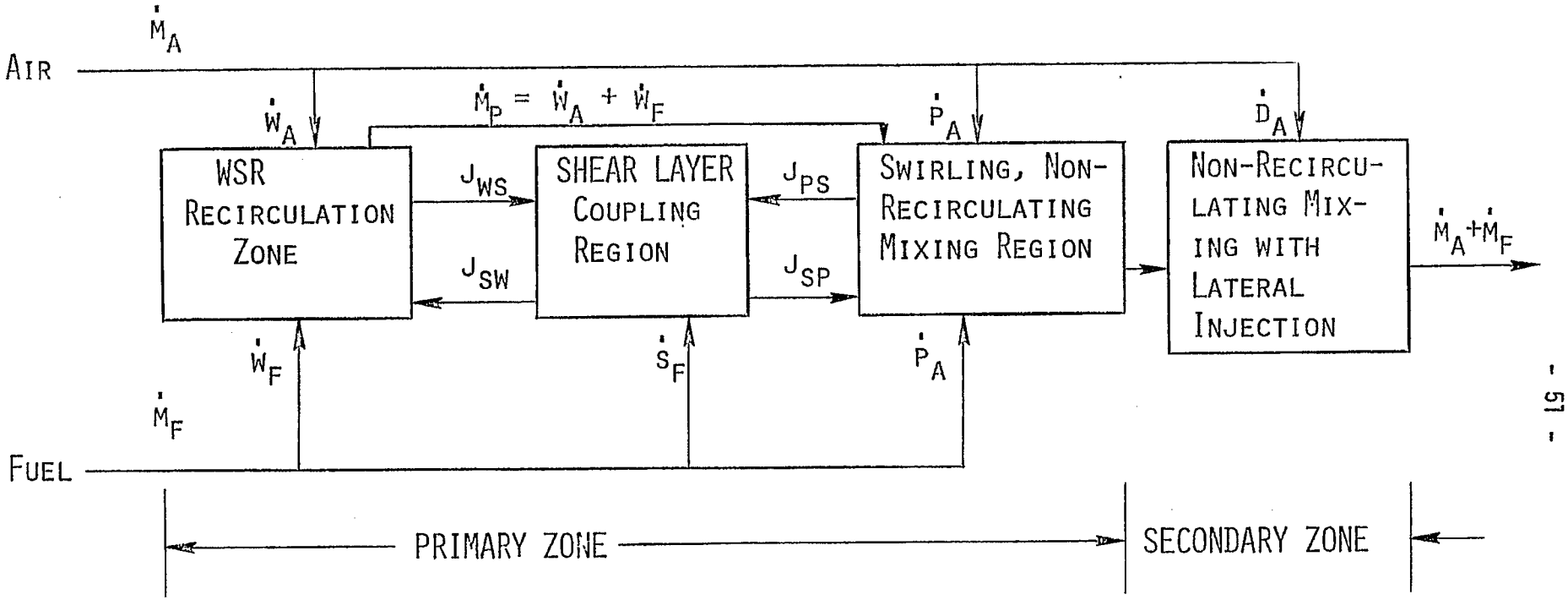

- WSR - Well Stirred Reactor Theory
- SHEAR LAYER and Non-Recirculating Flow - Parabolic Flow Theory
- Quasiglobal Kinetics
- Turbulence Modeling - Turbulent Kinetic Energy and Micromixing Theories

techniques such as those developed by Rhodes, et al. (34), Khalil (35), and Pratt (36). Multiple well-stirred reactors can also be easily introduced for more detailed modeling of the recirculation region. The detail available in the parabolic flowfield computation allows the inclusion of models for processes such as liquid fuel injection, and the spread and vaporization of the resulting spray, treated either in bulk or through the use of detailed spray modeling. Thus, modular modeling of the type described here offers considerable potential for systematic development with increasing complexity. It offers the prospect of providing computational capabilities substantially equivalent to those available from direct solution of the elliptic equations, while at the same time providing greater insight into the physical details involved in a generalized combustor flowfield.

1. Modular Model Formulation--The basic elements of the current modular model formulation are the parabolic finite-difference computational technique developed by Boccio, Weilerstein and Edelman (37), modified to incorporate the turbulent kinetic energy model developed by Harsha (38), used for the directed-flow portion of the analysis, and the stirred reactor computation developed by Edelman and Weilerstein (39). Both of these elements make use of the quasi-global model developed by Edelman and Fortune (32) for rapid computation of finite-rate hydrocarbon-air kinetics. The crucial feature of the modular model concept is the coupling between the directed-flow and recirculating flow elements of the model. In the present formulation, these elements are coupled together through a simplified representation of the turbulent shear layer which exists between the directed flow and the recirculation region; this shear layer representation is used to define the gradients in velocity, species, and enthalpy between the two regions of the flow, thus providing both the boundary condition on the directed flow and the stirred reactor feed rates. The mathematical formulations used for the flowfield region are briefly discussed in this section.

a. Coupling Rleations: The Shear Layer Model--The key feature of the modular concept lies in the coupling relations assumed along the dividing streamline that 1) supply the boundary conditions for the parabolic computations and 2) determine the feed rates for the stirred reactor computation. These coupling conditions are obtained through a model of the turbulent shear layer separating the recirculation zone from the directed flow. Within the general concept of the modular model, this shear layer region can be treated in as much detail as is desired, for example, using the component synthesis method of Korst (40), or through a solution of the boundary-layer equations governing free shear layer development. However, in the present modular formulation, a simplified model of the shear layer is introduced. The shear layer is assumed to be vanishingly thin, that is, the gradients established through the shear layer model are applied along the dividing streamline.

It is assumed that the shear layer can be modeled as a region of width $\ell(x)$ across which all dependent variables (i.e., velocity, temperature, turbulent kinetic energy, and species mass fractions) vary linearly. The width of the shear layer is itself assumed to be specifiable by the relation

$$\ell = a + bx \tag{1}$$

in which a and b are constants. Since for a planar shear layer the growth rate can be related to the dividing streamline shear stress, specification of the

constant b implies a shear stress distribution along the dividing streamline, while the constant a can be taken to be a parameter which is related to the initial boundary layer thickness.

The dividing strealine shape, $R_c(x)$, is specified; this specification also defines the dividing streamline stream function value $\psi=\psi_w$. Along ψ_w, the turbulent shear stress τ_w is defined as described above, and thus the turbulent kinetic energy k_w is defined through the relation

$$\tau_w = 0.3\ \rho k_w \tag{2}$$

To obtain the gradients in temperature and species mass fraction, linear profiles across the shear layer are assumed. If ψ_p is defined as the streamline immediately "outside" the recirculation region (i.e., within the directed flow) and ψ_R is the streamline immediately "inside" the recirculation zone, then, for species i

$$\left(\frac{\partial \alpha_i}{\partial r}\right)_w = \frac{\alpha_{ip} - \alpha_{iR}}{\ell} \tag{3}$$

and for the temperature

$$\left(\frac{\partial T}{\partial r}\right)_w = \frac{T_p - T_R}{\ell} \tag{4}$$

where α_{ip} and T_R are the values of species mass fractions and temperature obtained from the stirred reactor solution.

b. Well-Stirred Reactor: The Recirculation Zone Model--Flowfield regions in which intense backmixing occurs can approach the limit of complete mixing, and thus the well-stirred reactor concept is attractive for representing the recirculation regions in continuous flow combustors. If the mixing process is considered to be complete, the mathematical formulation for the perfectly stirred reactor is applicable and is straightforward, as has been described, for example, in Ref. 41. The result is a set of transport equations for enthalpy and species mass fractions written in terms of the enthalpy and species mass fraction fluxes across the boundaries of the recirculation zone. In the present modular model, net inflow of species and enthalpy can be expressed as line integrals involving gradients evaluated along the dividing streamline, so that for the modular model the energy and species conservation equations for the stirred reactor can be written

Energy

$$-2\pi \int_0^S R_c(x)\rho\varepsilon_D \sum_i \left[h_i^I\ (T^I)\ \frac{\partial \alpha_i^I}{\partial r}\right] ds + \dot{Q}$$

$$-2\pi \int_0^S R_c(x)\kappa \frac{\partial T}{\partial s}\, ds = -2\pi \int_0^S R_c(x)\rho\varepsilon_D \sum_i \left[h_i^o(T_R) \frac{\partial \alpha_i^o}{\partial r} \right] ds \qquad (5)$$

Species

$$\frac{d\alpha_i}{dt} = \frac{-2\pi}{\rho_c V} \int_0^S R_c(x) \left[\rho\varepsilon_D \frac{\partial \alpha_i^I}{\partial r} \right] ds - \frac{2\pi}{\rho_c V} \int_0^S$$

$$R_c(x) \left[\rho\varepsilon_D \frac{\partial \alpha_i^o}{\partial r} \right] ds + \frac{\dot{W}_i}{\rho_c} \qquad (6)$$

Here the superscript I refers to inflow into the stirred reactor (recirculation region) and superscript o refers to outflow from the stirred reactor, V is the reactor volume, ρ_c a characteristic density of the stirred reactor region, and $\rho\varepsilon_D$ a characteristic eddy diffusivity, evaluated from the outer flowfield solution in the region of the dividing streamline. The term $\dot{W}_i$ represents the rate of production of species i caused by chemical reactions and $\dot{Q}$ represents the heat input to the stirred reactor region through the combustor walls.

Equations (5) and (6), along with an equation of state

$$\rho = \frac{P}{RT \sum_i \frac{\alpha_i}{M_i}} \qquad (7)$$

where

R = the universal gas constant

M_i = the molecular weight of species i

are used to establish a new reactor state, given the feed rates established form the parabolic directed flow solution; i.e., given the diffusive fluxes of species and energy across the dividing streamline, Equations (5), (6), and (7) are solved for new values of the α_i and the recirculation zone temperature, T_R.

c. Parabolic Mixing: The Non-Recirculating Model--The next major element of the modular model is the formulation for the non-recirculating flow portion of the combustor flowfield. It is assumed that the boundary layer approximations apply to this part of the flowfield, so that the describing equations are parabolic. A full description of the governing equations and their numerical solution technique may be found in Refs. 31, 37, and 42. Since the directed flow is assumed to be turbulent, a model for the turbulent shear stress is required, and in the present version of the model the one-equation

turbulent kinetic energy model described by Harsha (38,41,43) is used. Briefly, this model involves the solution of a modeled form of the turbulent kinetic energy equations, with an algebraic specification for the dissipation length scale which appears in that equations; the turbulent shear stress is then related to the local turbulent kinetic energy through the relation

$$\tau_T = a_1 \rho k \tag{8}$$

The dissipation length scale is defined in terms of the local width of the mean turbulent flowfield; the definition of this length scale and of the parameter a_1 is discussed in detail in Refs. 38,41 and 43. This turbulence model has been successfully applied to a wide variety of flows, with and without variation in density.

d. Chemical Kinetics: The Quasiglobal Model--This model has as a key element one or more subglobal oxidation steps, coupled to intermediate reversible reaction chains involving well known reaction systems. The philosophy behind the quasiglobal kinetics model is similar to that applied to the overall modular formulation itself: relevant empirical information is used to simplify the overall kinetics computation without significant loss in accuracy. The existing scheme is given in Table 5. Results obtained using the quasiglobal scheme as incorporated in the modular model have shown excellent agreement with experimental data (41,44).

e. Outline of the Modular Computation--The overall flowfield computation using the modular approach proceeds as follows. A dividing streamline shape $R_c(x)$ is assumed, and the shear layer width expression and shear stress distribution is defined. An initial state for the stirred reactor computation is assumed, resulting in values of α_{iR} and T_R. With these data available as boundary conditions, the parabolic mixing calculation is carried out to the end of the recirculation zone. This calculation defines the species mass fraction and temperature gradients at $\psi=\psi_w$, and these values are used to obtain the stirred reactor feed rates. A new stirred reactor computation is carried out using the new feed rates, resulting in a new specification of α_{iR} and T_R, and the parabolic computation is repeated. The procedure is repeated until the changes in the stirred reactor composition from computation to computation become small, at which point the coupling iteration has converged. The parabolic calculation is then carried out to the end of the combustion chamber, completing the solution.

The modular model approach has yet another advantage in addition to those cited above: each of the elements may be independently developed and proved prior to coupling them to characterize a particular combustion system. This feature is particularly relevant to the current program where emphasis is placed upon the fuel related chemical aspects of the combustion of alternative fuels. The jet stirred combustor (JSC) used as a primary experimental tool by Exxon in this program (Section II) is an example of the direct correspondence of a major element of the modular combustor model to the experimental configuration. The JSC is ideally suited for the determination of kinetic rate information for subglobal reaction steps which is directly relevant to the development of the quasiglobal model. The development of the quasiglobal model in conjunction with the JSC data has been the major area of attention during this phase of the program.

TABLE 5: Extended C-H-O Chemical Kinetic Reaction Mechanism $k_f = AT^b \exp(-E/RT)$

Reaction	A	Forward	E/R
1) $C_nH_m + \frac{n}{2}O_2 \rightarrow \frac{m}{2}H_2 + n\,CO$	A. Long Chain 6.0×10^4	1	12.2×10^3
	B. Cyclic 2.08×10^7	1	19.65×10^3
2) $CO + OH = H + CO_2$	5.6×10^{11}	0	0.543×10^3
3) $CO + O_2 = CO_2 + O$	3.0×10^{12}	0	25.0×10^3
4) $CO + O + M = CO_2 + M$	1.8×10^{19}	-1	2.0×10^3
5) $H_2 + O_2 = OH + OH$	1.7×10^{13}	0	24.7×10^3
6) $OH + H_2 = H_2O + H$	2.19×10^{13}	0	2.59×10^3
7) $OH + OH = O + H_2O$	5.75×10^{12}	0	0.393×10^3
8) $O + H_2 = H + OH$	1.74×10^{13}	0	4.75×10^3
9) $H + O_2 = O + OH$	2.24×10^{14}	0	8.45×10^3
10) $M + O + H = OH + M$	1.0×10^{16}	0	0
11) $M + O + O = O_2 + M$	9.38×10^{14}	0	0
12) $M + H + H = H_2 + M$	5.0×10^{15}	0	0
13) $M + H + OH = H_2O + M$	1.0×10^{17}	0	0
14) $O + N_2 = N + NO$	1.36×10^{14}	0	3.775×10^4
15) $N_2 + O_2 = N + NO_2$	2.7×10^{14}	-1.0	6.06×10^4
16) $N_2 + O_2 = NO + NO$	9.1×10^{24}	-2.5	6.46×10^4
17) $NO + NO = N + NO_2$	1.0×10^{10}	0	4.43×10^4
18) $NO + O = O_2 + N$	1.55×10^9	1.0	1.945×10^4
19) $M + NO = O + N + M$	2.27×10^{17}	-0.5	7.49×10^4
20) $M + NO_2 = O + NO + M$	1.1×10^{16}	0	3.30×10^4
21) $M + NO_2 = O_2 + N + M$	6.0×10^{14}	-1.5	5.26×10^4
22) $NO + O_2 = NO_2 + O$	1.0×10^{12}	0	2.29×10^4
23) $N + OH = NO + H$	4.0×10^{13}	0	0
24) $H + NO_2 = NO + OH$	3.0×10^{13}	0	0
25) $CO_2 + N = CO + NO$	2.0×10^{11}	-1/2	4.0×10^3
26) $CO + NO_2 = CO_2 + NO$	2.0×10^{11}	-1/2	2.5×10^3

$$\frac{d[C]_{C_nH_m}}{dt} = A\,T^b\,P^{0.3}\,C_{C_nH_m}^{1/2}\,C_{O_2}\,\exp\left(-\frac{E}{RT}\right);\ [C] = \frac{\text{gm moles}}{\text{cc}},\ [T] = K,\ [P] = \text{atm.},\ [E] = \frac{\text{kcal}}{\text{mole}}$$

Reverse reaction rate k_r is obtained from k_f and the equilibrium constant K_c

B. Comparison With Data

The extension of the existing quasiglobal model has received the major emphasis during this phase of the program. The approach involves the comparison of predictions based upon the existing quasiglobal model with recent data obtained in this program and from other sources. The data derived in the current program has been obtained from the JSC. Other data that is being used in this study was derived from the plug flow reactor work carried out at Princeton University (Ref. 45). The purpose of this comparison is to provide information on appropriate directions to pursue in extending the existing quasiglobal model.

1. Current Quasiglobal Model--Work reported by Edelman and Fortune (31) in 1969 demonstrated that many observations on the rate of combustion of hydrocarbons could be predicted by a relatively simple kinetic scheme. One of the most significant observations made from the available data is the similarity of ignition delay times for hydrocarbons in homologous series. This seems to be true for hydrocarbons in the presence of oxygen at initial temperature above about 1000 K. There are exceptions to this behavior and methane is an important example of a hydrocarbon in the paraffin (alkane) series having significantly longer ignition delay times than the higher hydrocarbons in the same series. This difference can be traced to the importance of the methyl radical (CH_3) formed during the decomposition of methane. For the higher hydrocarbons (propane and above) the similarity in oxidation behavior suggested that the prediction of significantly more detail of the oxidation process might be obtainable by extending the notion of a single step overall reaction to a scheme which characterizes the initial pyrolysis and partial oxidation reactions with one of more "sub-global" steps coupled to a set of detailed reversible reactions to characterize the overall kinetics process. Edelman and Fortune (31) introduced the term "quasiglobal" as a definition of this type of kinetics modeling.

The basic quasiglobal scheme introduced by Edelman and Fortune (31) involves a single subglobal fuel oxidation step

$$C_nH_m + \frac{n}{2} O_2 \rightarrow \frac{m}{2} H_2 + n\ CO \tag{9}$$

with a rate given by

$$\frac{dC_{C_nH_m}}{dt} = - AT^b\ p^{0.3} \left[C_{C_nH_m}\right]^{\frac{1}{2}} C_{O_2} \exp\left(\frac{-E}{RT}\right) \tag{10}$$

with empirically determined values of A, b, and E/R as given in Table 5, in which the units of equation (9) are also indicated, coupled to the "wet CO" mechanism as also listed in Table 5.

Some observations on this scheme should be noted. First, it generally is agreed that in hydrogen-bearing systems carbon monoxide is oxidized rapidly to CO_2 via the reaction

$$CO + OH = CO_2 + H \quad (11)$$

We have, however, included other reactions involving CO and oxygen for completeness including

$$CO + O_2 = CO_2 + O \quad (12)$$

$$CO + O + M = CO_2 + M \quad (13)$$

where M is the general third body. Reactions (12) and (13) are much slower than reaction (11), but their inclusion was necessary for basic studies performed on systems, including the CO/air system reported in Ref. 44. In addition, a number of reactions involving NO_x are included which represent a necessary extension of the basic Zelodovich mechanism to account for certain of the ambient long-time NO-to-NO_2 conversion reactions which occur in the atmosphere, particularly when coupled with appropriate daylight photochemical mechanisms. These reactions have proven to be relatively unimportant in combustion processes. Note that the mechanism shown in Table 5 does not include the capability to predict either fuel nitrogen-to-NO_x conversion or soot production--inclusion of these features is a high priority goal of our future program.

2. Application of the Quasiglobal Model

a. Plug Flow Model--The data obtained by Glassman, et al. (45) include temperature and species histories for the combustion of several fuels with air or oxygen, at various equivalence ratios. These measurements were made in the Princeton adiabatic, high temperature, turbulent flow reactor, for which the flowfield was essentially one-dimensional.

One difficulty observed in analytically modeling this experimental configuration is the lack of detailed initial condition data. Thus the computations do not start at the injection station but rather at the first point downstream of the injection station at which detailed species measurements are available; these values (with all hydrocarbon fragments converted to equivalent fuel) and the measured temperatures are used to initiate the plug flow computation.

Several comparisons were made, including data for propane, ethylene, and butane fuels. The results for propane, at the low equivalence ratio of 0.079 are presented in Figures 27 and 28.

Figure 27, which shows both the temperature profile measured by Glassman et al. (45) and that computed for a plug flow using the current quasiglobal model indicates that the ignition delay time, as defined by a 5% rise in the temperature is well predicted in the case of propane. However, the temperature during combustion is underestimated by the model. This comes about because, as shown in Figure 28, the calculation predicts only a gradual and slowly decreasing fuel concentration, while the experimental measurements show that after a first stage (induction period) the fuel disappears rapidly. The data shows that the rapid disappearance of the fuel coincides in this case with the conversion of CO to CO_2 (see Figure 28) which is responsible for the temperature rise. Figure 28 also shows that the calculation predicts that the maximum amount of CO is produced during the first phase of combustion and that the peak mole fraction

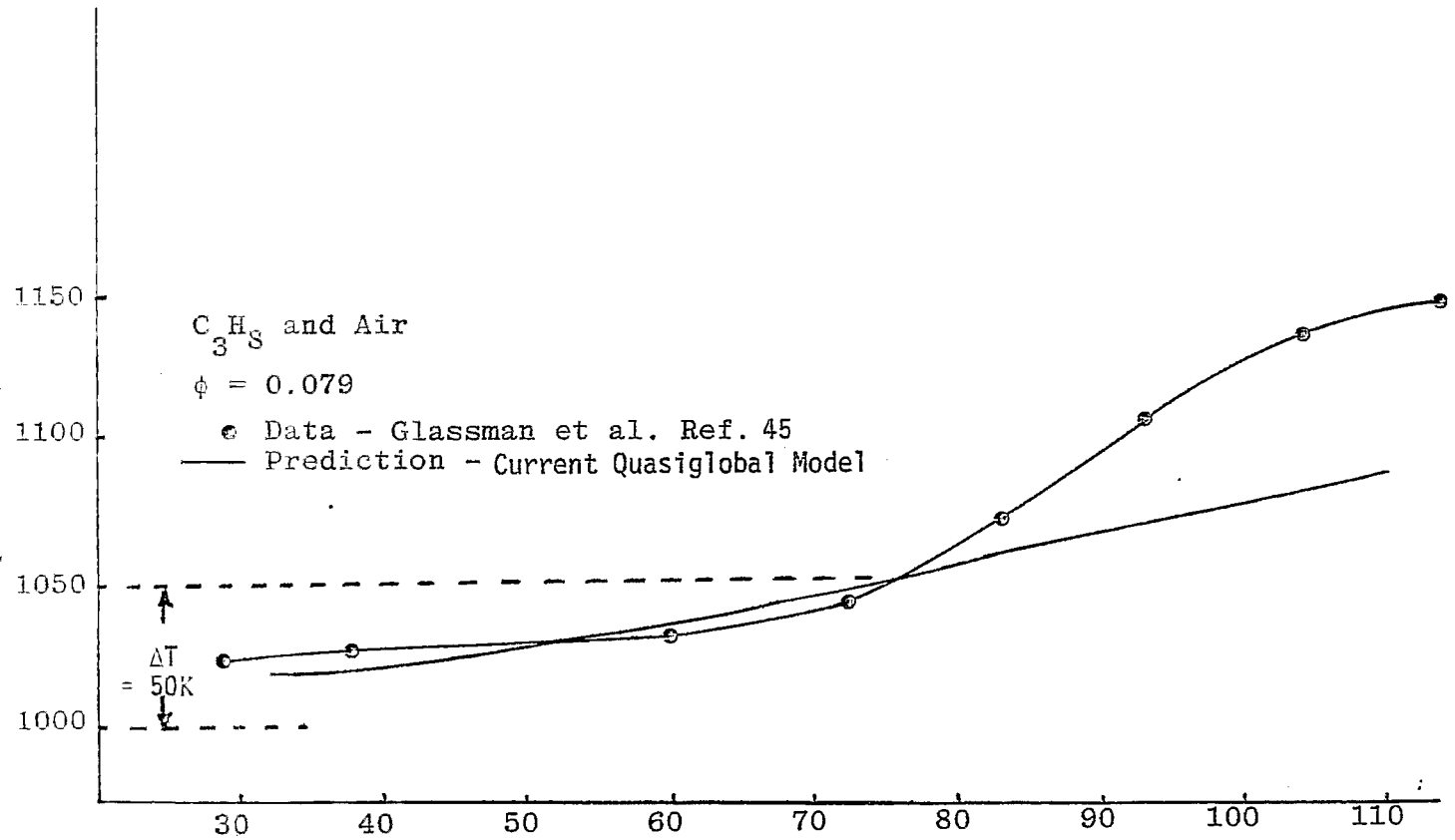

FIGURE 27: Temperature During Propane-Air Reaction

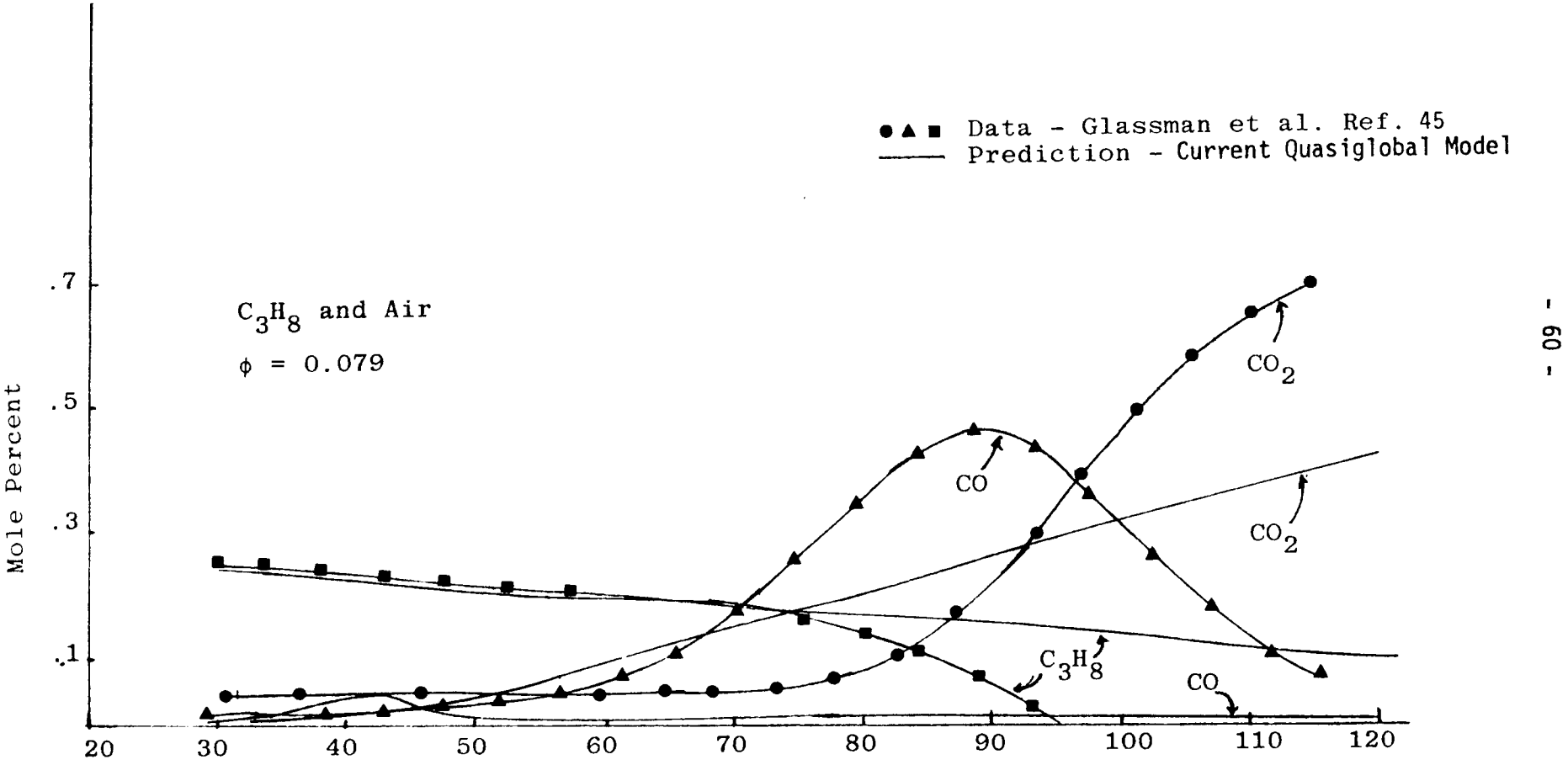

FIGURE 28: Chemical Composition of Spread Propane-Air Reaction

obtained is 0.05×10^{-2}; the experimental measurements show that the major CO production occurs during the latter part of the combustion process, peaking slightly before the total disappearance of fuel at a mole fraction of 0.46×10^{-2}. Both measurements and calculations show that the major amount of CO_2 is produced during the later part of the combustion process, however, the calculations first over predict and then under predict (by a factor of two) the measured values. Also, while the data shows a constant mole fraction of CO_2 during the gradual decrease in the amount of fuel, and then a rapid increase in CO_2 during the rapid decrease in the amount of fuel, the calculations predict that CO_2 increases at an almost constant rate throughout the burning.

For both ethane and butane, computations with the current quasiglobal model underestimate the igniton delay time as shown by the data while providing an increased temperature level compared to the experiment. Thus, the current model predicts the ignition delay time for propane well, but not the ignition delay time for butane or ethane. It should be noted, however, that the rate of the fuel consumption reaction in the quasiglobal model was determined from a series of experimental results and calculations for ten different fuels, which included propane but not ethane or butane.

b. Perfectly Stirred Reactor Model--Data obtained during this program for the concentration of CO observed in stirred reactor operation using toluene and ethylene as fuels at fuel lean operation showed a characteristic minimum in CO concentration as a function of fuel air ratio. Preliminary calculations of CO concentration in a stirred reactor configuration using the existing quasi-global model showed a moderate sensitivity of the predicted CO concentration to the rate used for the reaction.

$$CO + OH = CO_2 + H$$

for which a number of rate expressions exist in the literature.

In order to establish the effect of the rate used in predicting the observed CO vs fuel-air ratio trends, a series of stirred reactor computations was carried out using the following rate expressions.

(1) Gardiner, et al (1973) (Ref. 46)

$$k_f = 4.0 \times 10^{12} \exp(-4030/T)$$

(2) Baulch and Drysdale (1974) (Ref. 47) as reported by Engleman (Ref. 48)

$$k_f = 1.5 \times 10^{7} T^{1.3} \exp(+380/T)$$

(3) Baulch, et al (1968) (Ref. 49)

$$k_f = 5.6 \times 10^{11} \exp(-543/T)$$

Substantial differences in these rates exist over the temperature range of interest for comparison with the data obtained in this program. Forexample, at a temperature of 1000 K, the rate computed from expression (1) is a factor of 4.6 lower than

that from expression (3), while expression (2) is a factor of 2 lower than expression (3). Between 1000 K and 2000 K a crossover occurs in the relative rate comparison for expression (1) compared to the other expression: at 2000°K, expression (1) produces a rate a factor of 1.3 higher than expression (3) and expression (2) is a factor of 1.2 lower than expression (3).

A comparison of computed CO concentrations as a function of fuel-air equivalence ratio carried out for an adiabatic perfectly stirred reactor is shown on Figure 29 compared to a composite of the data from this program obtained by Exxon. The CO concentration data were plotted as a function of fuel-air ratio, and different fuel-air ratio values at which the minimum in CO occurred were apparent for toluene versus ethylene. When replotted in terms of equivalence ratio this shift in minimum location is considerably reduced, as can be seen from Fig. 29, indicating that fuel type produces only a relatively small effect on the observed equivalence ratio for minimum CO. This observation, and the objective of evaluating the performance of the existing quasi-global model in establishing trends in the predicted CO levels led to the use of propane as a representative conventional H/C ratio fuel for the purposes of these computations.

Two conclusions can immediately be drawn from the comparison presented in Fig. 29. First, the prediction of the minimum in CO concentration observed in the experimental data is highly sensitive to the expression chosen for the rate for the $CO + OH = CO_2 + H$ reaction: no minimum is observed over the equivalence ratio range of interest when the rates given by Baulch and Drysdale (Refs. 47, 48) and Baulch et al. (Ref. 49) are used, but the observed minimum is reproduced when the rate given by Gardiner et al. (Ref. 46) is used in the computation. Second, all of the CO predictions, irrespective of rate, are within a factor of two of the observed CO levels. Thus the existence of a minimum in the observed CO data provides a valuable characteristic in addition to blowout data for the evaluation of models for hydrocarbon oxidation under kinetically limited operation.

Because the early data obtained during this program did not include measured heat transfer rates, the computations shown in Fig. 29 were carried out for an adiabatic stirred reactor configuration. More recent measurements have included heat transfer rates, and Fig. 30 shows a comparison of stirred reactor computations carried out for isooctane, using both the measured heat transfer rates and the adiabatic assumption, with experimental data for several fuels.

It is of considerable interest to note, as shown on the figure, that the predictions of CO mole percent made using the current quasiglobal model are within a factor of two of all the data shown over the equivalence ratio range of the data. Furthermore, both the data and the predictions show the existence of the characteristic minimum in the CO mole percentage, which can be a sensitive indicator of the behavior of the chemical kinetic model used in the prediction. Although the jet stirred combustor data have shown that the soot formation behavior of toluene is considerably different from that observed for isooctane, for fuel rich operation, it is clear from Figure 30 that the CO production behavior of the two fuels is similar and that results for both fuels at lean operating conditions are predicted to within a factor of two by the current quasiglobal model. Even for ethylene, which generally behaves quite differently than the bulk of the higher petroleum-based hydrocarbons, the agreement between predicted and measured CO concentrations is within a factor of two.

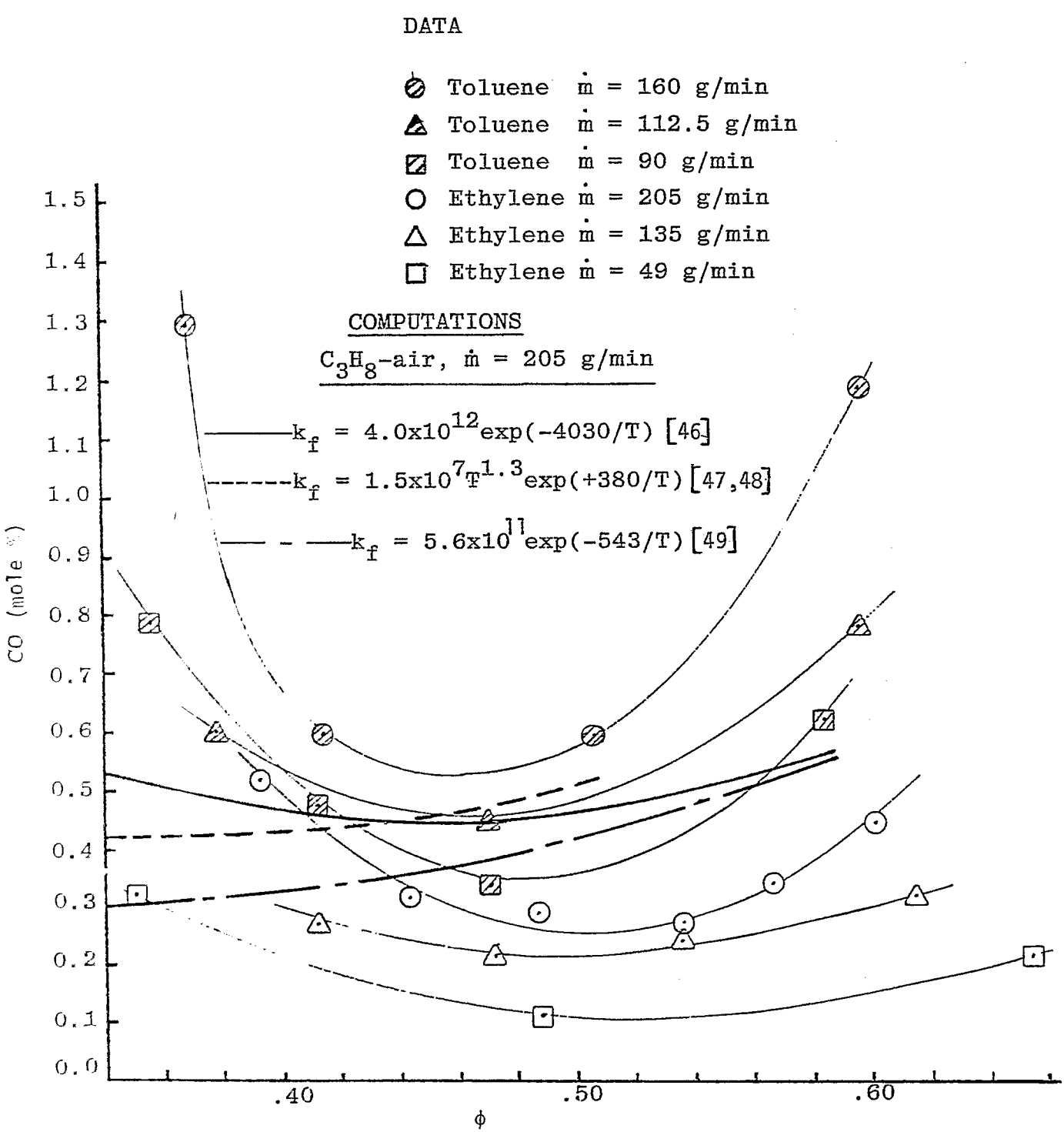

FIGURE 29: Comparison of Stirred Reactor Computations Using Different Rates for $CO+OH=CO_2+H$ Reaction with Experimental Data

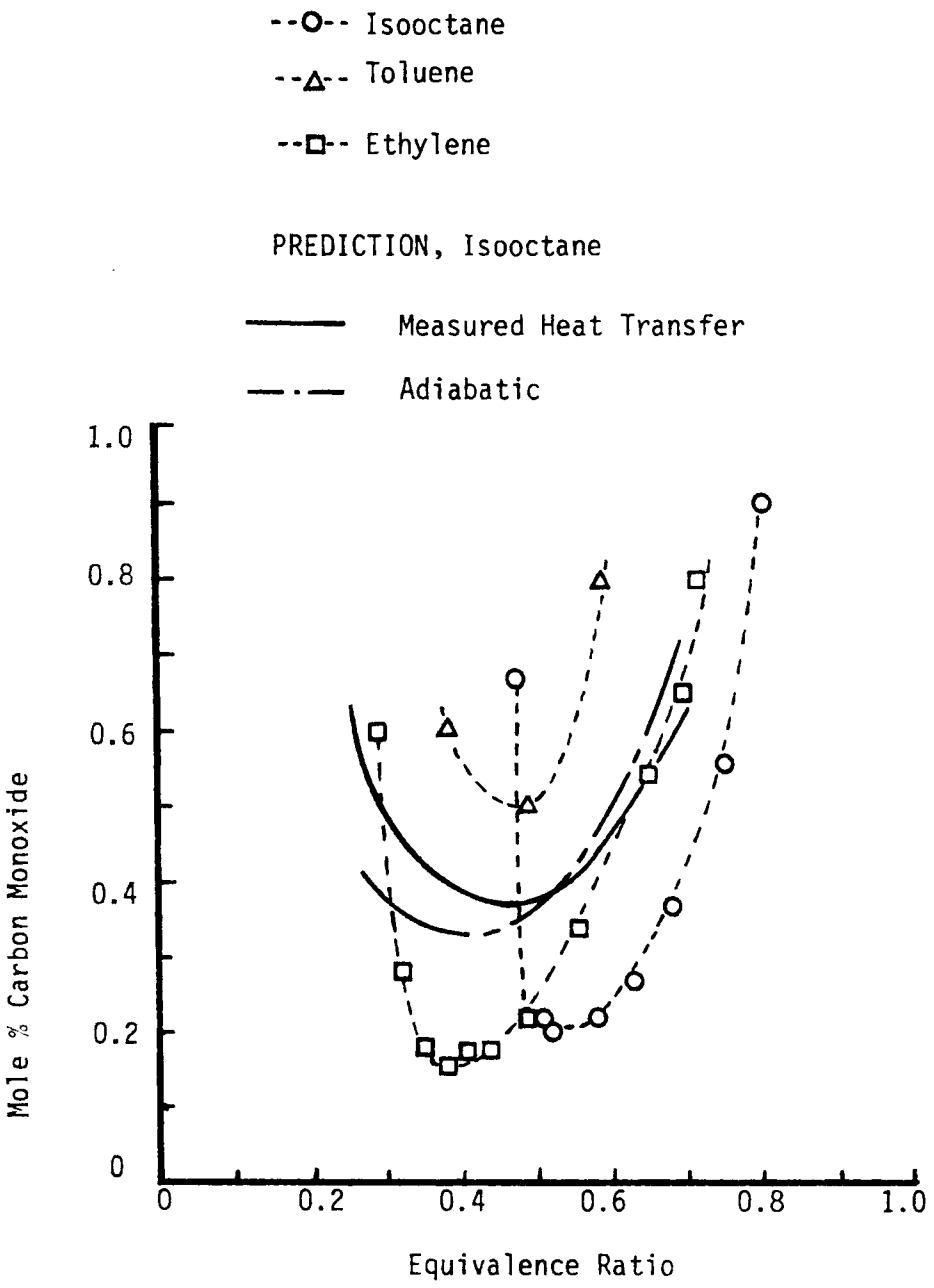

FIGURE 30: Comparison of Predicted with Measured CO Concentrations, Air Flow = 112.5 gm/min, Reactor Diameter = 5.08 cm

From Fig. 30 it can also be seen that it is important in making comparisons of experimental data and predictions for chemical kinetics model development to account for the effects of heat transfer. Note that the predicted curves for measured heat transfer and the adiabatic case show a crossover at an equivalence ratio of 0.53. This temperature sensitivity is indicative of the increasing importance of non-equilibrium behavior as the equivalence ratio is decreased.

Emphasis has been placed upon the comparison of predicted with measured CO concentrations because it is a key indicator of the performance of the kinetic scheme. However, additional comparisons have been made between predicted and experimentally determined temperatures, and CO_2, O_2 and unburned fuel concentrations. These comparisons are shown in Figures 31 through 34. The effect of heat transfer on the predicted temperatures is clearly shown on Figure 31 where from 50 to 100 K temperature differences are predicted between the adiabatic and non-adiabatic cases. The agreement between predictions and experimentally determined temperatures is excellent over most of the equivalence ratio range when the measured heat transfer is taken into account. Some deviation is noted near blowout. This shows up as well in the CO_2 comparison, Fig. 32, slightly in the O_2 comparison, Fig. 33, and in the fuel comparison, Figure 34. It should be noted that with the exception of the approach to blowout the levels of fuel concentrations, typically on the order of 3 hundreths of a percent, are predicted fairly well.

Only limited comparisons have been made in the fuel rich regime. Predictions for isooctane are compared with experimental data obtained from this program over an equivalence ratio range of 1.38 to 1.61, Figs. 35 and 36. These computations were carried out using measured heat transfer rates. Further computations carried out at equivalence ratios beyond the experimentally observed blowout point (under an adiabatic assumption) show that the rapid rise in HC mole percent seen in the data is also seen in the computed results, but at higher equivalence ratios: the 7.5% mole percent HC point reached at $\phi = 1.61$ in the data is not seen until $\phi = 2.28$ in the computed results. Further, the concave downward trend of the CO data seen in Fig. 35 is also observed in the computation, but stretched out over a wider equivalence ratio range, with a maximum of 11% CO reached (in the computation) at $\phi = 2.30$. Figure 36 shows predicted temperatures compared with measured values illustrating that significantly higher temperatures are predicted than are observed. Although this constitutes limited comparisons at fuel rich operation, apparent deficiencies in the existing quasiglobal model are indicated.

C. Discussion

The foregoing comparison of predictions with data has shown that the existing quasiglobal model does predict some of the important aspects of the oxidation process in the fuel lean regime. Furthermore, the data for toluene shows that the levels of CO are similar to those of the paraffins. Refering back, Fig. 30 shows this behavior and illustrates that the prediction (based upon the isooctane test conditions) falls in the middle of and within a factor of two of all the data. It is also clear from this comparison (Fig. 30) that the predictions do not agree in detail with the experimental results; in paritcular the predicted CO mininum for isooctane occurs at an equivalence ratio

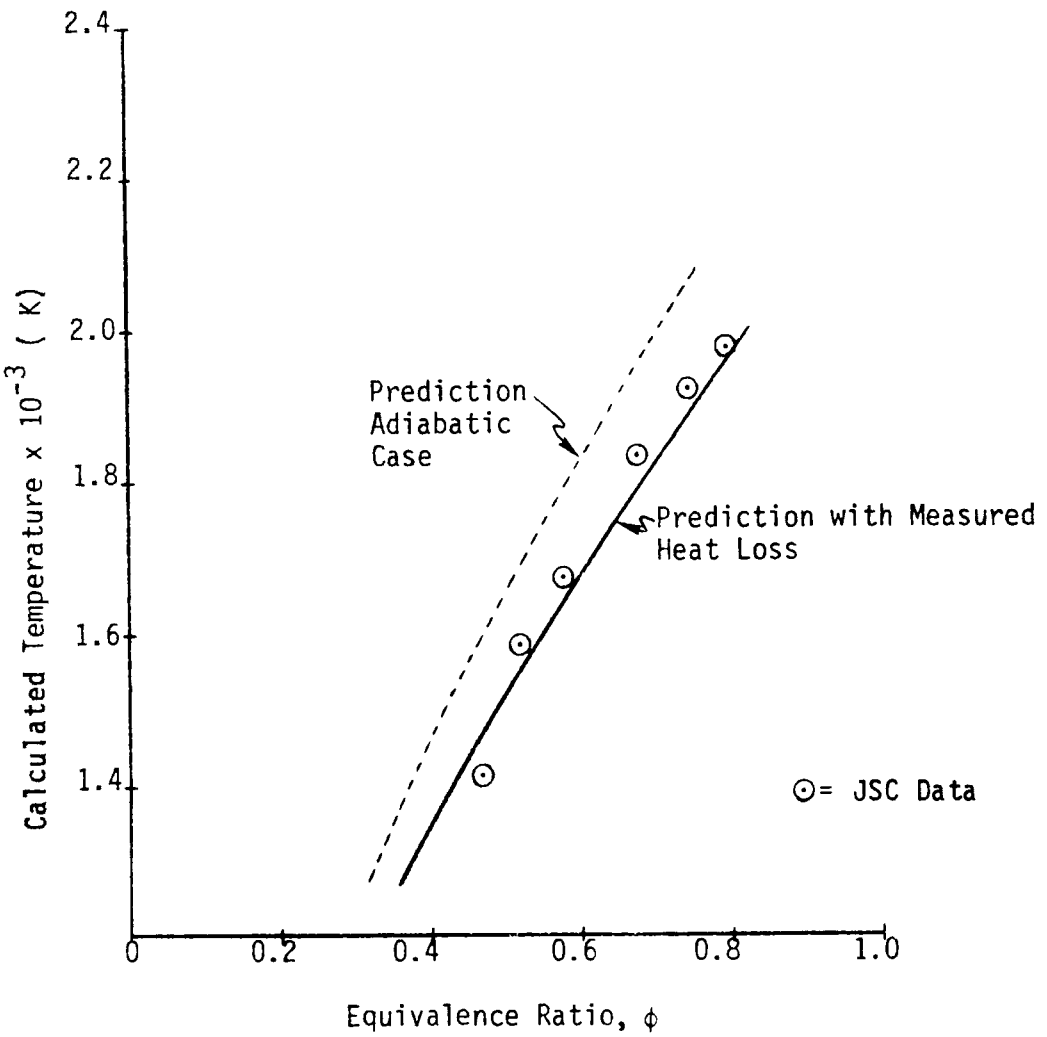

FIGURE 31: Comparison of Predicted Reactor Temperature with Reactor Temperature Computed from Experimental Data, Isooctane

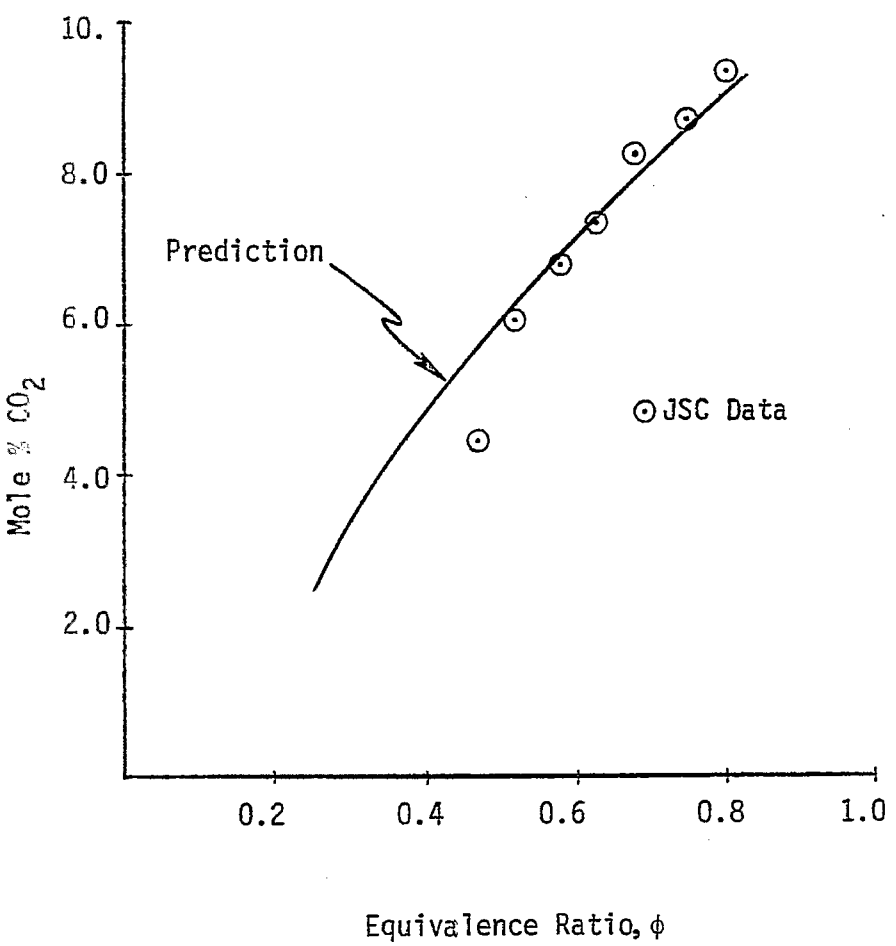

FIGURE 32: Comparison of Predicted and Measured CO_2 Concentration, Isooctane

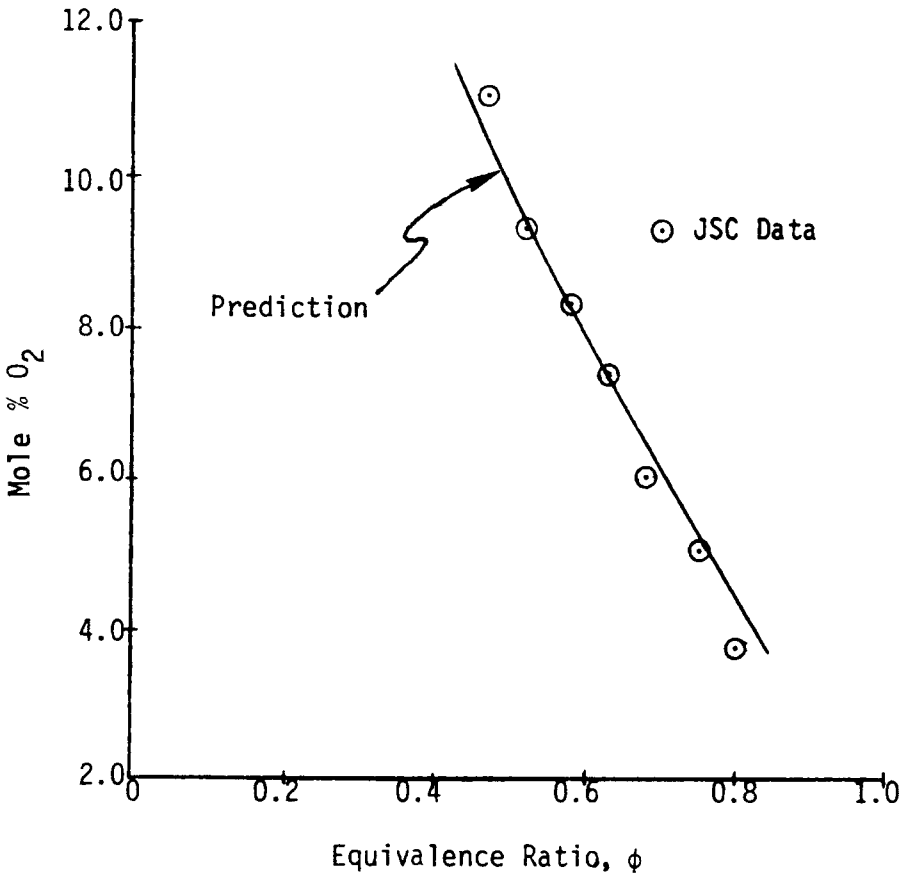

FIGURE 33: Comparison of Predicted and Measured O_2 Concentration, Isooctane

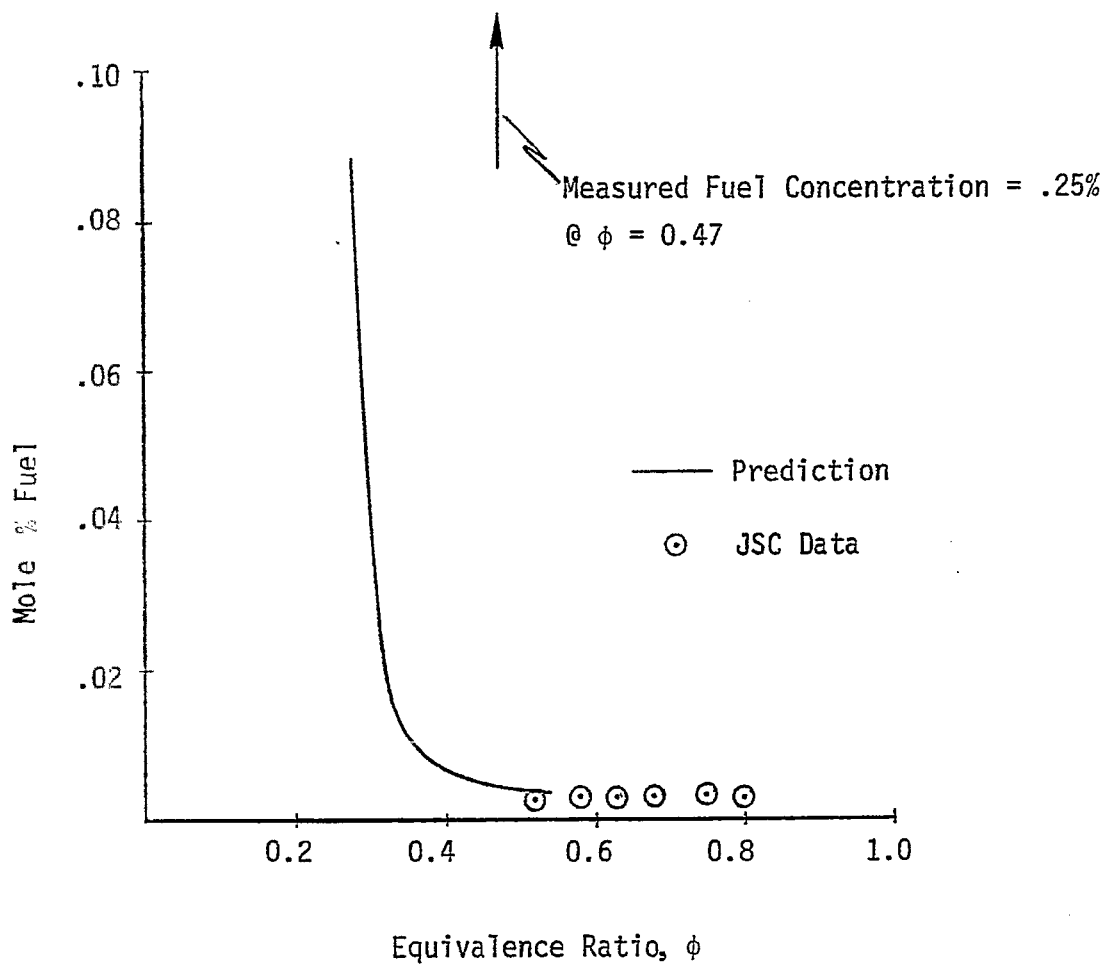

FIGURE 34: Comparison of Predicted and Measured Fuel Concentration, Isooctane

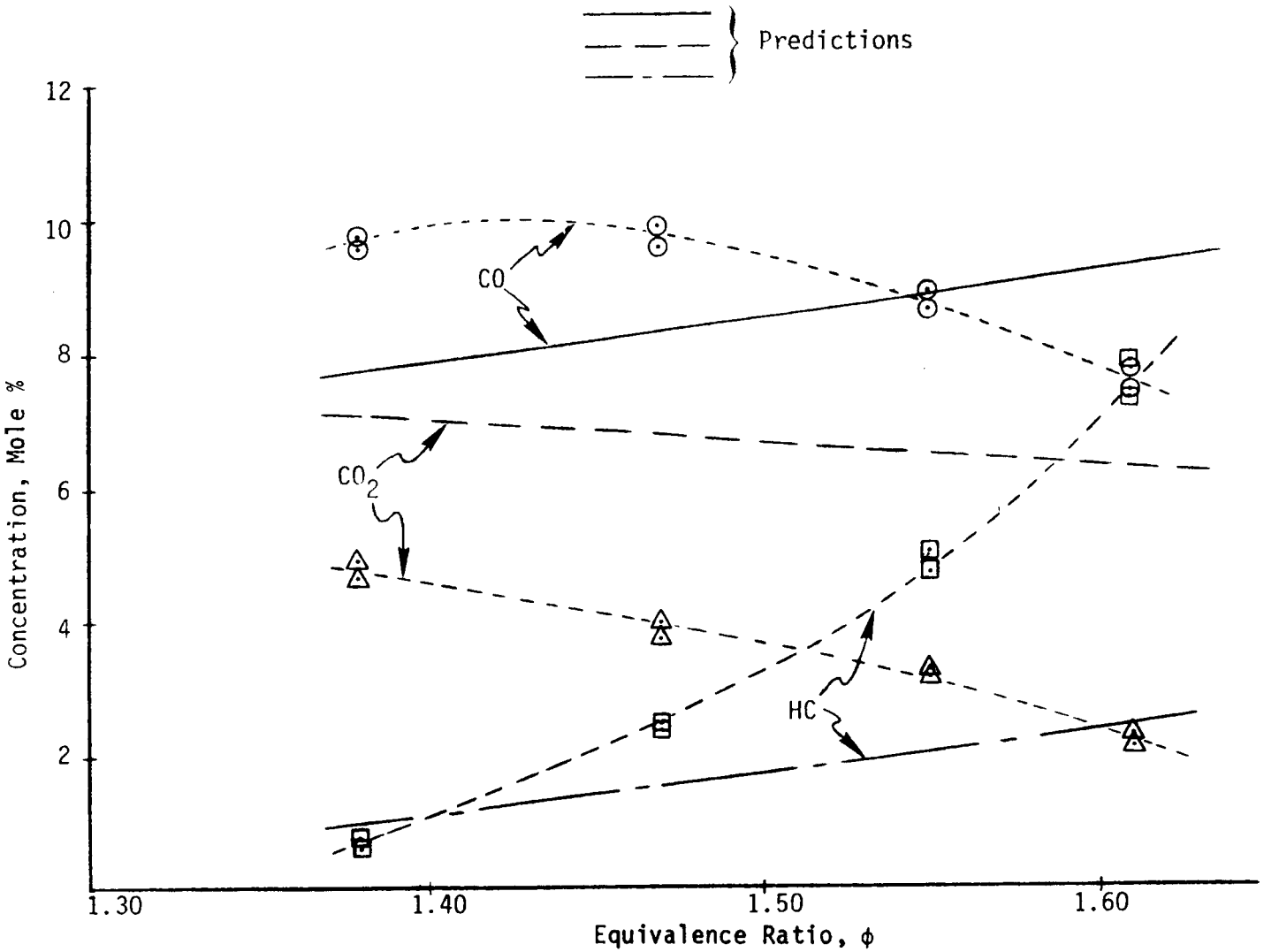

FIGURE 35: Comparison of Prediction with JSC Data for CO, CO_2, and HC in the Fuel Rich Regime, Iso-octane

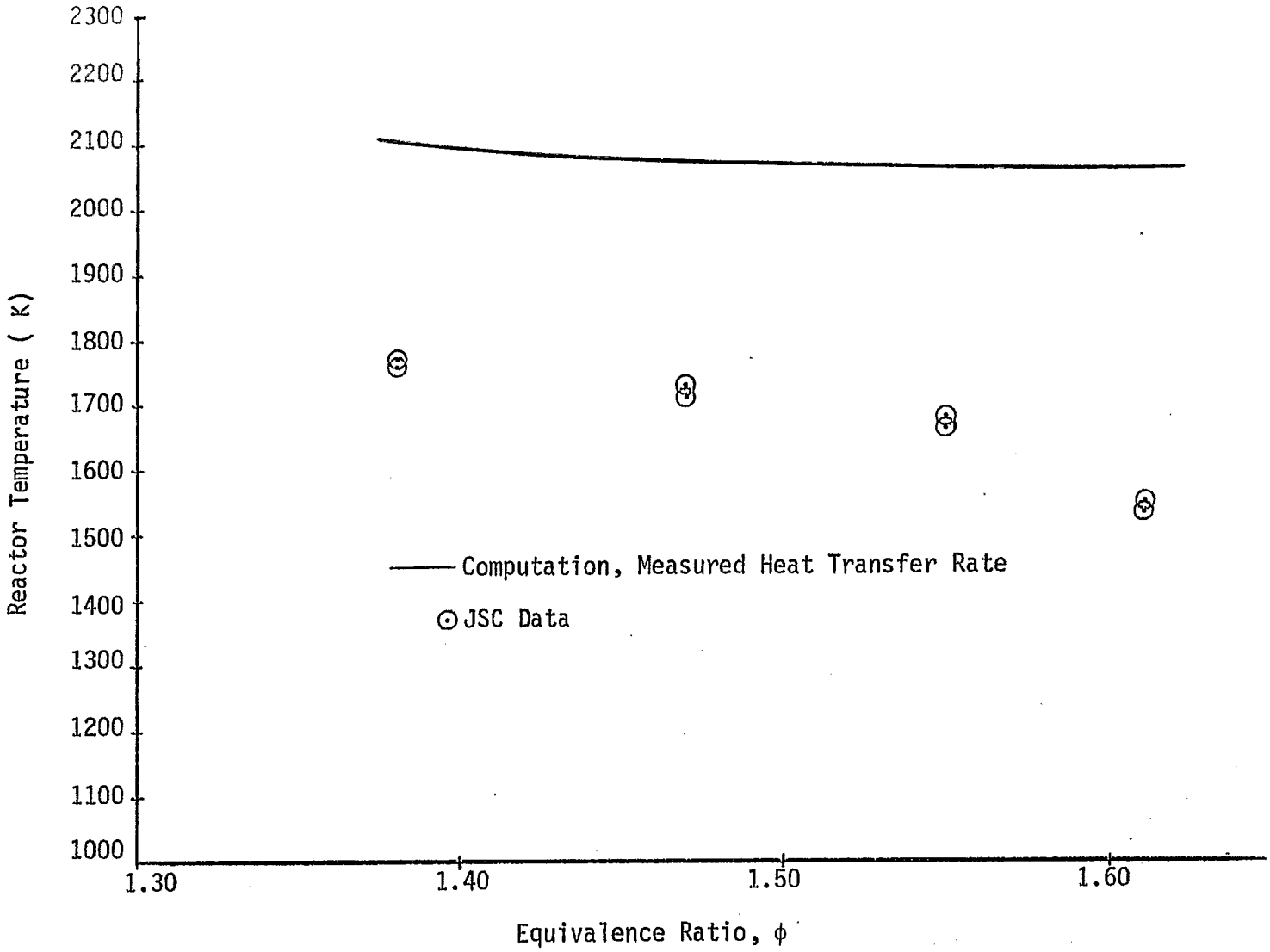

FIGURE 36: Comparison of Predicted and Measured Reactor Temperature, Isooctane

of 0.45 while the experimentally observed minimum occurs at an equivalence ratio of 0.53. Although the practical significance of this result would appear not to be of extreme importance it is necessary to have confidence in extrapolating these results, through prediction, to arbitrary operating conditions. In this regard the comparisons with the plug flow data (see Figure 27 and 28) is relevant. Here, very lean equivalence ratios (< .1) for initial temperatures on the order of 1000 K are investigated. The CO concentrations are underpredicted. While the predicted temperature (Fig. 27) rises steadily the observed temperatue rises slowly at first and then rises rapidly toward the end of the combustion process. The observed behavior of temperature is consistent with the observed CO history. This suggests that the OH radical concentration history may be a key factor responsible for this behavior. Since OH is the primary path for the formation of CO_2 from CO its history during the early stages of the plug flow reaction process is important. Two possible mechanisms for the underprediction of CO are (Reference 50): OH consumption through formation of HO_2 and H_2O_2 through the so-called "quenching" mechanism and consumption thru direct attack of the fuel by the OH radical. Both mechanisms will slow the consumption of CO through the reduction of the available OH radical. These mechanisms will be modeled in Phase II of the current program.

In the fuel rich regime the predictions indicate that the consumption of fuel is too rapid, resulting in stable combustion far beyond the observed blowout limits. Consideration of pyrolysis of the fuel in competition with the oxidation of the fuel may explain this behavior. Referring to Fig. 35, the underprediction of CO that occurs at the lower end of the fuel rich equivalence ratios may be due to the rapid consumption of the CO similar to what was observed in the very lean plug flow data. However, at somewhat higher equivalence ratios the predicted CO concentrations are higher than observed. Over the entire fuel rich equivalence ratio range beyond this point the predicted CO remains higher than observed while the predicted fuel concentration is lower than observed. This suggests that as the equivalence ratio increases pyrolysis becomes dominant and less CO is produced. These results suggest that both competing pyrolysis and partial oxidation steps are required in the extension of the quasiglobal model. However, the extensions that are required must also account for the additional observations made on the soot formation process. In fact, it appears that for the aromatic hydrocarbons (toluene, etc.) there is a direct correspondence between the breakthrough of unburned hydrocarbons and the incipient formation of soot. This global observation (see Section II) is in concert with the quasiglobal model concept and further supports the need for a multistep (subglobal) set of initiation reactions.

The observations described here and in Section II can be characterized by the following sequence of initiation steps:

Starting with a raw fuel, F_1, the competition will be accounted for through the follow set,

$$F_1 \rightarrow F_2 + \alpha(F_1,F_2)\ H_2 + NX$$

$$F_1 + O_2 \rightarrow CO + H_2,$$

where α depends upon the specification of the raw fuel and the fuel, F_2, manufactured by the pyrolysis step. NX represents a nitrogeneous compound released from its fuel bound state during the decomposition of the raw fuel.

The manufactured fuel also decomposes and oxidizes though the competitive steps:

$$F_2 \rightarrow C_s + H_2$$

$$F_2 + O_2 \rightarrow CO + H_2,$$

where C_s is solid carbon characterizing the soot. The sequential nature of the formation of F_2 prior to the formation of soot accounts for the lag in the formation of soot relative to pyrolysis. The sequential rate controlled competative mechanism also provides the means to account for the observation that incipient soot formation was not observed in the isooctane tests.

The final step in the subglobal scheme is the oxidation of soot,

$$C_s + O_2 \rightarrow CO_2.$$

The major products of these reactions (CO and H_2) react to completion through the extended detailed "wet" CO mechanism that includes the HO_2 and H_2O_2 species and reactions.

The development of this model will proceed during Phase II of the current program. The information to be developed experimentally in support of the model development will include: definition of the major products of pyrolysis (F_2), the major products of combustion, soot concentration and size. These data will be obtained over a full spectrum of equivalence ratios (rich and lean), residence times, initial temperatures and over a range of pressure levels. Both jet stirred combustors and plug flow reactors will be employed (experimentally and theoretically) to provide conditions relevant to reactions in parallel (recirculation zones) and reactions in series. This combination will provide the widest range of applicability of the quasiglobal model including turbulent diffusion regions relevant to the overall modeling of practical combustion systems.

A complete description of the future work which includes spray and aerodynamic considerations is discussed in the next section.

IV FUTURE WORK

This section is intended to provide an overview of future program plans. It is divided into two sub-sections. The first lists the technical areas requiring attention and the priorities of this work. The second describes our work plan for Phase II (FY 79 and FY 80).

A. Analysis of Required Effort

During the first quarter of this first program year an evaluation of combustion phenomena requiring further study was accomplished. This work is reported in detail in the first quarterly progress report (Reference 3). In brief, it was concluded that the following technical areas required study.

- Soot Formation
- Fuel Pyrolysis
- Soot Oxidation
- Flame Radiation
- Bound Nitrogen → NO_x Conversion
- Aerodynamic Chemical Interactions
- Fuel Vaporization and Spray Dynamics

It should be noted that these research areas are not very sharply defined. For example, soot formation occurs during fuel pyrolysis and one topic could not be totally excluded from study of the other. Further, the difference in the priority of the items is very small. Bound nitrogen conversion should be given urgent priority even though it is fifth on the list.

The experimental and analytical efforts of the past three quarters have provided additional information to refine and amplify this list of needs. These areas are discussed below and specific contributions which can be made as part of this program are identified.

Soot formation has been actively studied during this first program year and detailed needs can be defined. The nature of hydrocarbon species present at and beyond the sooting limit must be identified to establish the correct mechanism and constant T and ϕ experiments are required to develop quasi-global kinetics of the process. Fuel types similar to those investigated this past year must be utilized. The effects of unmixedness and the presence of fuel droplets are known to be very significant. These must also be incorporated into the model framework by employing the iterative experimental/analytical procedure which characterizes this program. Finally, the influence of pressure on soot formation in backmixed combustion must be determined.

Fuel pyrolysis can be thought of as a step in the overall soot formation process but the generation of new quasi-global characterizations of pyrolysis should be considered as a separate technical requirement. The pyrolysis process also affects the stability of the combustion process and combustion efficiency.

To better resolve the chemistry of this process, plug flow studies of hydrocarbon pyrolysis should be undertaken. Time resolution (not possible in the JSR) under realistic conditions of heat release, temperature, and time is necessary for appropriate understanding and quasi-global characterization of the fuel pyrolysis process.

Soot oxidation is a process which is generally thought to be well-characterized by the Strickland-Constable relationship. However, the key data from which this conclusion is drawn do not involve well-characterized sooting flames but, rather, shock tube experiments using pre-formed carbon. Further, little information is available regarding soot consumption under fuel rich conditions. The appropriate experimental/analytical approach to provide this information is again the highly-turbulent plug flow combustion device. Here the evolution and oxidation of soot can be followed in a time-resolved fashion at equivalence ratio and temperature conditions of interest.

Flame radiation, fuel vaporization, and spray dynamics are processes which will not be studied experimentally during this program. Our approach will be to use existing analytical models which are believed to be reliable if our predictions of other flame characteristics, especially soot production and the aerodynamic flow field, are accurate. A survey of existing analytical characterizations and selection of the most suitable approach will be a portion of our future work.

Fuel nitrogen conversion to NO_x must be studied, as the practical fuels of interest in the future will have high nitrogen content. Plug-flow investigations where the evolution and conversion of nitrogen containing intermediates can be time resolved, should be conducted and quasi-global models generated. These studies will be particularly important in defining conditions where rich combustion to promote N_2 formation can be achieved without the production of excessive soot. The parameters of ϕ and T which define the optimum combination of operating conditions should be investigated.

Aerodynamic/chemical interaction is the last area requiring study. It must be recognized that in real systems inhomogeniety is always present and we must analyze the nature by which turbulence and unmixedness influences the results we have obtained. Combined analytical/experimental studies will be performed in an interactive fashion. Current thinking is to perform a well-defined shear-flow experiment which can be analyzed for this purpose.

B. Phase II Program

This program has entered into its second phase which will have a much broader scope and invove a greater level of effort. The program will concentrate on solving the problems identified using the approaches defined in Phase I as described in Sections II and III. These efforts will be characterized by the broad application of larger-scale experiments involving backmixed, plug-flow, and shear flow combustion conditions. The SAI modeling work will not only attempt to better describe chemical and physical phenomena, but will also provide valuable guidance concerning the design of experiments. This cooperative, iterative procedure will optimize the improvements to fundamental understanding and the generation of an analytical model during this program.

Six tasks are incorporated into Phase II. The first involves additional JSC-type experiments which improve our knowledge of soot formation under strongly backmixed conditions. During this task, additional atmospheric JSC studies will be conducted to determine the nature of the combustion product hydrocarbons via gas chromatographic analysis of the sampled gas. In addition, experiments will be conducted where N_2/O_2 blends are used to study the influence of combustion product temperature on soot formation at constant ϕ and to evaluate the influence of ϕ at constant temperature.

Stirred combustors of a a larger scale capable of operating over a range of pressures will be constructed and tested. While studies at ER&E will encompass a range from 0.2-6.0 atm, the system will be designed for testing up to 40 atm for possible additional use at a larger government operated facility. These studies will permit the already recognized strong pressure effect to be evaluated and will allow the influence of pressure variation on the present conclusions to be ascertained. It is also planned that the effects of unmixedness and the presence of liquid droplets will be studied in this system. These experiments will be designed in close coordination with SAI. Methods of accounting for micro-scale unmixedness and analytical capabilities for analysis of droplet effects will be considered in developing the reactor and experimental procedure designs. These Task 1 efforts will comprise the experimental portion of the first year of Phase II.

The second task is also experimental in nature. It involves an improved version of the Exxon Continuous Flow System. Basically, the system will provide a highly turbulent plug flow for the study of hydrocarbon pyrolysis and soot production, soot oxidation, and fuel nitrogen to NO_x conversion. No attempt at isothermal operation is made in utilizing this system; instead, information is acquired at realistic conditions of mixture ratio, heat release, and temperature rise. Use of turbulent plug flow for this series of experiments will allow time/temperature resolution of soot formation and oxidation kinetics and fuel-N combustion chemistry. This information will complement that previously acquired in strongly backmixed combustion in that turbulent plug flow represents the other major aerodynamic portion of a continuous combustion system.

The final experimental portion, Task 3, to be undertaken late in the second year of Phase II involves the evaluation of aerodynamic/chemical interactions. An experimental study of the coupled effects of turbulence and mixing will be undertaken with the formal experimental design being strongly influenced by SAI modeling requirements. One potential configuration for this investigation is the well-characterized shear-flow experiment where the reacting flow process at the interface between two uniform parallel streams, one of fuel and one of air, are studied. The global kinetics of hydrocarbon consumption, CO oxidation, soot production, and soot burnout may be studied resulting in the development of methods to account for turbulence effects on combustion chemistry.

The fourth through sixth tasks involve the parallel analytical effort to be conducted. Task 4 will be a continuing effort which parallels the experimental program outlined in Tasks 1 and 2 above. Quasi-global modeling of soot formation will be undertaken which will encompass experimental information concerning the effects of stirred combustor dynamics, pressure, unmixedness of fuel-air mixtures at the stirred reactor inlet, and the presence of liquid droplets within the stirred reactor. In the case of the latter two phenomena, some analytical predictive work will be performed in advance of the relevant experiment and guidance in experiment design will thus be provided.

The results of experimental work in the plug flow system will also be analyzed for incorporation into the analytical model framework at this time. Quasi-global models for hydrocarbon pyrolysis, soot formation and oxidation, and fuel nitrogen conversion will be improved based on the information from the Continuous Flow System.

Task 5 provides for development of the non-chemistry aspects of the overall model which is to predict fuel effects in continuous combustion systems. Three specific objectives will be addressed.

a. Gas dynamic aspects important to the prediction of fuel effects in actual systems will be analytically investigated and predictive capability will be developed. The turbulence/unmixedness influence present in practical combustion systems will be investigated and the analytical capabilities developed will be utilized to assist ER&E in designing a shear flow experiment to verify the modeling approach taken (Task 3). Non-premixed combustion flows (i.e. diffusion flames) will also be modeled during this task. The importance of hydrocarbon pyrolysis on the fuel side of a diffusion flame will be ascertained.

b. Spray development and behavior during combustion will be analyzed and a model will be developed. It is anticipated that existing literature information and output from current DOE programs in this area will be utilized for this development.

c. A flame radiation model will be developed along with an analytical means for relating this information to combustor hardware conditions (i.e. prediction of combustor liner temperature). Existing radiation and hardware analytical capabilities will be utilized in this effort.

The final task involves development of a working gas turbine combustion system model which embodies the key aspects of the previously described submodels and the quasi-global chemistry developed. The emphasis in modeling the complex gas dynamics of the turbine system will be to utilize combinations of well-characterized combustion models (i.e. well-stirred and plug flow) with appropriate means of relating combustion system design details (i.e. amount and location of secondary flow injection) to model input. Parameters predicted will include flame radiation, liner metal temperature, soot emission, hydrocarbon, CO, and NO_x emission, and blowout limits.

C. Technology Transition

The information being generated in this program provides an improved understanding of the processes important to alternate fuels utilization. The "end item" is an analytical model which allows prediction of fuel effects in various types of continuous combustion devices, particularly utility gas turbines. Such a development will provide combustor designers with a tool to develop fuel flexible combustion systems which can utilize synfuels which are produced with minimum refining/upgrading and, hence, minimum cost and energy consumption during refining.

Transition of this information to the eventual user--the combustion system designer-- must be considered a major objective of this overall program. As has been the case historically, the trends taken in future combustion system development will depend only upon the skills of the hardware designer. Many examples of information and analytical models which have been developed only to remain within the academic research community can be sighted. If the results of this program are not transitioned into the store of skills familiar to the hardware designer, our advancements will not provide the desired crucial payoff in future system fuel flexibility.

We recognize our responsibility to transfer the results of this program to combustion system designers. Three actions will be taken to accomplish this. First, our experimental findings/conclusions and analytical models will be presented in a manner understandable to the hardware developers. In particular, the final analytical model will be designed to be as simple as possible. Second, we will publish information at meetings and in journals which are oriented towards the development community. This policy will assure that the appropriate individuals are present during our communications of important information. Finally, we will attempt to form a special committee of users--people involved in hardware design--to advise us regarding program orientation and to receive the program results. Such a forum would allow a detailed examination/evaluation of our findings and foster important ties of communication which, hopefully, will facilitate the task of transition and result in immediate use of information and models developed.

References

1. Longwell, J. P., "Synthetic Fuels and Combustion," Sixteenth International Symposium on Combustion, The Combustion Institute, Pittsburgh, PA, August 1976, pp. 1-15.

2. Cooper, V., and Duncan, R., "Baseload Reliability in a Combustion Turbine?", EPRI Journal, June 1978, pp. 17-21.

3. Blazowski, W. S., Bellan, J. R., Harsha, P. T., and Edelman, R. B., "Fundamental Characterization of Alternate Fuel Effective Continuous Combustion Systems," Technical Progress Report No. 1, Contract EC-77-C-03-1543, January 1978.

4. Longwell, J. P. and Weiss, M. A., Ind. Eng. Chem., 47, 1634, 1955.

5. Wright, F. J., "The Formation of Carbon Under Well-Stirred Conditions," 12th Symposium (International) on Combustion, The Combustion Institute, Pittsburgh, PA., pp. 867-875, 1968.

6. Wright, F. J., "Carbon Formation Under Well-Stirred Conditions, Part II," Combustion and Flame, Vol. 15, pp. 217-222, 1970.

7. Jackson, T. A., and Blazowski, W. S., "Fuel Hydrogen Content as an Indicator of Radiative Heat Transfer in an Aircraft Gas Turbine Combustor," in Gas Turbine Combustion and Fuels Technology, ASME, United Engineering Center, 345 E. 47th St., New York, N.Y., November 1977, pp 59-65.

8. Cullis, C. F., "Role of Acetylenic Species in Carbon Formation," ACS Symposium Series, 21, 1976, pp 348-357.

9. Daniels, P. H., "Carbon Formation in Premixed Flames," Combustion and Flame, Vol. 4, pp. 45-49, 1960.

10. Fenimore, C. P., and Jones, G. W., "Comparative Yields of Soot from Premixed Hydrocarbon Flames," Combustion and Flames, Vol. 12, No. 3, June 1968, pp. 196-200.

11. Fenimore, C. P., and Jones, G. W., "Coagulation of Soot to Smoke in Hydrocarbon Flames, "Combustion and Flame, Vol. 13, No. 3, June 1969, pp. 303-310.

12. Fennimore, C. P., Jones, G. W., and Moore, G. E., "Carbon Formation in Quenched Flat Flames at 1600^{o}K," 6th Symposium (International) on Combustion, pp. 242-246, 1956.

13. Gaydon, A. G., and Wolfhand, H. G., "Solid Carbon in Flames," Chapter VIII in Flames, pp. 175-210.

14. Graham, S. C., Homer, J. B., and Rosenfeld, J. L. J., "The Formation and Coagulation of Soot Aerosols Generated by the Pyrolysis of Aromatic Hydrocarbons," Proc. Roy. Soc. London A., Vol. 344, 1978, pp 259-285.

15. Graham, S. C., Homer, J. B., and Rosenfeld, J. L. J., "The Formation and Coagulation of Soot Aerosols," Int. Shock Tube Symposium, 10th Proceedings, July 1975, pp. 621-631.

16. Hein, K., "Recent Results on the Formation and Combustion of Soot in Turbulent Oil and Gas Flames," Combustion Science and Technology, Vol. 5, 1972, pp. 195-206.

17. Holderness, F. H., and MacFarlane, J. J., "Soot Formation in Rich Kenosene Flames at High Pressure," Paper No. 18, AGARD Conference Proceedings No. 125, Atmospheric Pollution by Aircraft Engines, April 1973.

18. Homann, K. H., "Carbon Formation in Premixed Flames," Combustion and Flame, Vol. 11, pp. 265-287, 1967.

19. Howard, J. B., "On the Mechanism of Carbon Formation in Flames," 12th Symposium (International) on Combustion, 1968, pp. 877-887.

20. Jensen, D. E., "Prediction of Soot Formation Rates: A New Approach," Proc. Roy. Soc. London A. 338, 1974, pp. 375-396.

21. MacFarlene, J. J., Holderness, F. H., and Whiteher, F. S. E., "Soot Formation Rates in Premixed C_5 and C_6 Hydrocarbon-Air Flames at Pressure Up to 20 Atmospheres," Combustion and Flame, Vol. 8, pp. 215-229, 1964.

22. Palmer, H. B., and Cullis, C. F., "The Formation of Carbon from Gases," Chapter 5 in Chemistry and Physics of Carbon, edited by P. L. Walker, 1965.

23. Stehling, F. C., Frazee, J. D., and Anderson, R. C., "Carbon Formation from Acetylene," 6th Symposium (International) on Combustion, pp. 247-254, 1956.

24. Street, J. C., and Thomas, A., "Soot Formation in Premixed Flames," Fuel, Vol. 34, pp. 4-36, 1955.

25. Tesner, P. A., "Formation of Dispersed Carbon by Thermal Decomposition of Hydrocarbons," 7th Symposium on Combustion, 1959.

26. Thomas, A., "Carbon Formation in Flames," Combustion and Flame, Vol. 6, March 1962, pp. 46-62.

27. Hutchinson P., Khalil, E. E., and Whitelaw, J. H., "Measurement and Calculation of Furnace-Flow Properties," Journal of Energy, Vol. 1, No. 4, July-August 1977, pp. 212-219.

28. Abou Ellail, M. M. M., Gosman, A. D., Lockwood, F. C., and Megahead, I. E. A., "Description and Validation of a Three-Dimensional Procedure for Combustion Chamber Flows," Report FS/77/27, Imperial College, Oct. 1977.

29. Roberts, R., A. Aceto, L. D., Kollrack, R., Teixeira, D. P., and Bonnell, J. M., "An Analytical Model for Nitric Oxide Formation in a Gas Turbine Combustor," AIAA Journal, Vol. 10, No. 6, June 1972.

30. Swithenbank, J., Poll, I., Vincent, M., W., and Wright, D. D., "Combustion Design Fundamentals," Fourteenth Symposium (International) on Combustion, The Combustion Institute, Pittsburgh, 1973, pp. 627-636.

31. Edelman, R. B. and Harsha, P. T., "AFOSR Interim Report on Mixing and Combustion in High Speed Air Flows," RDA-TR-0700-002, R&D Associates, Marina del Rey, CA, April 1976.

32. Edelman, R. B. and Fortune, O., "A Quasi-Global Chemical Kinetic Model for the Finite Rate Combustion of Hydrocarbon Fuels," AIAA Paper 69-86, 1969.

33. Kattan, A. and Adler, R. J., "A Stochastic Model for Homogeneous, Turbulent, Tubular Reactors," AICHE Journal, Vol. 13, May 1967, pp. 580-585.

34. Rhodes, R. P., Harsha, P. T. and Peters, C. E., "Turbulent Kinetic Energy Analyses of Hydrogen-Air Diffusion Flames," Acta Astronautica, Vol. 1, 1974, pp. 443-470.

35. Khalil, E. E., "Flow and Combustion in Axisymmetric Furnances," Ph.D. Thesis Univ. of London, 1977.

36. Pratt, D. T., "Mixing and Chemical Reaction in Continuous Combustion," Progress in Energy and Combustion Science, Vol. 1, No. 2/3, 1976, pp. 73-86.

37. Boccio, J. L., Weilerstein, G., and Edelman, R. B., "A Mathematical Model for Jet Engine Combustor Pollutant Emissions," NASA CR-12108, GASL TR-781, General Applied Science Laboratories.

38. Harsha, P. T., "A General Analysis of Free Turbulent Mixing," AEDC TR-73-177, Arnold Engineering Development Center, 1974.

39. Edelman, R. B., and Weilerstein, G., unpublished work, 1971.

40. Korst, H. H., Chow, W. L., Hurt, R. F., White, R. A., and Addy, A. L., "Analysis of Free Turbulent Shear Flows by Numerical Methods," Free Turbulent Shear Flows, Vol. 1, Conference Proceedings, NASA SP-321, 1973, pp. 185-232.

41. Edelman, R. B. and Harhsa, P. T., "Some Observations on Turbulent Mixing With Chemical REactions, " AIAA Paper 77-142, 15th AIAA Aerospace Sciences Meeting, January 1977; to appear in Progress in Aeronautics and Astronautics, Vol. 58, Turbulent Combustion, edited by Lawrence Kennedy, April 1978.

42. Edelman, R. B and Harsha, P. T., "AFOSR Interim Scientific Report: Mixing and Combustion in High Speed Air Flows," Report SAI-78-008-WH, Science Applications, Inc., April 1978.

43. Harsha, P. T., "Kinetic Energy Methods," Chapter 8 of Handbook of Turbulence, Vol. 1, W. Frost and T. Moulden, Eds., Plenum Publishing Corp., 1977.

44. Engleman, V. S., Edelman, R. B., Bartok, W. and Longwell, J. P., "Experimental and Theoretical Studies of NO_x Formation in a Jet-Stirred Combustor, 14th Symposium (International) on Combustion, The Combustion Institute, 1973, pp. 755-765.

45. Glassman, I., Dryer, F. L., and Cohen R., "Combustion of Hydrocarbons in an Adiabatic Flow Reactor: Some Considerations and Overall Correlations of Reaction Rate," Princeton Report No. 1223, presented at the Joint Meeting of the Central and Western States Section of the Combustion Institute, April 1975.

46. Gardiner, W. C., Jr., Mallard, W. G., McFarland, M., Morinaga, K., Owen, J. H., Rawling, W. T., Takeyama, T., and Walker, B. F., "Elementary Reaction Rates from Post-Induction-Period Profiles in Shock-Initiated Combustion," Fourteenth Symposium (International) on Combustion, The Combustion Institute, 1973, pp. 61-72.

47. Baulch, D. L. and Drysdale, D. D., Combustion and Flame, Vol. 23, p. 215, 1974.

48. Engleman, V. S., "Survey and Evaluation of Kinetic Data on Reactions in Methane/Air Combustion," Report EPA-600/2-76-003, Environmental Protection Agency, January 1976.

49. Baulch, D. L., Drysdale, D. D., and Lloyd, A. C., "Critical Evaluations of Rate Data for Homogeneous, Gas-Phase Reactions of Interest in High Temperature Systems," No. 1, Leeds University, 1968.

50. Private Communication between R. Edelman (SAI) and Charles Westbrook (L.L.L.) and Dr. Fredrick Dryer (Princeton University), Doe Workshop, January 1978.

U.S. DEPARTMENT OF COMMERCE
Technology Administration
National Technical Information Service
Springfield, VA 22161 (703) 605-6000